

Cyber Resilience in Next-Generation Networks: Threat Landscape, Theoretical Foundations, and Design Paradigms

Junaid Farooq

University of Michigan-Dearborn

Quanyan Zhu

New York University

Abstract

The evolution of networked systems, driven by innovations in software-defined networking (SDN), network function virtualization (NFV), open radio access networks (O-RAN), and cloud-native architectures, is redefining both the operational landscape and the threat surface of critical infrastructures. This book offers an in-depth, interdisciplinary examination of how resilience must be re-conceptualized and re-engineered to address the multifaceted challenges posed by these transformations.

Structured across six chapters, this book begins by surveying the contemporary risk landscape, identifying emerging cyber, physical, and AI-driven threats, and analyzing their implications for scalable, heterogeneous network environments. It then establishes rigorous definitions and evaluation frameworks for resilience, going beyond robustness and fault-tolerance to address adaptive, anticipatory, and retrospective mechanisms across diverse application domains.

The core of the book delves into advanced paradigms and practical strategies for resilience, including zero trust architectures, game-theoretic threat modeling, and self-healing design principles. A significant portion is devoted to the role of artificial intelligence, especially reinforcement learning and large language models (LLMs), in enabling dynamic threat response, autonomous network control, and multi-agent coordination under uncertainty.

Recognizing the convergence of digital and physical domains, the final chapters synthesize resilience design principles through detailed case studies in software-defined 5G and O-RAN systems, including trust-aware resource management, risk-aware edge–cloud orchestration, multi-agent reinforcement learning, and LLM-driven network control. The concluding chapter then distills overarching lessons and outlines future directions, emphasizing AI-enabled and vertical-aware resilience requirements in industrial automation and smart manufacturing contexts.

Contents

1 Risk Landscape in Next Generation Networks	5
1.1 Understanding Next-Generation Networks	5
1.2 Integrated Risks Across Next-Generation Networks	12
2 Defining and Measuring Resilience	16
2.1 Understanding Network Resilience in 5G Networks	16
2.1.1 Resilience vs. Fault-Tolerance and Reliability	17
2.1.2 Multi-Dimensional and Dynamic Nature of 5G Resilience	19
2.2 Types of Resilience Mechanisms in 5G Networks	20
2.2.1 Proactive Resilience	21
2.2.2 Responsive Resilience	23
2.2.3 Retrospective Resilience	25
2.2.4 Integration of Proactive, Responsive, and Retrospective Mechanisms	27
2.2.5 Quantitative Approach to Resilience Design	29
2.3 Metrics and Evaluation	30
2.3.1 Discrete-Time Formalism for Resilience	31
2.3.2 General Temporal Metrics	32
2.3.3 Domain-Specific Metrics	33
2.3.4 Composite and Cost-Aware Metrics	35
2.3.5 Integration with Control and Learning Frameworks	36
3 Theoretic Foundations for Resilient Network Management	39
3.1 Control-Theoretic Foundation	40
3.1.1 System Model	40
3.1.2 Moving Target Defense.	49
3.2 Dynamic Game Foundation	53
3.2.1 Model Definition	54
3.2.2 Resilience as an equilibrium property	58

3.2.3	Equilibrium Solution Via Dynamic Programming	59
3.2.4	Equilibria and dynamic programming.	62
3.3	Learning as the Foundation	64
3.3.1	Learning dynamics in games	64
3.3.2	Resilience control as a learning process	65
3.3.3	Feedback structures and observability	66
3.3.4	Reinforcement and Meta-Learning	66
3.3.5	Toward Predictive Resilience	67
3.4	Network-Theoretic Foundation	68
4	Cyber Risk Assessment for NextG Networks	73
4.1	Probabilistic Risk Assessment with Digital Twins	73
4.1.1	State-Space View and Twin Synchronization	74
4.2	Strategic Risk Assessment	76
4.2.1	Red-Blue Teaming as a Game	77
4.2.2	Integration with Digital Twins	79
4.2.3	Evaluating Resilience Metrics	79
4.2.4	Insights from the Game to DT Pipeline	80
4.3	Network Analytics for Risk Analysis	81
4.4	Agentic AI and Large Language Models for Risk Assessment	85
4.4.1	What is Agentic AI?	85
4.4.2	What are Large Language Models (LLMs)?	86
4.4.3	Distributed Agent Roles in NextG	87
4.4.4	Agentic AI Workflow Across Resilience Stages	89
4.4.5	Integration Across Mechanisms in Large-Scale Contexts	90
5	Resilient System Designs	92
5.1	Trust-Aware Resource Management for Resilient Network Slicing	92
5.2	Risk-Aware Resource Orchestration in Multi-Tier 5G Edge-Cloud Systems	100
5.2.1	Risk Modeling and Application Beliefs	101
5.3	Resilient Slice Management through Multi Agent Reinforcement Learning	107
5.4	LLM Driven Resilient Slice Management	115
5.4.1	Performance Implications and Observed Gains	118
5.4.2	Discussion	119
6	Concluding Remarks	123
6.1	Summary of the Article	123

6.2	AI-Enabled Resilience and Vertical-Specific Challenges	124
6.2.1	AI as an Enabler of Resilience	125
6.2.2	Vertical Domains and Domain-Specific Resilience Specifications . . .	125

Chapter 1

Risk Landscape in Next Generation Networks

1.1 Understanding Next-Generation Networks

Next-generation (NextG) networks, particularly those underpinned by 5G and its successors, represent a transformative shift from traditional telecommunications paradigms [1, 2, 3]. They are not merely incremental upgrades in bandwidth or speed, but comprehensive re-architectures of the communication stack. NextG networks introduce architectural innovations such as software-defined networking (SDN) [4, 5], network function virtualization (NFV) [6, 7], and open interfaces (e.g., O-RAN) [8, 9], coupled with unprecedented service flexibility enabled by network slicing, edge computing, and integration with cloud-native principles. These capabilities allow the network to evolve from a rigid infrastructure into a programmable platform that can dynamically host diverse services: from enhanced mobile broadband (eMBB) to ultra-reliable low-latency communication (URLLC) and massive machine-type communication (mMTC) [10].

NextG networks play a central role as the enabling fabric of the digital economy. Beyond supporting consumer connectivity, it underpins critical infrastructures such as smart grids [11, 12], intelligent transportation [13, 14], remote healthcare [15, 16], and industrial automation [17, 18]. In many cases, mission-critical and safety-critical operations, such as autonomous vehicles coordinating in real time, tele-surgery surgeons or factories running with digital twins, depend directly on the deterministic performance and reliability of NextG services. Unlike previous generations, where mobile networks were largely confined to consumer use cases, NextG is tightly interwoven with societal functions, making its dependability a matter of public safety, national security, and economic competitiveness.

The same innovations that make NextG powerful also expand its attack surface [19]. Virtualization and softwarization increase the number of components and interfaces that must be secured. Disaggregated RAN architectures introduce new trust boundaries between radio units (RU), distributed units (DU), and centralized units (CU), each with their own control and data flows [20, 21]. Cloud-native deployments inherit the vulnerabilities of container platforms, orchestration systems, and third-party software supply chains [22]. Multi-tenant network slicing, while enabling efficiency and customization, raises the risk of cross-slice leakage and resource contention attacks [23]. Moreover, the reliance on third-party vendors and open interfaces (e.g., O-RAN Alliance specifications) means that security is no longer centrally enforced but must be coordinated across heterogeneous ecosystems [24].

The stakes are high: adversaries can target not only consumer data but also industrial processes, public safety systems, and national infrastructure [25, 26]. State-sponsored actors may view NextG as a strategic battleground for espionage and disruption. Criminal organizations may exploit vulnerabilities for ransomware or denial-of-service campaigns. Even unintentional misconfigurations in such complex systems can cause widespread outages, as recent incidents in cloud services have demonstrated [27]. Thus, the security of NextG networks is not an auxiliary concern but a prerequisite for their safe adoption.

Architectural Overview. Fig. 1.1 provides a high-level view of a NextG network, organized into three main domains, core, transport, and RAN, with external interfaces to the Internet, cloud platforms, and end-user devices [28, 29]. This layered view reflects both the functional separation of modern mobile networks and the trust boundaries across which data and control traffic must pass. Unlike legacy monolithic architectures, NextG systems are deeply disaggregated and virtualized, meaning that control and user planes are distributed across software-defined functions running on commodity hardware, often orchestrated in multi-vendor, cloud-native environments. This shift amplifies flexibility but simultaneously creates a much larger and more complex attack surface.

The red numbering in Fig. 1.1 highlights potential threat points, many of which cluster at inter-domain interfaces where assumptions of trust are weakest [30]. Specifically, points (1)–(2) capture risks introduced by external connectivity to the Internet and cloud services. These connections expose NextG infrastructure to volumetric distributed denial-of-service (DDoS) attacks, cloud-side supply chain risks, and data exfiltration attempts that originate outside the operator’s administrative control [31]. Point (3) highlights vulnerabilities in Core network compute, memory, and bandwidth resources. Here, threats include denial-of-service against control-plane virtual network functions (VNFs), exploitation of software bugs in user-plane functions, and abuse of APIs in the service-based architecture (SBA) [32].

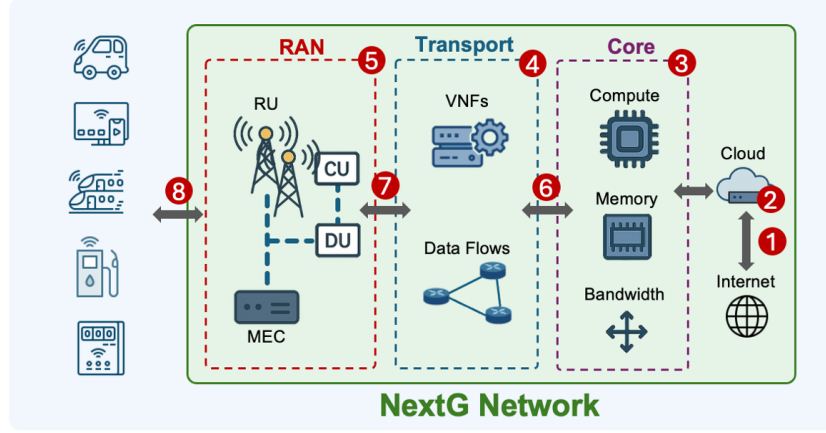


Figure 1.1: Architecture of a NextG network showing Core, Transport, and RAN domains, with interfaces to the Internet, Cloud, and end-user devices. Red numbering highlights potential threat points: (1)–(2) external connectivity through Internet and Cloud; (3) vulnerabilities in Core compute, memory, and bandwidth; (4) risks in virtualized Transport functions and data flows; (5)–(7) exposed surfaces in disaggregated RAN (RU, DU, CU, MEC); and (8) end-user and critical-infrastructure edges. Several of these occur at inter-domain interfaces, underscoring the importance of boundary security.

Point (4) identifies risks in the Transport domain, which is increasingly virtualized and programmable. Software-defined backhaul and fronthaul links enable flexible routing but also introduce susceptibility to mis-configuration, routing manipulation, and man-in-the-middle attacks [33]. Points (5)–(7) focus on the disaggregated RAN, where RUs, DUs, CUs, and MEC nodes interact over open interfaces. While this disaggregation allows multi-vendor deployments and fine-grained scalability, it also exposes additional attack vectors such as rogue RUs injecting false signals, tampering with DU-CU fronthaul protocols, or exploiting MEC workloads that lack strong isolation [34].

Finally, point (8) highlights risks at the end-user and critical-infrastructure edges, where heterogeneous devices connect to the network. These include consumer smartphones, IoT sensors, industrial control devices, and safety-critical endpoints in transportation and healthcare [35, 36, 37, 38]. Many of these devices operate with limited security features, making them attractive entry points for adversaries who can pivot into the core network. Their compromise can lead not only to localized data breaches but also to systemic effects such as botnet-driven DDoS, signaling storms, or manipulation of mission-critical services [39, 40, 41, 42].

In what follows, we provide a detailed description of the background and function of each architectural component, followed by an analysis of its associated threat vectors. This approach highlights how the same architectural features that empower NextG networks with

unprecedented flexibility and programmability also introduce novel security challenges that demand proactive, responsive, and retrospective resilience mechanisms.

External Interfaces: Internet and Cloud

NextG networks interface with the global Internet and cloud infrastructures to deliver agile, scalable services. The cloud provides elastic compute and storage resources for hosting network functions, analytics platforms, and AI/ML workloads, while Internet connectivity ensures global reachability and interconnection with third-party services. These interfaces form the bridge between telecom infrastructure and the broader digital ecosystem, enabling cloud gaming, edge AI inference, and global roaming. In practice, major operators already deploy critical control-plane functions in public or hybrid clouds to take advantage of scalability, but this also shifts the trust boundary beyond traditional telecom domains.

At threat points 1–2, these same interfaces create the most exposed attack surfaces. Malicious or unverified cloud updates can compromise workloads, as seen in recent supply-chain attacks where adversaries inserted backdoors into software libraries [43]. Misconfigured APIs in the SBA may allow unauthorized requests or privilege escalation [44]. Cloud-side compromises, such as a breach of an orchestration platform, can propagate directly into the control and user planes, undermining both confidentiality and availability [45]. Peering and interconnection points with the Internet are also targets: attackers may inject spoofed BGP updates to reroute traffic, launch volumetric DDoS attacks that overwhelm ingress points, or exploit DNS misconfigurations to hijack sessions [46].

Defenses must therefore include strong API authentication with mutual TLS, fine-grained access policies, encrypted traffic inspection to detect anomalies without violating privacy constraints, and hardware-based attestation of workloads to ensure that functions running in the cloud have not been tampered with. Current best practices also involve continuous posture assessment of cloud services [47], supply-chain verification pipelines [48], and DDoS scrubbing at peering edges [49]. Yet, despite these defenses, the speed and scale of cloud-native updates mean that even small lapses can expose entire operator networks to cascading risks.

Core Network: SDN and NFV Foundations

The Core (threat point 3) is the programmable heart of NextG networks. It embodies the shift from hardware appliances to flexible, software-defined infrastructures. SDN centralizes policy and routing control, while NFV allows functions such as user plane functions (UPFs), session management functions (SMFs), and firewalls to run as virtualized workloads

on commodity servers. Together, SDN and NFV enable elasticity, service agility, and cost efficiency: operators can spin up new slices for enterprises in minutes rather than months, dynamically reconfigure routing, or scale security functions with changing load.

However, the same virtualization and programmability that enable flexibility also concentrate risk. The SDN controller is a single point of control; if compromised, it can alter forwarding rules to reroute or drop traffic, perform traffic interception, or disable entire network slices [50]. Similarly, a compromised NFV orchestrator could halt service instantiations, inject malicious VNFs, or disable defensive functions [51]. Vulnerabilities in hypervisors or container runtimes further expand the attack surface, allowing adversaries to escape virtualized environments and access host infrastructure [52].

Interfaces between the Core and Transport (threat point 4) are particularly critical, since they connect logical control functions with heterogeneous physical backhaul resources. Attackers who pivot across this boundary can perform lateral movement: e.g., leveraging a compromised control-plane API in the core to disrupt multipath routing in the transport. In the status quo, operators mitigate these risks with role-based access controls [53], segmented management planes [54], and continuous vulnerability scanning of VNFs [55]. Yet, many deployments still rely on legacy VNFs with limited patch cycles, leaving core functions exposed to evolving zero-day exploits.

Transport Network: Programmable Data Flows

The Transport domain (threat point 4) provides the backbone interconnecting Core and RAN. It carries high-capacity data flows over backhaul and fronthaul links, supporting programmable traffic handling for bandwidth allocation, quality-of-service (QoS) enforcement, and tunneling. The shift to programmable transport allows dynamic reconfiguration of flows, enabling better load balancing and resilience against failures. VNFs in this domain manage traffic engineering, policy enforcement, and encryption services, bringing agility that was not possible with static hardware routers.

At the same time, programmable transport introduces new vulnerabilities. Attacks against VNFs, such as traffic shapers or firewalls, can degrade data-plane integrity or bypass enforcement rules. Control-plane signaling in transport networks is also a target; for example, compromised SDN controllers managing transport switches could alter routing policies, enabling blackholing or interception of traffic [56]. Physical sabotage remains a real threat: cutting fiber links or tampering with roadside transport nodes can cause wide-area outages, while natural disasters (e.g., earthquakes, floods) highlight the fragility of centralized transport hubs [57].

Defensive practices today include encrypted overlays (e.g., IPsec or TLS tunnels) to

protect data-plane confidentiality [58], multipath routing to ensure that traffic can be rerouted around compromised or failed links [59], and automated recovery protocols that detect faults and restore flows rapidly [60]. Some operators are experimenting with AI-based transport anomaly detection, analyzing flow-level measurement to identify rerouting attacks or sudden congestion indicative of malicious interference. Still, these systems are often reactive, and ensuring provable guarantees of transport resilience under adversarial conditions remains an open challenge.

Radio Access Networks

The Radio Access Network (RAN, threat points 5–7) is undergoing a fundamental transformation with the advent of Open RAN (O-RAN) [9], which supports disaggregation and openness. In this new architecture, monolithic base stations have been decomposed into Radio Units (RUs), Distributed Units (DUs), and Central Units (CUs), interconnected by standardized fronthaul and midhaul protocols [8]. This split architecture allows multi-vendor interoperability, flexible deployment, and optimized resource utilization. Multi-access Edge Computing (MEC) extends compute and storage into the RAN domain, enabling ultra-low-latency services such as augmented/virtual reality, autonomous driving, and industrial process control [61]. The RAN Intelligent Controller (RIC), both near-real-time and non-real-time, introduces programmability into the RAN, supporting AI-driven optimization of spectrum allocation, handover management, and interference mitigation [62].

This disaggregation, however, significantly enlarges the attack surface. Interfaces between RU, DU, and CU are susceptible to man-in-the-middle and replay attacks, where adversaries manipulate control messages to degrade performance or exfiltrate data. Rogue base stations (so-called “IMSI catchers” or “stingrays”) can spoof legitimate signals, harvest subscriber data, or force devices into weaker encryption modes [63]. Jamming and interference remain perennial threats, but in NextG they pose amplified risks to URLLC applications where even millisecond disruptions may lead to catastrophic outcomes [64]. Vulnerabilities in RIC xApps or rApps could propagate faulty policies across the entire RAN, creating systemic instability [65, 66]. MEC nodes, positioned at the edge, inherit risks from both the cloud and RAN domains: a compromised MEC platform could host malicious workloads, manipulate latency-sensitive data flows, or serve as a pivot for lateral movement into core functions [67, 68, 69].

In the status quo, operators deploy measures such as mutual authentication across fronthaul links, encryption of control-plane signaling, and geofencing of base stations. RIC security frameworks are still nascent, with ongoing work in the O-RAN Alliance to define trust anchors and policy controls for xApp/rApp onboarding. MEC security largely depends

on cloud-native defenses (container isolation, trusted execution environments), but uniform standards are lacking, leaving implementations uneven across vendors.

Heterogeneity, Scalability, and Edge Integration

NextG networks must simultaneously support eMBB, URLLC, and mMTC. This heterogeneity drives the deployment of dense small-cell infrastructures, mobility-aware scheduling, dynamic spectrum sharing, and real-time orchestration at the edge. It also requires seamless integration of heterogeneous devices, from smartphones and IoT sensors to industrial robots and connected vehicles, each with distinct performance and security profiles.

At threat point 8, the diversity of endpoints multiplies attack opportunities. Millions of IoT devices, often designed with minimal security features, represent a vast distributed attack surface [70]. Weak authentication, default credentials, or unpatched firmware allow adversaries to conscript devices into botnets, launch DDoS attacks, or act as footholds for lateral movement into higher-value network domains [71]. Smart vehicles and industrial robots, if compromised, can be manipulated to cause physical damage or safety incidents [35]. Edge integration further complicates matters: workloads that migrate between devices, MEC nodes, and cloud data centers create opportunities for adversarial tampering with data-in-transit or manipulation of scheduling decisions [72].

In practice, today’s defenses include device attestation protocols [73], slice-aware access control at the RAN [74], and anomaly detection for IoT traffic patterns [75]. However, the scale of device diversity makes centralized approaches difficult to sustain. Emerging research emphasizes AI-driven interference management [76], federated learning for anomaly detection at the edge [77], and trust frameworks that can dynamically assign risk scores to endpoints based on behavioral evidence [21]. Despite these developments, the heterogeneity of endpoints remains one of the weakest links in NextG security.

Interfaces with Critical Infrastructures and Supply Chains

Beyond consumer connectivity, NextG networks are envisioned as enablers for critical infrastructures such as healthcare, transportation, logistics, and energy systems. These verticals rely on NextG’s low-latency, high-reliability features to deliver real-time monitoring, automation, and control. Examples include telesurgery relying on URLLC slices, autonomous vehicles coordinated through V2X communications, and energy grid management via mMTC-enabled sensors. This deep integration means that NextG is not simply a communications platform—it becomes a foundational pillar for future smart societies.

The risks at threat point 8 therefore extend beyond technical failures to systemic con-

sequences. A vulnerability in a baseband unit sourced from an untrusted supplier could be exploited to surveil or disrupt entire regions of critical infrastructure [78]. Firmware backdoors in MEC equipment could allow attackers to trigger cascading failures across hospitals or transportation hubs [79, 80]. Supply chain dependencies are especially concerning: as disaggregation encourages multi-vendor ecosystems, ensuring that every component (hardware, firmware, orchestration software) is free from hidden vulnerabilities becomes a daunting task. Nation-state actors may exploit these dependencies to insert long-term backdoors, while criminal organizations may leverage counterfeit or tampered equipment to launch persistent attacks.

Mitigation requires secure development lifecycles across all vendors, rigorous vendor validation and certification, and application of Zero Trust principles not just within the telecom network but across sectoral boundaries [81]. Current efforts include initiatives like the GSMA’s Network Equipment Security Assurance Scheme (NESAS) [82] and U.S./EU proposals for trusted vendor certification [83, 84]. However, global supply chains remain opaque, and geopolitical tensions complicate consensus on trust anchors. As a result, securing critical infrastructure integration with NextG remains one of the most pressing challenges for both operators and policymakers.

1.2 Integrated Risks Across Next-Generation Networks

While individual vulnerabilities in NextG networks are serious on their own, the most disruptive scenarios often arise when adversaries combine multiple threat vectors across domains. These integrated risks highlight the systemic nature of next-generation networks and demonstrate why piecemeal defenses are inadequate. Unlike isolated incidents, integrated attacks exploit interdependencies between cloud, Core, Transport, and RAN domains, amplifying their impact and complicating detection and mitigation. Table 1.1 organizes the heterogeneous threat space of NextG networks into a layered taxonomy that links vectors, targets, and representative real world incidents.

Advanced Persistent Threats (APTs)

APTs represent long-term, stealthy campaigns typically orchestrated by nation-states or highly resourced adversaries [85]. Their hallmark is patience: adversaries infiltrate gradually, establish persistence mechanisms, and move laterally to expand control [86, 87, 88]. In NextG networks, the programmability of SDN and the elasticity of NFV create attractive avenues for APT operators. Similarly, the disaggregated and open interfaces of O-RAN provide additional footholds for exploitation.

A hypothetical but plausible chain of events begins with adversaries gaining initial access through a misconfigured cloud API (threat point 2), as seen in the 2019 Capital One breach, where a misconfigured cloud firewall exposed sensitive data [89]. From there, attackers could compromise an NFV orchestrator in the Core (threat point 3), similar in spirit to the SolarWinds supply-chain compromise of 2020, where trusted software updates were weaponized to deploy malicious code across thousands of organizations [90]. Once persistence is established, adversaries could pivot into RAN controllers (threat points 5–7). Rogue base stations like IMSI catchers are already widely documented in law enforcement and criminal contexts, showing that manipulation of signaling channels is feasible [91]. In an integrated APT scenario, this could escalate to manipulating radio scheduling or selectively disrupting connectivity in politically sensitive regions [92, 93].

Real-world parallels exist: the U.S. Cybersecurity and Infrastructure Security Agency (CISA) has repeatedly warned that advanced state-backed actors are probing telecom networks for long-term access. Incidents like the compromise of Ukraine’s telecom providers during the early stages of the 2022 war illustrate how adversaries use cross-domain access, spanning network control and radio functions, to monitor and disrupt communications on a scale [94]. Such integrated footholds allow covert traffic monitoring, long-term data exfiltration, or synchronized disruption campaigns designed to evade conventional detection, ultimately eroding trust in the entire NextG ecosystem.

Ransomware in Telecom Infrastructure

Ransomware, once confined to laptops and enterprise IT, has evolved into a strategic weapon against critical infrastructure [95]. In NextG networks, where continuous availability underpins essential services, from emergency dispatch to industrial automation, the stakes are exponentially higher. Telecom operators also manage vast orchestration platforms and virtualized services, making them prime ransomware targets [96, 97].

The 2021 Colonial Pipeline attack [98] demonstrated how ransomware against operational technology (OT) can cascade into widespread economic disruption, while the 2021 Kaseya VSA incident [99] showed how attackers can simultaneously compromise hundreds of organizations by targeting a single orchestration platform. Similar logic applies in NextG contexts. A sophisticated ransomware campaign might launch simultaneously across multiple domains: disrupting Transport VNFs managing QoS and tunneling (threat point 4) [51], degrading connectivity across metropolitan areas, while simultaneously locking MEC nodes (threat point 7) to paralyze latency-sensitive workloads such as telemedicine or AR/VR services [100].

Real-world telecom incidents show the plausibility of such campaigns. In 2022, Costa

Rica's government was crippled by Conti ransomware, which disrupted tax collection and customs systems [101]. In 2021, Irish health services were paralyzed by a ransomware attack, leading to canceled medical appointments and delayed emergency care [102]. While not limited to NextG infrastructure, these incidents illustrate the societal stakes when connectivity and cloud orchestration are held hostage. In a NextG context, ransomware could encrypt orchestration databases or slice management functions, preventing operators from controlling traffic flows or restoring workloads. The leverage comes not just from data encryption but from paralyzing service continuity across critical sectors. Even short-lived outages could ripple into public safety failures or financial market disruptions, making operators highly vulnerable to extortion.

Table 1.1: Layered Taxonomy of Emerging Threats in NextG Networks

Threat Category	Threat Vector	Target Components	Attack Surface	Representative Examples
Infrastructure & Physical Layer	Power outages, fiber cuts, sabotage, spectrum interference	RUs, DUs, transport links, MEC servers	(5), (7), (8) RAN and edge infra	Maui wildfires disrupting 5G infra; submarine cable sabotage in Europe (2022–23)
Virtualization & Network Functions	VNF compromise, hypervisor exploits, supply-chain injection	VNFs, NFV/SDN controllers, container orchestrators	(3), (4), (6) Core VNFs, data flows	Backdoored baseband VNF image; supply chain exploit in CI/CD for MEC
Data & Control Plane	Signaling storms, slice misconfiguration, API abuse	AMF, SMF, network orchestrators, slice managers	(2), (3), Cloud–Core signaling paths	Slice flooding via malicious UE; orchestrator API exploitation disabling policies
AI/Automation & Cognitive Layer	Model poisoning, adversarial examples, data drift	Traffic classifiers, anomaly detectors, ML-based resource schedulers	(3), (4), (6) Core measurement-driven VNFs	Adversarial routing in SDN; poisoning AI-based radio resource scheduling (2022 demo)
Cross-Domain Composite	Multi-vector, cascading failures, tenant interference	Service chains, inter-slice dependencies, inter-domain workflows	(1)–(8) Full NextG pipeline	Combined jamming + firmware exploit impacting smart grid and public safety slices

Chapter 2

Defining and Measuring Resilience

2.1 Understanding Network Resilience in 5G Networks

Network resilience in the context of 5G refers to the ability of next-generation communication systems to **prepare for, withstand, recover from, and adapt to disruptions**, particularly those induced by cyber threats, software misconfigurations, or cascading hardware failures. Unlike previous generations of networks, 5G introduces new complexities through *ultra-dense deployments, virtualization, network slicing, and multi-access edge computing (MEC)*, all of which necessitate a fundamental shift from classical robustness-focused designs to resilience-centered architectures. The dynamic, programmable, and distributed nature of 5G infrastructure demands mechanisms that can autonomously respond to failures, maintain service continuity across heterogeneous domains, and evolve in response to emerging threats.

Resilience vs. Robustness

Robustness in 5G networks typically entails the design of base stations (gNodeBs), core components, and control functions to *withstand predefined disruptions*. For example, a robust 5G base station might incorporate dual power sources, redundant transmission links, and hardened hardware to tolerate power failures or backhaul outages [103, 104, 105]. Robust control planes may include failover routes and standby network functions to handle predefined load spikes or equipment faults [106, 107]. However, robustness assumes *static failure models* and is primarily aimed at preserving normal operations under known or statistically likely stressors [108]. It does not fully account for intelligent, evolving, or stealthy threats, such as a novel zero-day exploit or an adversarial AI agent manipulating control messages.

In contrast, **resilience** in 5G embraces the reality that disruptions, especially those from *adaptive cyber attackers, supply-chain exploits, or unforeseen cross-slice dependencies*, cannot always be predicted [109, 110]. Resilience emphasizes the capacity of the network to detect anomalies, contain damage, restore functionality, and adapt over time [111]. For instance, if a rogue application in a network slice causes signaling storms that congest shared core functions (such as the Access and Mobility Management Function, AMF), a resilient architecture would leverage real-time measurement and AI-driven diagnostics to detect irregularities, automatically quarantine or rate-limit the faulty slice, and re-balance affected virtual network functions (VNFs) using orchestration platforms like O-RAN Service Management and Orchestration (SMO) or Kubernetes-based network function virtualization (NFV) managers [112, 113].

Example: Consider a 5G-enabled autonomous vehicle that relies on an ultra-reliable low-latency (URLLC) slice to communicate with roadside units and edge-hosted control services [114]. Suppose an adversary initiates a volumetric DDoS attack against the edge server hosting the URLLC slice’s control logic, thereby overwhelming the MEC node [115]. In a merely robust system, protective firewalls or ingress filtering might block known traffic sources or hardcoded IP addresses, but this would be insufficient if the attack employs distributed botnets with adaptive spoofing or uses legitimate service ports to evade detection.

In a resilient 5G network, the MEC controller would first detect abnormal traffic patterns through real-time flow analytics and alert the central orchestrator [116]. The affected URLLC slice would then be migrated to a neighboring edge site using live VNF migration [117], preserving critical communication for the autonomous vehicle. Non-essential services such as vehicle infotainment or measurement might be de-prioritized or throttled to ensure that bandwidth and compute resources remain available for safety-critical operations [118]. Simultaneously, the orchestration system could initiate a forensic analysis to trace the attack origin [119], update threat intelligence repositories [120], and generate new traffic rules to prevent recurrence [121]. As a result, the vehicle would maintain its control plane connection with negligible latency variation, preserving navigational safety and mission continuity.

This sequence of detection, containment, service continuity, and adaptive learning demonstrates how resilience in 5G systems exceeds classical robustness by enabling autonomous, context-aware, and mission-prioritized responses in the face of unpredictable disruptions.

2.1.1 Resilience vs. Fault-Tolerance and Reliability

5G networks employ **fault-tolerant components**, such as redundant core servers, geographically distributed gNodeBs, and standby VNFs, to ensure that localized faults, such as

hardware failures, software crashes, or power disruptions, do not result in a complete service outage [110]. These fault-tolerance mechanisms are typically designed to absorb failures within narrowly defined bounds and are often evaluated using **reliability metrics** such as “five nines” (99.999%) availability [122]. These metrics quantify the expected uptime of system components and provide assurances that under nominal operating conditions, critical functions will remain continuously available. This level of availability is particularly important for mission-critical services, including emergency communications [123], industrial automation [17], and autonomous vehicle coordination [124].

However, fault-tolerance in 5G systems is generally *pre-configured*, meaning that it depends on static redundancy models and assumptions about the nature of failures. For instance, a centralized 5G core deployment might rely on active-passive replication, where a primary node manages operations and a standby replica takes over in the event of failure [125]. While effective for isolated hardware issues or predictable load spikes, this model becomes inadequate in scenarios involving *multi-site failures*, such as those triggered by cascading software misconfigurations introduced through continuous integration/continuous deployment (CI/CD) pipelines [126]. Additionally, coordinated cyber-attacks targeting shared management APIs or exploiting overlooked inter-slice dependencies can propagate rapidly across control and user planes, rendering static redundancy models insufficient.

In contrast to static fault-tolerance, **resilience** in 5G networks encompasses a dynamic and adaptive approach to failure management that spans detection, containment, recovery, and adaptation. Resilience begins with real-time detection, wherein measurement data, such as slice-level latency, packet loss, and signaling rate, are continuously monitored by AI-powered analytics engines to uncover abnormal patterns that might signal imminent failures or security breaches [127]. Upon detection of an anomaly, containment mechanisms are activated. These may involve automated micro-segmentation of affected network functions [128], isolation of suspicious user equipment (UE), or even temporary quarantine of compromised network slices to prevent lateral threat propagation [117].

Once the immediate impact is contained, resilient 5G systems initiate recovery by real-locating services and workloads to unaffected parts of the infrastructure. This may include dynamic migration of VNFs to alternate MEC sites or centralized clouds using Kubernetes-based orchestration platforms, ensuring service continuity with minimal human intervention [129]. Finally, adaptation involves post-incident analysis, during which logs, alarms, and incident traces are analyzed to refine detection thresholds, update security policies, and optimize traffic engineering rules, thereby improving the network’s ability to cope with similar incidents in the future.

Consider, for example, a 5G-enabled smart manufacturing facility that relies on private

network slicing to support distinct workflows, such as robotic control, quality assurance, and remote monitoring [130]. Suppose a routine firmware update introduces unintended latency in a critical robotic controller operating on an URLLC slice. A fault-tolerant system might attempt to roll back the firmware if a snapshot is available, but this assumes that the error was detected quickly and that the backup mechanism is reliable. However, a truly resilient system would respond more intelligently. It could detect the latency anomaly through slice-level measurement [131], deprioritize or throttle non-essential background processes such as periodic sensor uploads, and reallocate compute resources to latency-sensitive control functions [132]. Furthermore, the system could autonomously reschedule a full maintenance window during a low-activity shift and use predictive analytics to validate that other slices or services would not be impacted by the update.

2.1.2 Multi-Dimensional and Dynamic Nature of 5G Resilience

Resilience in 5G networks is inherently **multi-dimensional**, operating across cyber, physical, organizational, and temporal layers. In the **cyber domain**, 5G networks rely heavily on software-defined components such as SDN controllers, VNFs, and MEC platforms. These components are vulnerable to zero-day exploits, misconfigurations, and privilege escalations, particularly in containerized or virtualized environments. A resilient system incorporates safeguards such as secure boot protocols, runtime attestation for trust verification, and continuous intrusion detection mechanisms that can flag anomalous behaviors across the service-based architecture (SBA) interfaces [133, 134].

In the **physical dimension**, threats such as localized power failures, electromagnetic interference, or RF jamming can compromise the availability of radio resources, especially in dense urban small cell deployments. Resilience strategies at this layer may involve power-aware load balancing, fallback to macro cells with acceptable latency penalties, or even the use of hybrid satellite-terrestrial links for emergency failover [135].

On the **human and organizational front**, operator errors, poor policy management, and inadequate role-based access controls continue to pose major risks to network reliability. To mitigate these, 5G management frameworks must integrate tools that enforce policy compliance, audit configuration changes, and provide automated rollback capabilities to revert to known good states when anomalies are detected [136, 137, 138, 139, 140].

Finally, resilience unfolds along the **temporal dimension**. It must account not only for immediate responses to incidents but also for long-term adaptations. Short-term responses may involve sub-second failover to alternate nodes or spectrum slices, while longer-term adaptation might include retraining AI models used for threat detection, refining orchestra-

tion workflows based on observed inefficiencies, or reallocating spectrum in anticipation of future usage patterns. These dimensions define the evolving and context-aware character of resilience in 5G systems, distinguishing it fundamentally from static fault-tolerance and traditional reliability engineering.

2.2 Types of Resilience Mechanisms in 5G Networks

Fig. 2.1 illustrates the dynamic interaction between adversarial attack vectors, system vulnerabilities, network state, and resilience mechanisms. An attacker exploits a vulnerability, driving the system into a perturbed state X_t , which in turn degrades the observable performance Y_t . Resilience mechanisms intervene at three stages: proactively by anticipating and mitigating vulnerabilities before they are exploited [141, 142], responsively by adapting to changes in the network state as attacks unfold [143, 144], and retrospectively by analyzing outcomes to recover performance and strengthen defenses [145, 146]. This tripartite structure highlights that resilience in 5G is not a static attribute, but a dynamic process that unfolds across time.

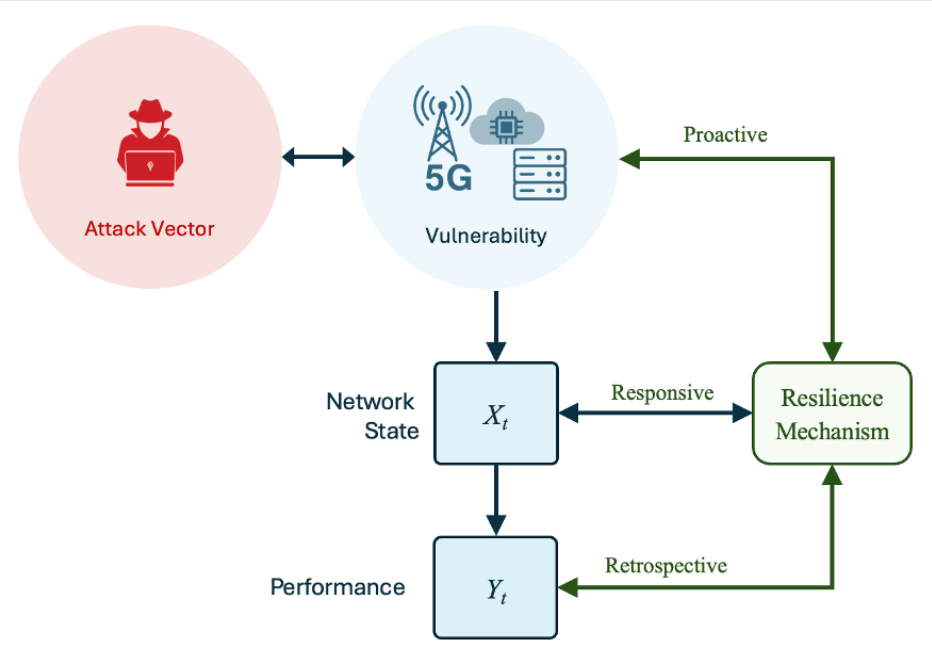


Figure 2.1: Interaction between attack vectors, vulnerabilities, network state, and resilience mechanisms. The diagram highlights three classes of defense: proactive (anticipating and hardening against vulnerabilities), responsive (adapting to the current network state X_t), and retrospective (learning from performance outcomes Y_t to improve future resilience).

2.2.1 Proactive Resilience

Proactive resilience corresponds to the upper branch of Fig. 2.1, where defenses act upstream of disruption, before an attack has an opportunity to take effect. The essence of this stage is to design solutions ahead of time that eliminate or neutralize vulnerabilities that are already known and prevent them from being exploited [147, 148, 149, 150]. In 5G, the importance of proactive resilience is amplified by the vast attack surface created through virtualization, multi-tenant network slicing, and reliance on heterogeneous third-party software and hardware components [78]. Because many of these risks stem from well-characterized classes of threats, such as unpatched software vulnerabilities, misconfigured APIs, or insecure interfaces, they can, in principle, be mitigated or prevented through deliberate architectural choices and rigorous security engineering.

In today’s deployments, proactive resilience is primarily realized through layered security hardening and standards-driven compliance. NFV on cloud-native platforms are hardened with continuous patching pipelines [151], container scanning [152], and automated vulnerability assessments [153]. Yet, patching cycles often lag behind zero-day exploit timelines, leaving windows of exposure. Similarly, API protection mechanisms such as TLS encryption and access tokens are widely deployed, but misconfiguration or insufficient key management still accounts for a significant portion of breaches. The SBA, while enabling agility and programmability, expands the number of interfaces to be secured, multiplying opportunities for attackers.

Operators currently mitigate these risks by enforcing security baselines mandated by 3GPP and ETSI standards, but adoption is uneven across vendors and regions. Multi-vendor interoperability, especially in O-RAN ecosystems, complicates proactive resilience: a gNodeB provided by one vendor may not seamlessly integrate with the security hardening protocols of a RAN Intelligent Controller (RIC) from another [21]. As a result, despite the availability of proactive mechanisms in principle, the operational reality is one of patchwork integration, where the weakest link may dictate the effective resilience of the system [154].

Examples of Proactive Measures. Examples of proactive measures span architectural design, access control, redundancy, and automated assurance. One foundational mechanism is logical segmentation through network slicing, which confines faults and attacks to the affected slice and prevents lateral propagation across services. For instance, a denial-of-service attack targeting an enhanced mobile broadband (eMBB) slice should not impair URLLC slices supporting critical functions such as telemedicine or industrial automation. Slice-aware resource allocation at the RAN and core further reinforces this isolation, ensuring that bandwidth, processing, and control signaling are insulated across tenants.

Another pillar of proactive resilience is *zero-trust authentication* [155, 156], implemented across the SBA. In this model, every API call and microservice interaction must be explicitly authenticated and authorized, eliminating implicit trust assumptions between network functions. Techniques include mutual TLS for service-to-service authentication, token-based access enforcement through OAuth 2.0 or JSON Web Tokens, and fine-grained policy enforcement points deployed within the Service Mesh. By enforcing least-privilege access across hundreds of microservices, zero-trust frameworks eliminate entire categories of lateral movement attacks that have historically compromised monolithic core networks [157].

Hardware and service redundancy provide a complementary layer of defense. Redundant gNodeBs, distributed UPFs (User Plane Functions), and geo-redundant data centers ensure that failures or targeted attacks against single nodes do not escalate into systemic outages. High-availability orchestration frameworks (e.g., Kubernetes with self-healing deployments) can restart failed network functions automatically, while distributed consensus mechanisms in control-plane clusters maintain service continuity even under node compromise. This approach shifts the system away from fragile single points of failure and toward fault-tolerant cloud-native operations.

In practice, major operators are also beginning to implement *continuous compliance pipelines*. These pipelines automatically test slice configurations, access policies, and orchestration templates against predefined security baselines before deployment [158]. For example, Infrastructure-as-Code templates are validated for adherence to 3GPP, ETSI, and operator-specific security policies, reducing the risk of misconfiguration-induced vulnerabilities. Emerging industry roadmaps go further by integrating AI-driven configuration management. Machine learning models trained on historical misconfigurations and threat intelligence can proactively detect anomalous parameter settings or deviations from expected baselines, flagging them before adversaries can exploit them. Such approaches are already being prototyped within the O-RAN Alliance’s security work groups, where AI-enabled RICs are envisioned to continuously monitor and enforce compliance [159].

Collectively, these measures illustrate how proactive resilience transforms knowledge of known vulnerabilities into preventive safeguards embedded at the infrastructure, orchestration, and policy layers. By confining failures, eliminating implicit trust, building redundancy, and automating compliance, proactive strategies reduce the effective attack surface of 5G/O-RAN systems long before disruptions materialize.

Limitations and the Need for Quantitative Modeling. Yet, anticipation alone cannot guarantee comprehensive protection. Novel attack vectors inevitably emerge, and vulnerabilities cannot be exhaustively enumerated in such a dynamic and evolving ecosystem. For

example, increasing reliance on supply chain components introduces risks that may bypass even rigorously designed controls [78]. Moreover, proactive measures may introduce their own trade-offs: extensive redundancy raises cost and energy consumption, while zero-trust architectures increase signaling overhead and complexity [81].

This limitation highlights the importance of quantitative modeling. Proactive resilience must be assessed not only in terms of whether safeguards exist but also in terms of how effectively they reduce risk relative to cost, complexity, and performance constraints. Developing models that capture preparedness as a measurable state, linking vulnerability coverage, attack likelihood, and resilience investment, provides a principled way to evaluate trade-offs. Such models can represent resilience readiness through metrics such as coverage ratios (fraction of known vulnerabilities addressed), protection depth (layers of defense applied), or risk-weighted benefit-cost indices. These foundations allow designers to move beyond heuristic defenses and toward systematically engineered architectures that balance efficiency with security, ensuring that 5G networks enter the operational environment with robust, verifiable resilience against known threats.

2.2.2 Responsive Resilience

Responsive resilience lies at the core of real-time adaptation. It is invoked when proactive defenses prove insufficient—either because adversaries exploit zero-day vulnerabilities that could not be anticipated in advance, or because known threats bypass preventive mechanisms due to configuration gaps or operational oversights. Once an attack perturbs the system state X_t , the resilience layer must react rapidly to prevent localized disruptions from escalating into systemic failures. In 5G networks, this requirement is amplified by URLLC applications, where even millisecond-scale delays can compromise safety-critical services such as autonomous vehicle coordination, industrial robot control, or remote telesurgery [110].

Today, responsive resilience is largely realized through a combination of monitoring platforms, orchestration systems, and security appliances integrated into the 5G/O-RAN stack. Most operators deploy Security Operations Centers (SOCs) with real-time analytics pipelines that ingest measurement from RAN, transport, and core domains [160]. Near-real-time RAN Intelligent Controllers (near-RT RICs) use xApps for anomaly detection and resource optimization, while non-real-time RICs (non-RT RICs) provide policy guidance. Cloud-native orchestration frameworks such as Kubernetes add auto-healing capabilities, restarting failed pods and redistributing workloads when anomalies are detected. However, these responses are often best-effort and heuristic rather than quantitatively guaranteed. For example, anomaly detection systems may raise alarms too late to prevent service-level

agreement (SLA) violations, and current orchestration policies may not differentiate sufficiently between mission-critical and best-effort slices. This leaves a gap between the vision of responsive resilience and the operational practices that dominate current deployments.

Examples of Responsive Measures. Responsive resilience mechanisms act directly on the evolving network state through dynamic orchestration, anomaly detection, fault isolation, and controlled degradation. Their purpose is not necessarily to fully neutralize the attack, but to contain its impact, preserve continuity of essential services, and maintain graceful degradation rather than abrupt collapse.

Dynamic orchestration allows workloads to be reallocated in response to localized disruptions [161, 162]. For instance, if an MEC node is compromised, overloaded, or disconnected, latency-tolerant workloads (e.g., content caching, video streaming) can be migrated to centralized cloud resources. This preserves edge capacity for URLLC applications that cannot tolerate disruption. Cloud-native platforms support such failovers through container migration, traffic redirection, and dynamic slice reconfiguration. However, in the status quo, many operators still rely on static orchestration rules, limiting the speed and efficiency of such migrations.

Anomaly detection serves as the first line of defense against stealthy or fast-spreading attacks [75, 100]. Responsive anomaly detection modules analyze signaling patterns, traffic volumes, and device behaviors in real time to detect events such as signaling storms, botnet-driven DDoS, or misbehaving IoT devices. For example, if a surge of attach requests destabilizes control-plane functions, anomaly detection can trigger throttling or quarantining of suspicious traffic sources. In practice, anomaly detection is typically implemented via rule-based intrusion detection systems (IDS) and threshold monitors [134, 163, 164, 165]. While these systems are widely deployed, they often suffer from high false positive rates or limited ability to adapt to evolving adversarial strategies. Research prototypes are increasingly exploring machine-learning-based anomaly detectors, but deployment at scale remains limited due to explainability and trust concerns.

Fault isolation mechanisms explicitly contain failures or attacks by segmenting affected subsystems [166]. For example, if a slice orchestration component exhibits abnormal behavior, responsive mechanisms can isolate that slice to prevent control-plane instability across other tenants. Similarly, service mesh firewalls can block compromised microservices from interacting with neighboring functions. Today, such isolation is often manual or policy-driven, with limited automation, which delays the response window and risks cascading failures before isolation takes effect.

Controlled degradation ensures continuity of essential services even when full performance

cannot be maintained [167]. For instance, in the event of resource exhaustion, responsive policies may prioritize URLLC slices by shedding non-critical eMBB traffic, preserving life-critical applications while gracefully degrading best-effort services. Current operator practices include basic traffic shaping and prioritization [168], but fine-grained and adaptive degradation strategies, such as dynamically adjusting quality-of-experience targets or selectively offloading workloads, are still in their early stages of adoption.

Need for Quantitative Guarantees. The effectiveness of responsive resilience hinges on the ability to provide quantitative guarantees [110]. Critical questions include: How quickly must a control action be executed to satisfy stringent service-level agreements? What level of performance loss can be tolerated in a degraded mode before cascading failures occur across interdependent services? How can false positives in anomaly detection be balanced against the risk of delayed containment? Addressing these challenges requires rigorous mathematical formulations that link adversarial actions, state transitions, and control responses. By embedding responsiveness into models of stochastic dynamics, hybrid control, and adversarial interaction, we can move from heuristic responses to provably effective real-time resilience mechanisms. This is particularly vital in 5G/O-RAN, where the margin for error is narrow and disruptions in milliseconds can ripple across safety-critical ecosystems.

2.2.3 Retrospective Resilience

Retrospective resilience closes the loop by addressing the residual consequences of disruptions that could not be fully prevented or neutralized in earlier stages. It begins once performance outcomes Y_t have already been degraded, and its primary function is to transform these outcomes into actionable knowledge for future preparedness [169]. Unlike proactive and responsive measures, which focus on anticipation and real-time adaptation, retrospective resilience is inherently reflective. It recognizes that not all failures can be foreseen or contained, and therefore emphasizes recovery, learning, and long-term adaptation.

In today’s networks, retrospective resilience is implemented through post-incident response frameworks that combine operational, organizational, and financial tools. Telecom operators typically maintain Security Operations Centers (SOCs) and Network Operations Centers (NOCs) that conduct forensic analysis after a breach or outage [170]. For example, when a slice outage occurs due to a misconfigured VNF or API abuse, logs and measurement are gathered to reconstruct the sequence of events. Recovery is often achieved through restoring from snapshots or redeploying cloud-native functions using orchestration tools such as Kubernetes. Vulnerabilities discovered in the aftermath are patched in subsequent software updates, though patch latency remains a critical weakness, as operators must test

updates across heterogeneous vendor equipment before deployment. At the organizational level, retrospective resilience often relies on financial instruments such as cyber insurance and compensation schemes for SLA violations. While these mechanisms are widespread, they remain fragmented, with lessons from one incident not always systematically incorporated into future architectures.

Examples of Retrospective Measures. Retrospective mechanisms span several layers of response and adaptation:

Forensic investigations reconstruct the timeline of a disruption, identifying the initial vector, propagation path, and defensive breakdowns. For example, in the wake of a signaling storm that crashed a control-plane VNF, forensic analysis might reveal abnormal registration requests from compromised IoT devices, alongside misconfigured throttling policies [119]. These insights not only resolve attribution but also provide feedback to refine anomaly detection thresholds and slice isolation rules.

Recovery and restoration procedures aim to bring services back online as quickly as possible, even if at reduced capacity [171]. In cloud-native 5G, this typically involves redeploying containerized VNFs, restoring MEC workloads from backups, or shifting services to unaffected geographic regions. In practice, operators often employ automated “runbooks” integrated with orchestration frameworks, though their coverage is incomplete. Mission-critical URLLC applications, such as telesurgery or autonomous vehicle platooning, highlight the limits of retrospective recovery: workloads may be restored, but degraded latency or jitter performance may render the restored service unsafe for real-time use.

Post-incident patch development addresses the vulnerabilities exploited in the disruption [19]. In the status quo, patches are released by vendors on varying timelines and must be tested across diverse hardware and virtual environments before rollout. This lag creates recurring exposure windows. Some operators have begun integrating retrospective vulnerability discovery directly into CI/CD pipelines, where measurement and forensic artifacts automatically trigger patch generation, regression testing, and staged rollout across slices.

Financial and organizational mechanisms mitigate the long-term impact of disruptions. SLA violation penalties provide immediate compensation to customers when performance falls below contractual thresholds. Cyber insurance policies cover broader losses, such as reputational damage or large-scale service outages [172, 173, 174, 175, 176]. Although these mechanisms are widely adopted, they are often reactive and do not inherently improve technical resilience unless coupled with systematic feedback loops that invest the proceeds of such penalties into resilience upgrades.

Limits of Recovery. A defining feature of retrospective resilience is that recovery may not always be complete. Some disruptions result in irrecoverable data loss, long-lasting service degradation, or systemic architectural weaknesses. For example, a ransomware attack on a MEC cluster may allow operators to restore workloads from backups, but applications requiring strict latency guarantees may still be rendered unusable due to degraded performance. Similarly, a compromise of core orchestration software may undermine trust in future updates, necessitating costly revalidation of the entire stack. Retrospective resilience therefore acknowledges these limits and emphasizes not only minimizing immediate damage but also capturing lessons to prevent recurrence.

Toward Quantitative Retrospective Resilience. If left purely qualitative, retrospective resilience risks becoming anecdotal, i.e., dependent on operator intuition rather than embedded in formal design processes. What is required is a quantitative framework that measures how much knowledge is gained from each incident, how effectively this knowledge reduces the probability or severity of future risks, and how quickly resilience mechanisms adapt across successive disruptions. Candidate metrics include:

- *Knowledge gain ratio*: fraction of incident root causes for which new defensive rules, patches, or detection signatures are generated.
- *Patch latency*: average delay between vulnerability discovery and deployment of effective remediation across all affected nodes.
- *Learning curve slope*: rate at which incident recurrence frequency declines across successive disruptions.

By formalizing retrospective mechanisms such as forensics, patching, recovery, and insurance, networks can convert disruption into an opportunity for improvement. Every incident becomes a driver for more robust architectures, tighter integration with CI/CD pipelines, and adaptive security policies. In this way, retrospective resilience ensures that 5G/O-RAN and cloud-native infrastructures evolve dynamically, continuously strengthening their preparedness against an ever-changing adversarial landscape.

2.2.4 Integration of Proactive, Responsive, and Retrospective Mechanisms

The resilience of 5G networks cannot be secured by any single class of mechanism in isolation. Instead, it depends on the integration of proactive, responsive, and retrospective approaches

into a coherent lifecycle [177]. This integration is essential because the threat landscape is characterized not only by well-known vulnerabilities that can be prevented, but also by unknown risks that cannot be anticipated in advance, and by adversarial actions that are difficult to mitigate fully in real time.

Proactive mechanisms form the first line of defense by hardening the system against known threats. In 5G, measures such as network slicing, zero-trust authentication, redundancy in RAN deployments, and rigorous patch management reduce the probability that an attacker can gain a foothold. If proactive mechanisms were perfect, eliminating every vulnerability and anticipating every possible exploit, then responsive and retrospective layers would be unnecessary. In practice, however, this ideal is unattainable. The sheer complexity of cloud-native architectures, the continual discovery of zero-day vulnerabilities, and the sophistication of adaptive adversaries ensure that some threats will bypass even the most carefully engineered proactive safeguards.

Responsive mechanisms serve as the safety net once proactive measures are breached. They detect anomalies, isolate faults, and contain unfolding attacks in real time. For example, when a misconfigured API in the 5G Core is exploited to escalate privileges, responsive defenses, such as anomaly detection and adaptive access control, can contain the intruder before lateral movement compromises multiple slices. Similarly, in the event of jamming attacks on a RAN fronthaul, responsive orchestration can reroute traffic to alternative links or degrade non-essential services to preserve mission-critical URLLC. However, relying too heavily on responsiveness is costly: it requires continuous monitoring, high-speed analytics, and dynamic reallocation of resources under strict latency constraints, which consume substantial computational and operational overhead. Moreover, some attacks, such as stealthy data exfiltration or firmware-level compromises, may not be easily neutralized online.

Retrospective mechanisms address residual consequences that proactive and responsive measures cannot fully prevent. They enable recovery, forensic investigation, patch development, and post-incident learning. For instance, if ransomware encrypts MEC workloads despite anomaly detection, retrospective recovery procedures may restore services from backups while forensic analysis identifies the exploit vector. Post-incident patching then prevents recurrence in future releases. Retrospective mechanisms also include financial and organizational tools such as cyber insurance to manage long-term impacts. However, relying primarily on retrospective resilience is also costly and inefficient, as it accepts disruption as inevitable and shifts the burden to recovery, sometimes partial and incomplete, rather than prevention or containment.

The interdependencies among these mechanisms reveal the trade-offs in designing resilient 5G networks. Strong proactive defenses reduce the frequency of incidents, lowering the

reliance on costly responsive and retrospective actions. Robust responsive mechanisms limit the severity of incidents that bypass proactive safeguards, reducing the scale of retrospective recovery needed. Retrospective resilience ensures that every disruption generates knowledge that improves both proactive preparation and responsive agility in the future. The balance among these mechanisms depends on the threat environment: for well-characterized risks such as DDoS attacks, proactive measures like traffic filtering and redundant paths are cost-effective. For unpredictable or rapidly evolving threats such as AI-driven adversarial manipulation of MEC scheduling, responsive and retrospective layers become indispensable.

In practice, no single mechanism suffices. Proactive defenses can never be perfect, and responsiveness and retrospection are too costly to serve as the sole basis of resilience. It is only through their integration, including anticipating, adapting, and learning, that 5G networks can minimize the overall impact of disruptions while optimizing the trade-offs between cost, complexity, and risk tolerance [178, 179, 180, 181, 182].

2.2.5 Quantitative Approach to Resilience Design

The three stages depicted in Fig. 2.1 form a resilience lifecycle that is both dynamic and recursive. Proactive mechanisms operate on the timescale of anticipation, reducing the probability that known threats will materialize by hardening the system in advance. Responsive mechanisms operate on the timescale of real-time adaptation, intervening in the system dynamics as adversarial activity perturbs the network state X_t . Retrospective mechanisms extend the horizon further by converting performance outcomes Y_t into actionable insights that strengthen future preparedness. Although conceptually distinct, these stages are deeply interdependent. Proactive defenses must be guided by knowledge distilled from retrospective analysis, and responsive strategies must be designed within the constraints created by proactive design choices while also benefiting from retrospective feedback. Resilience is therefore not a static collection of safeguards but a co-designed, adaptive process that evolves with the system it protects [177, 183].

This recursive and interdependent structure underscores the urgent need for quantitative modeling and analysis. Qualitative descriptions alone cannot capture the complexity of 5G networks, where adversaries adapt strategically, interdependencies span multiple domains, and service requirements are safety-critical. Quantitative frameworks are needed to characterize how threats propagate through vulnerabilities, how mechanisms interact across timescales, and how resource trade-offs shape achievable resilience [184]. For instance, perfecting proactive defenses would, in theory, reduce reliance on responsive and retrospective mechanisms, but this comes at escalating costs that may be impractical. Conversely, relying

too heavily on responsiveness or recovery places a high burden on monitoring, orchestration, and post-incident remediation. The optimal balance depends on the type of threat, its likelihood, and the cost-effectiveness of each layer of defense. A rigorous analytical foundation is required to formalize and solve these trade-offs.

We will present foundations based on control theory, game theory, learning theory, and network theory to address this challenge [169]. Control theory provides models of the temporal dynamics of network states and feedback mechanisms that stabilize performance under perturbations [107, 185, 186, 187]. Game theory captures the strategic interplay between attackers and defenders, enabling the study of equilibria, incentives, and adversarial adaptation [88, 188, 150, 189]. Learning theory supports adaptive mechanisms that improve with experience, extracting patterns from retrospective data to refine proactive planning and responsive detection [189, 190, 178, 191, 192, 193]. Network theory offers structural insights into interdependencies, cascading effects, and systemic vulnerabilities in interconnected large-scale infrastructures [194, 195, 196, 197, 198].

To build truly resilient 5G networks, these foundations must be synthesized into principled models that represent resilience as a lifecycle process rather than a static property. Such models must capture adversarial interactions as stochastic or dynamic games, quantify performance trade-offs among security, latency, and availability, and embed learning modules that evolve with the threat landscape. By moving beyond ad hoc defenses and embracing mathematically grounded optimization frameworks, resilience can be designed, analyzed, and assured as a first-class property of next-generation communication systems.

2.3 Metrics and Evaluation

Resilience in next-generation networks is a multifaceted attribute that captures a system's ability to withstand, recover from, and adapt to adverse conditions. Unlike classical notions of reliability or robustness, which focus on steady-state operation or tolerance to bounded perturbations, resilience emphasizes the *entire lifecycle* of a disruptive event: anticipation, real-time response, and long-term recovery. Rigorous quantification of resilience is crucial for ensuring operational continuity, guiding architectural decisions, benchmarking infrastructure deployments, and informing investment strategies [199, 200].

Fig. 2.2 illustrates this lifecycle. During prevention (t_0-t_1), the system sustains nominal performance despite emerging stressors. At t_2 , a disruption triggers performance degradation, reaching a maximum shortfall M . Responsive mechanisms act during t_2-t_3 to limit both the depth and duration of this decline. Recovery begins at t_4 , where performance stabilizes, often with a residual deficit D if the system cannot fully return to baseline. These

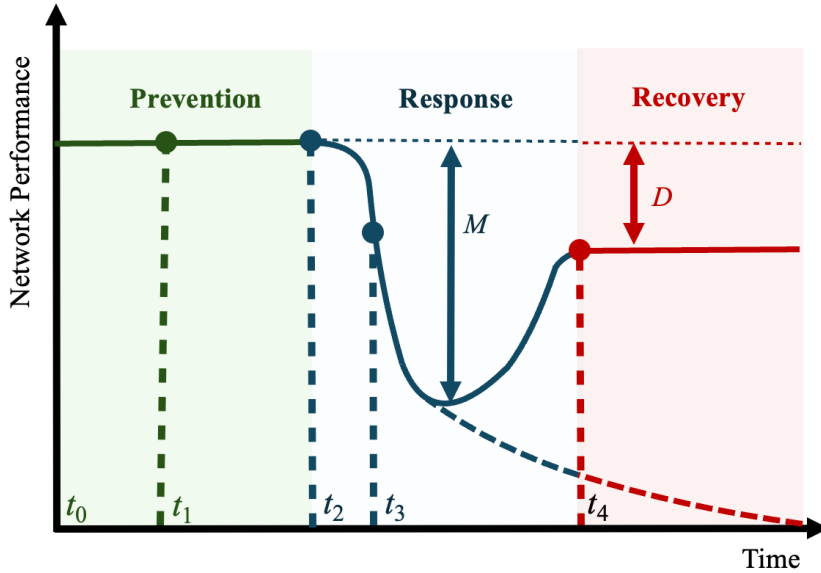


Figure 2.2: Illustration of network resilience across three phases: prevention, response, and recovery. The vertical axis represents network performance, and the horizontal axis represents time. Preventive mechanisms delay or avoid the onset of disruption (t_0-t_1). Responsive mechanisms act during the disruption window (t_2-t_3), limiting the maximum performance degradation M . Recovery mechanisms operate after t_4 , aiming to restore performance, though often with a residual deficit D . The shaded regions emphasize the temporal domains of each class of resilience mechanism.

temporal markers anchor the formal definitions and metrics developed below [201].

2.3.1 Discrete-Time Formalism for Resilience

To formalize resilience, we adopt a discrete-time representation that is well suited for cyber-physical networks, where events are logged, monitored, and acted upon at discrete epochs. Let the system evolve at times $t = 0, 1, \dots, T$, where each step represents a measurable operational interval (e.g., seconds, control cycles, or monitoring windows). At each t , the system is characterized by a performance level Q_t , which is bounded between zero and a nominal maximum Q_{\max} . The baseline Q_{\max} corresponds to ideal operating conditions such as target throughput, latency compliance, or service-level guarantees.

A disruptive event is defined by two critical instants. The failure onset occurs at t_f (denoted t_2 in Fig. 2.2), marking the departure from nominal behavior. The recovery time is t_r (t_4 in the figure), when the system stabilizes in a recovered or steady state, which may or may not fully achieve Q_{\max} . Between t_f and t_r , the trajectory $\{Q_t\}$ reflects both the severity of the disruptive impact and the efficacy of the system's detection, mitigation, and recovery mechanisms.

The cumulative resilience loss is then defined as

$$L = \sum_{t=t_f}^{t_r} \left(1 - \frac{Q_t}{Q_{\max}} \right), \quad (2.1)$$

which integrates the depth and duration of degradation into a single measure, corresponding geometrically to the shaded area between the degraded trajectory and the baseline in Fig. 2.2. Systems with rapid detection and efficient recovery achieve smaller L , whereas systems with sluggish or incomplete responses accumulate larger resilience loss.

2.3.2 General Temporal Metrics

While L in (2.1) captures the overall severity of a disruption, more granular temporal metrics provide insights into specific phases of the disruption-recovery cycle shown in Fig. 2.2. *Down-time* D_k quantifies the period during which performance falls below an acceptable service threshold δQ_{\max} for the k -th disruptive event:

$$D_k = \sum_{t=t_f}^{t_r} \mathbb{I}(Q_t < \delta Q_{\max}), \quad (2.2)$$

where $\mathbb{I}(\cdot)$ is the indicator function. This corresponds to the interval t_2-t_4 in Fig. 2.2, where user-perceived quality of service requirements are not met.

Mean Time to Failure (MTTF) measures the average length of normal operation between disruptive events, corresponding to the prevention or steady phases (t_0-t_1). Large MTTF indicates rare disruptions and effective preventive controls, whereas small MTTF indicates recurrent or persistent threats.

Mean Time to Detect (MTTD) captures the responsiveness of monitoring mechanisms by measuring the delay between the true failure onset t_f (t_2) and the detection instant t_d :

$$\text{MTTD}_k = t_d - t_f, \quad (2.3)$$

which measures the critical “blind window” during which the system is already degraded but not yet alerted.

Mean Time to Recovery (MTTR) reflects the speed of corrective actions by measuring the interval between detection and recovery:

$$\text{MTTR}_k = t_r - t_d, \quad (2.4)$$

corresponding in Fig. 2.2 to the trajectory from detection at t_d to stabilization at t_4 .

Two additional structural metrics capture the magnitude of degradation. The *maximum performance drop*,

$$M = \max_{t \in [t_f, t_r]} (Q_{\max} - Q_t), \quad (2.5)$$

represents the most severe instantaneous degradation (vertical arrow M). The *residual deficit*,

$$D = Q_{\max} - Q_{t_r}, \quad (2.6)$$

represents the long-term shortfall that persists after recovery (vertical arrow D). Together, M and D distinguish between transient acute shocks (large M but small D) and lasting structural damage (nonzero D).

2.3.3 Domain-Specific Metrics

While general temporal metrics characterize resilience broadly, domain-specific indicators capture properties critical for 5G/O-RAN and cloud-native contexts. These metrics extend the logic of Fig. 2.2 by linking performance deviations Q_t to service-level and architectural requirements such as slice isolation, latency guarantees, elastic scaling, and availability. By tailoring resilience assessment to these dimensions, operators can align quantitative measurements with concrete service-level objectives (SLOs) and SLAs.

Slice Isolation Index. In network slicing, multiple tenants and services coexist on the same physical infrastructure, relying on logical isolation to ensure that one slice’s disruption does not cascade into others. This makes isolation a cornerstone of resilience in multi-tenant environments. The *Slice Isolation Index* (SII) measures the extent to which a disruption in slice i affects other slices $j \neq i$:

$$\text{SII}_i = 1 - \frac{\sum_{j \neq i} \max_{t \in [t_f, t_r]} \left(1 - \frac{Q_t^{(j)}}{Q_{\max}^{(j)}}\right)}{(N - 1)}. \quad (2.7)$$

High values of SII_i (close to 1) indicate strong isolation, where slice i ’s failure is contained. Low values suggest cross-slice propagation, which undermines multi-tenancy guarantees and may lead to cascading failures across RAN, core, or MEC domains.

Latency Compliance. URLLC applications, such as autonomous driving or industrial control, impose stringent delay requirements. Even brief violations can cause safety or operational hazards. Let L_t denote the observed latency at time t , and L_{\max} the contractual

bound. The *Latency Compliance* is defined as

$$\Lambda = \frac{1}{T} \sum_{t=0}^T \mathbb{I}(L_t \leq L_{\max}), \quad (2.8)$$

representing the fraction of epochs in which latency remains acceptable. In Fig. 2.2, this corresponds to epochs where Q_t is above the latency threshold. A high Λ value reflects robust scheduling, congestion control, and RIC policies that maintain end-to-end delay guarantees even during disruptions.

SLA Violation Rate. SLAs in 5G cover multiple KPIs, including throughput, jitter, and reliability, and failing to meet them directly impacts operator revenue through penalties or reputational loss. Let Q_{SLA} denote the minimum contractual guarantee. The *SLA Violation Rate* is given by

$$V_{\text{SLA}} = \frac{1}{T} \sum_{t=0}^T \mathbb{I}(Q_t < Q_{\text{SLA}}), \quad (2.9)$$

which measures the proportion of time contractual guarantees are not satisfied. This metric is closely related to the shaded degradation region in Fig. 2.2. High violation rates signal systemic vulnerabilities in orchestration, scaling, or RAN scheduling that prevent the system from meeting promised service guarantees.

Auto-Scaling Efficiency. Cloud-native platforms rely heavily on elasticity: scaling microservices, MEC resources, or RAN functions up or down in response to load variations or disruptive events. Poor scaling may either over-provision (wasting resources) or under-provision (failing to recover quickly). Let R_t denote the actual resources allocated at time t , and R_t^* the optimal allocation that minimizes degradation. The *Auto-Scaling Efficiency* is defined as

$$\eta_{\text{scale}} = 1 - \frac{\sum_{t=t_f}^{t_r} |R_t - R_t^*|}{\sum_{t=t_f}^{t_r} R_t^*}. \quad (2.10)$$

High η_{scale} indicates close tracking of resource demand and fast adaptation to failures or adversarial load shifts. Low values indicate sluggish scaling, which prolongs recovery and increases both resilience loss L and MTTR.

Availability. Traditional availability metrics measure uptime, but in resilient systems, availability must account for degraded yet still functional states. Let Q_{avail} be the minimum performance threshold required for safe or acceptable operation (e.g., minimum data rate

for emergency services). The *Availability* metric is

$$A = \frac{1}{T} \sum_{t=0}^T \mathbb{I}(Q_t \geq Q_{\text{avail}}). \quad (2.11)$$

This metric synthesizes both the prevention phase (t_0 – t_1) and the post-recovery plateau ($t > t_4$), providing a global view of how often the system remains usable. In O-RAN settings, high availability reflects effective coordination between RIC policies, SMO functions, and cloud-native orchestration even under compound disruptions.

Together, these domain-specific metrics—slice isolation, latency compliance, SLA violation rate, auto-scaling efficiency, and availability—provide a multidimensional lens on resilience. They not only quantify recovery speed and degradation magnitude but also address whether the system continues to uphold the economic and service commitments that define 5G/O-RAN deployments. In practice, operators must track these indicators jointly to balance technical robustness with business viability.

2.3.4 Composite and Cost-Aware Metrics

No single metric can fully capture the multifaceted nature of resilience. For example, a system may recover quickly (low MTTR) but experience frequent failures (low MTTF), or maintain high availability while sustaining a large residual deficit D . Similarly, minimizing downtime D_k may come at the expense of larger resource expenditures or aggressive failover mechanisms. This tradeoff motivates the design of composite indices that aggregate multiple resilience indicators into a single figure of merit.

A general formulation is a weighted combination:

$$R_{\text{composite}} = \sum_{i=1}^n w_i \cdot M_i, \quad (2.12)$$

where M_i are normalized resilience metrics (e.g., L , MTTR, MTTD, availability, latency compliance), and w_i are application- or domain-specific weights satisfying $\sum_i w_i = 1$. The weights allow tailoring the composite measure to heterogeneous service requirements. For URLLC slices, larger weights may be assigned to latency compliance and SLA violation rate. For eMBB, throughput and availability may dominate. For massive machine-type communications (mMTC), long-term availability and energy efficiency could be emphasized.

Composite indices are particularly useful for comparing candidate architectures or resiliency mechanisms (e.g., static redundancy vs. dynamic orchestration). By compressing

multiple metrics into a single index, $R_{\text{composite}}$ enables benchmarking and ranking of system designs under consistent weighting schemes. However, the choice of weights w_i must be transparent, as they encode implicit priorities and tradeoffs that may differ across operators, regulators, and end-users.

Cost-Aware Resilience. While L in (2.1) measures total performance degradation, it does not account for heterogeneous costs associated with different degradation scenarios. A more realistic measure attaches monetary, operational, or societal costs to each unit of performance loss:

$$C_{\text{resilience}} = \sum_{t=t_f}^{t_r} C_t \cdot \left(1 - \frac{Q_t}{Q_{\max}}\right), \quad (2.13)$$

where C_t is a time-varying cost coefficient. In Fig. 2.2, this corresponds to weighting the shaded degradation area by its impact severity. For example:

- In URLLC telemedicine, C_t may represent risk-adjusted costs of violating latency constraints, reflecting potential harm to patients.
- In cloud services, C_t can encode SLA penalty charges or reputational costs for downtime.
- In industrial automation, C_t may represent opportunity costs due to halted production lines.

Thus, $C_{\text{resilience}}$ generalizes resilience loss into an economically meaningful quantity, making it possible to compare strategies not only on technical but also financial grounds. This is critical for operators deciding between competing resilience mechanisms that differ in cost structure (e.g., proactive redundancy vs. on-demand recovery).

2.3.5 Integration with Control and Learning Frameworks

The discrete-time formulation of resilience metrics makes them naturally compatible with control-theoretic and learning-based frameworks. In modern networks, system performance evolves over time as a consequence of both endogenous policies and exogenous disturbances. In this setting, Q_t becomes part of the observable system state, while proactive, responsive, and recovery actions influence its trajectory across disruption and recovery phases. By embedding resilience metrics such as L , MTTR, or cost-aware loss $C_{\text{resilience}}$ into optimization objectives or operational constraints, one can obtain principled designs of resilience-enhancing mechanisms that go beyond ad hoc heuristics. This approach provides a systematic bridge

between theoretical metrics and the concrete policies executed by controllers, orchestrators, and learning agents in 5G/O-RAN and cloud-native infrastructures.

Control-Theoretic Integration. Control theory provides a natural language for modeling resilience as a closed-loop property. In model predictive control (MPC), the controller predicts future trajectories of Q_t under possible failure scenarios and selects actions that minimize a cumulative cost function [202, 203, 204, 205]. Minimizing resilience loss L in (2.1) can be cast directly as such a cost minimization problem, with additional temporal constraints to ensure recovery within a specified MTTR. Robust control formulations extend this approach by explicitly accounting for uncertainty and adversarial disturbances, guaranteeing that Q_t remains above operational thresholds even in worst-case conditions. Hybrid control models [206, 207], combining continuous-time traffic dynamics (e.g., queue evolution, SINR variability) with discrete failure events (e.g., gNodeB outage, backhaul disconnection), are particularly relevant in O-RAN, where abrupt failures interact with continuous flows of data and control traffic. In such models, resilience metrics serve both as performance objectives and safety constraints, guiding the system toward guaranteed levels of service continuity.

Reinforcement Learning Integration. Resilience can also be optimized through reinforcement learning (RL), where metrics play the role of reward signals [208, 209]. An RL agent, observing network states $\{Q_t\}$ and exogenous inputs (e.g., traffic load, alarms, or anomaly scores), can be trained to select actions such as spectrum reallocation, slice migration, or MEC resource scaling. For instance, during the t_2-t_3 response window in Fig. 2.2, the agent may learn scaling policies that minimize MTTR or reduce cost-aware loss $C_{\text{resilience}}$ in (2.13). Multi-agent RL extends this formulation to settings where distributed controllers (e.g., near-RT and non-RT RICs, or federated operators) must coordinate decisions while optimizing resilience jointly. By aligning resilience metrics with RL reward design, networks can autonomously discover recovery strategies that adapt to evolving adversarial tactics and traffic dynamics.

Game-Theoretic Integration. In adversarial environments, resilience is inherently strategic: attackers attempt to maximize disruption, while defenders attempt to minimize it. Game-theoretic models provide a principled way to capture these interactions. Metrics such as maximum performance drop M in (2.5) and residual deficit D in (2.6) can serve directly as attacker and defender payoffs. Zero-sum games formalize the tradeoff: an attacker's gain (larger M or D) is precisely the defender's loss. More nuanced formulations (e.g., Stackelberg or Bayesian games) capture asymmetric information, where the attacker hides its type

or timing [210, 211, 181]. Equilibrium analysis then identifies achievable resilience levels under rational strategies. Such models motivate the design of adaptive defenses, such as moving-target configurations [189], deception strategies [212, 213, 214], and slice isolation policies [215, 216, 217], all of which can be evaluated through the lens of resilience metrics.

Adaptive Resilience. The ultimate goal is to move beyond passive measurement toward *adaptive resilience*. By embedding resilience metrics into control and learning objectives, networks gain the ability not only to quantify their performance after a disruption but also to evolve dynamically in response to repeated adversarial encounters. Adaptive resilience entails learning from past disruptions, refining recovery strategies, and reconfiguring policies to preempt future attacks or failures. In 5G/O-RAN and cloud-native architectures, this manifests as self-optimizing loops where RIC controllers, orchestration layers, and learning agents use resilience metrics to continuously update their policies. Thus, resilience becomes both a measurable property and an explicit control objective, shaping the architecture of next-generation communication systems toward self-healing, self-adaptive, and economically sustainable operation.

Chapter 3

Theoretic Foundations for Resilient Network Management

The preceding chapters established the evolving threat landscape of next-generation networks and introduced resilience as a multidimensional property that extends beyond fault-tolerance and reliability [147, 218]. We also explored proactive, responsive, and retrospective mechanisms and presented metrics to quantify resilience over time. Building on this groundwork, the next logical step is to develop rigorous theoretical foundations that allow resilience to be systematically modeled, analyzed, and engineered. This chapter presents the core mathematical and conceptual underpinnings of resilient network management. Four complementary perspectives: control theory, dynamic game theory, learning theory, and network theory, form the pillars of this foundation [150, 219, 197]. From a control-theoretic perspective, resilience is framed as an optimal performance regulation problem under adversarial perturbations, leveraging runtime monitoring, safe fallback mechanisms, and moving-target defense to ensure effective response to adversarial impacts. Game theory introduces the strategic dimension, modeling the interplay between adaptive attackers and defenders as dynamic games where equilibria encode resilience properties. Learning theory provides mechanisms for adaptation, enabling networks to evolve defenses based on feedback, reinforcement, and predictive inference. Finally, network theory captures the structural interdependencies and cascading vulnerabilities inherent in large-scale infrastructures, offering insights into systemic robustness and fragility. Together, these frameworks provide not only explanatory power but also actionable methodologies for designing and ensuring resilience. By integrating feedback control, strategic reasoning, adaptive learning, and structural analysis, this chapter lays the foundation for principled, mathematically grounded approaches to resilient network management, approaches that can scale with the complexity and adversarial dynamics of NextG environments.

3.1 Control-Theoretic Foundation

Control theory provides a foundational lens for understanding and managing resilience because it formalizes the dynamic, multi-stage evolution of network states under both adversarial attacks and natural disruptions. Unlike static reliability models, control theory explicitly accounts for feedback, adaptation, and time-varying uncertainties, making it ideally suited to capture the continuous interplay between system dynamics and external perturbations [220, 221]. In networked cyber-physical systems, disruptions emerge from two principal sources. On the one hand, adversarial threats come from intelligent and adaptive opponents that look for vulnerabilities and adjust their strategies in response to defenses. However, natural failures such as hardware crashes, fiber cuts, and power outages also degrade performance and can cascade across interdependent infrastructures. A resilient network must therefore regulate its performance in the presence of both strategic and stochastic disturbances [222, 223]. Next-generation networks (5G and beyond) further challenge this challenge. The adoption of SDN, NFV, O-RAN, and MEC introduces programmability and flexibility, but also enlarges the attack surface and creates tighter coupling between components [224, 78]. These architectures transform resilience from a static design problem into a real-time control problem, where monitoring, decision-making, and actuation must occur continuously to preserve service continuity. As a foundation, control theory contributes three essential principles to resilience engineering. First, it provides stability analysis, ensuring that, despite shocks, malicious or accidental, the system returns to an acceptable operating region. Second, it offers feedback mechanisms, allowing the network to sense deviations, adapt policies, and prevent small perturbations from escalating into systemic failures. Third, it enables the design of robust and adaptive controllers, which anticipate uncertainties and adjust to evolving environments without requiring complete foresight of every possible disruption.

3.1.1 System Model

Resilience requires reasoning about how a network evolves under normal operation and disruption. A control-theoretic abstraction provides this capability by capturing the *system state*, the *defender’s actions*, the *uncertainties* introduced by adversaries and the environment, and the *disruption state* that signals mode switches in the network. We model the

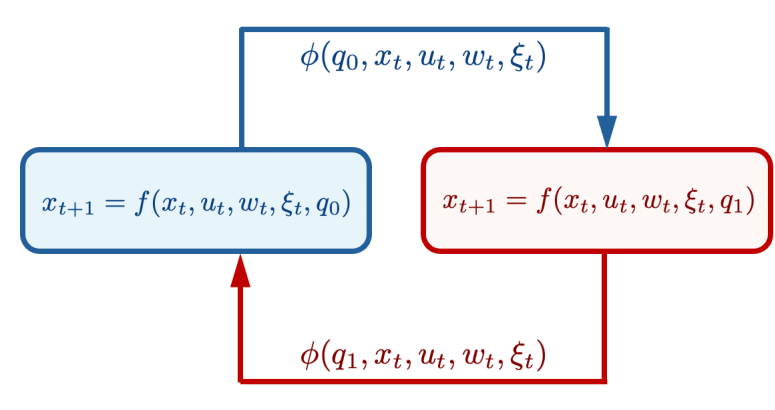


Figure 3.1: Hybrid dynamics with two disruption modes: q_0 (normal) and q_1 (abnormal). Within each mode, the network state x_t evolves according to the map $f(x_t, u_t, w_t, \xi_t, q_i)$, while transitions between modes are governed by $\phi(q_t, x_t, u_t, w_t, \xi_t)$. This captures how adversarial disturbances, natural hazards, or defensive actions can trigger shifts between normal and abnormal regimes.

hybrid dynamics as a stochastic process:

$$x_{t+1} = f(x_t, u_t, w_t, \xi_t, q_t), \quad (3.1)$$

$$q_{t+1} = \phi(q_t, x_t, u_t, w_t, \xi_t), \quad (3.2)$$

where x_t is the continuous-valued *network state*, u_t the defender's control input, w_t an *adversarial disturbance*, ξ_t a *natural disturbance*, and $q_t \in \mathcal{Q}$ the *disruption state*. The operators f and ϕ may be deterministic maps or stochastic kernels, so that both continuous dynamics and mode transitions can evolve probabilistically depending on the current state, inputs, and disturbances [218, 225].

The set \mathcal{Q} may include labels such as {normal, degraded, attack, failure}. Equation (3.1) describes the (possibly random) evolution of performance variables within each regime, while Equation (3.2) characterizes random mode transitions triggered by adversarial activity, natural hazards, or defensive reconfiguration. Fig. 3.1 illustrates this process for the simple case with two disruption modes: q_0 representing normal operation and q_1 representing an abnormal regime. Within each mode, the network state x_t evolves according to f , while the transition map ϕ determines when the system switches between modes.

By adapting both x_t and q_t to the domain, this hybrid model provides a unifying foundation for designing *tailored resilience strategies* while preserving a coherent framework for analysis. In what follows, we illustrate how different network components induce distinct choices of the continuous state x_t , the disruption state q_t , adversarial disturbances w_t , natural disturbances ξ_t , and defender inputs u_t . Each example highlights how the abstract hybrid model specializes to concrete resilience objectives in 5G and beyond [224, 226].

Core Network (Service-Based Architecture). The 5G Core relies on a Service-Based Architecture (SBA), where network functions interact through APIs. In this setting, signaling storms or API abuse can overwhelm the control plane. The state x_t is described by variables such as the signaling queue length x_t^{queue} , the control-plane processing rate μ_t , and the slice-level latency ℓ_t . The disruption mode m_t switches among {normal, overload, attack} depending on signaling arrival rates. Adversarial disturbances w_t manifest as malicious signaling arrivals λ_t^q , while legitimate arrivals are denoted by λ_t^0 . A representative queueing dynamic is

$$x_{t+1}^{\text{queue}} = x_t^{\text{queue}} + \lambda_t^0 + \lambda_t^q - \mu(u_t),$$

where the service rate $\mu(u_t)$ depends on elastic scaling of control-plane VNFs. Resilience objectives in this context are twofold: ensuring queue stability, i.e., maintaining bounded x_t^{queue} , and enforcing latency guarantees $\ell_t \leq \ell^{\max}$ even under abnormal operating modes.

Backhaul Transport. The transport domain carries data between the core and the RAN. Natural disturbances ξ_t , such as fiber cuts, reduce capacity, while $q_t \in \{\text{normal, degraded, partitioned}\}$ indicates disruption status. The state x_t includes available link capacity B_t , coverage set \mathcal{C}_t , and active connections N_t . A fault induces a drop

$$B_{t+1} = B_t - \Delta B(\xi_t, q_t),$$

where ΔB reflects disruption severity. The defender input u_t consists of rerouting or activating backup links. Resilience requires maintaining coverage \mathcal{C}_t and throughput above thresholds across disruption states.

Edge Computing (MEC). Multi-access edge computing nodes host latency-critical services. The state x_t includes compute capacity C_t , workload utilization ρ_t , and slice deadlines ℓ_t^{URLLC} , while $q_t \in \{\text{normal, congested, failure}\}$ captures disruptions. Adversarial inputs w_t may inject excess load ω_t , while natural failures ξ_t reduce available capacity. The utilization evolves as

$$\rho_{t+1} = \rho_t + \frac{\lambda_t^u + \omega_t}{C_t - \Delta C(\xi_t, q_t)}.$$

Resilience requires ensuring that URLLC slice deadlines are met even when the disruption state indicates capacity collapse.

Radio Access Network (RAN / O-RAN). In the RAN, resilience is tied to access reliability. The state x_t includes SINR, spectrum assignment, and coverage areas, while

$q_t \in \{\text{normal, jammed, outage}\}$ encodes disruption. Natural disturbances ξ_t may disable distributed units (DUs), while adversarial inputs w_t may jam signals or corrupt RIC commands. The SINR dynamics can be written

$$\text{SINR}_{t+1} = h(\text{SINR}_t, -\Delta R(\xi_t, q_t), w_t, u_t),$$

where $\Delta R(\xi_t, q_t)$ captures resource losses in different disruption modes. Defender inputs u_t include adaptive power control and spectrum reassignment. Resilience requires sustaining spectral efficiency and handover stability across disruption states.

Feedback and OODA Loop for Responsive Resilience. Resilience in cyber-physical networks is fundamentally a property of closed-loop systems in which sensing, reasoning, and actuation interact with evolving dynamics. In classical control, the loop consists of measurement, control law computation, and actuation applied to the system state x_t . In cyber resilience, this cycle is generalized to the OODA loop, *Observe, Orient, Decide, Act*, as illustrated in Fig. 3.2. Unlike static fault-tolerance mechanisms, the OODA loop explicitly enables *responsive resilience*, adapting in real time to adversarial adaptation, stochastic uncertainty, and disruptive mode switching [150, 227].

In the **Observe** phase, measurements y_t are collected from diverse sources, including MEC resource monitors, RAN physical-layer indicators such as SINR and PRB utilization, and SBA counters of signaling activity. Formally, this corresponds to a measurement equation $y_t = h(x_t, q_t)$ that maps the hybrid state (x_t, q_t) , combining continuous network variables and the discrete disruption mode, into observable quantities.

The **Orient** phase processes these observations to make sense of the environment. It not only constructs an estimate \hat{x}_t of the hidden state but also analyzes patterns, infers intent, and identifies where adversarial actions are concentrated. This step distinguishes between adversarial disturbances w_t and natural disturbances ξ_t , contextualizes the information, and determines the most critical vulnerabilities or targets for defense. Methodologically, it links to filtering and inference problems under uncertainty, employing tools such as Kalman or particle filters, Bayesian changepoint detection, and adversarially robust estimators to separate natural noise from intentional manipulation.

In the **Decide** phase, the defender computes a control input $u_t = \pi(\hat{x}_t, q_t)$ that specifies a resilience action conditioned on the interpreted hybrid state. Decisions may include migrating slices, reallocating spectrum, throttling malicious flows, or deploying deception-based defenses, and they are often derived from optimization, reinforcement learning, or game-theoretic control policies.

Finally, the **Act** phase enforces the control action through programmable interfaces such as SDN southbound APIs, MEC orchestration commands, or O-RAN RIC control loops. This input u_t directly influences the system dynamics described in Equations (3.1)–(3.2), closing the loop between perception, decision, and system evolution. The feedback paths in Fig. 3.2 emphasize this loop: control flows from *Decide* into *Act* and loops back into *Observe*, enabling continual adaptation across time.

This recursive cycle allows the defender not only to react to immediate disruptions but also to adapt policies under evolving adversaries and uncertain fault dynamics. Traditional telecom systems rely on static fault-tolerance mechanisms—redundant gNodeBs, backup batteries, overprovisioned links—that suffice against isolated natural failures but collapse under coordinated attacks or compound disruptions. A control-theoretic approach, grounded in the OODA loop, generalizes fault-tolerance into a dynamic feedback framework. Natural faults, such as fiber cuts or power outages, alter topology or capacity, requiring SDN controllers to reroute flows in real time. Adversarial disturbances, such as signaling storms or RIC command abuse, drive queue divergence and control misconfigurations, necessitating adaptive defenses such as traffic shaping, microsegmentation, or moving target defense. When both occur simultaneously, composite strategies are required: redundancy activation combined with deception to mislead adversaries exploiting weakened infrastructures.

From a systems perspective, these scenarios constitute a hybrid control problem in which discrete disruption events interact with continuous dynamics. Embedding the OODA loop into this hybrid modeling framework provides the structured feedback needed to sustain *responsive resilience* under adversarial, stochastic, and compound disturbances.

Multi-Horizon Optimization for Optimal Responsive Resilience. This section focuses on the notion of *responsive resilience*, which emphasizes online adaptation to unfolding disturbances and disruptions. In contrast, the *proactive* and *retrospective* resilience approaches are often carried out offline, involving long-term design, planning, and post-event analysis. Here, control-theoretic methods are particularly suitable, as they enable online decision-making and closed-loop adjustment in the face of adversarial uncertainty. In the *responsive* stage, closed-loop feedback policies adapt rapidly to disturbances w_t and ξ_t , containing degradation in Q_t and steering (x_t, q_t) back toward admissible regions.

When disturbances and disruption modes evolve stochastically, resilience is naturally formulated as a *stochastic* receding-horizon control problem over the hybrid state (x_t, q_t) . At decision time t , given the information set \mathcal{I}_t (measurements, state estimates, and mode), the defender must predict the system’s evolution H steps into the future using models, statistical

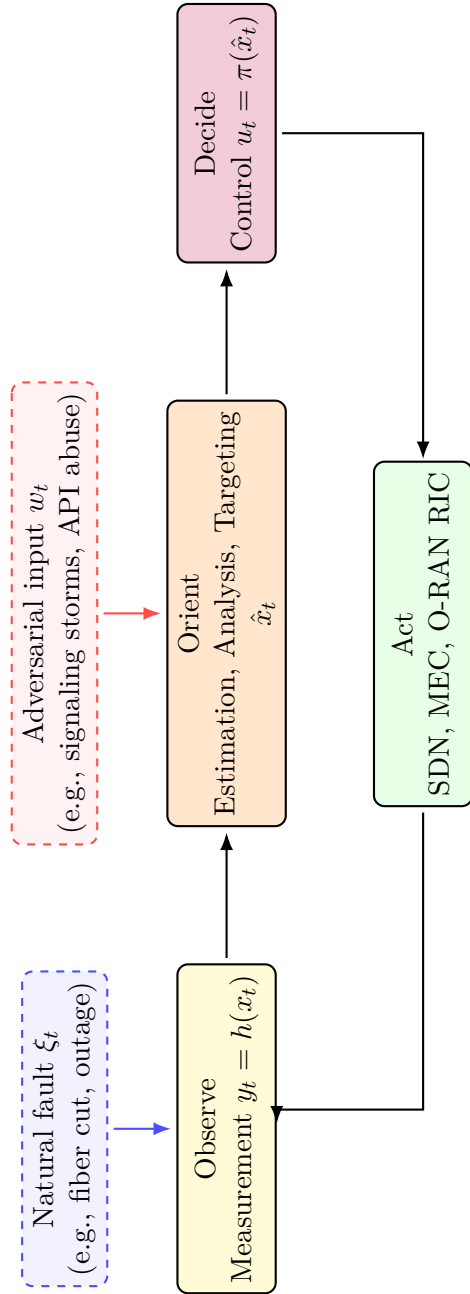


Figure 3.2: OODA feedback loop for *responsive resilience* in cyber-physical networks. The top row follows **Observe** → **Orient** → **Decide**; feedback proceeds via **Act**: *Decide* → *Act* (down, then right) and *Act* → *Observe* (left, then up). Unlike static fault-tolerance, the OODA loop supports adaptive responses under adversarial, stochastic, and compound disturbances.

forecasting, or digital twins. The resulting optimization problem is

$$\min_{u_{t:t+H-1} \in \mathcal{U}^H} \mathbb{E} \left[\sum_{\tau=t}^{t+H-1} (\ell(x_\tau, u_\tau, q_\tau) + c(u_\tau, q_\tau)) + V(x_{t+H}, q_{t+H}) \middle| \mathcal{I}_t \right], \quad (3.3)$$

subject to the stochastic hybrid dynamics in Equations (3.1)–(3.2), the initial condition (x_t, q_t) , and additional operational constraints

$$g(\hat{x}_\tau, u_\tau, \hat{q}_\tau) \leq 0, \quad \forall \tau \in [t, t+H-1],$$

where $\hat{x}_\tau, \hat{q}_\tau$ denote state and mode estimates obtained from \mathcal{I}_t .

Here H is the prediction horizon, and the expectation in (3.3) is taken with respect to the distribution of future disturbances and mode transitions $(w_{t:t+H-1}, \xi_{t:t+H-1}, q_{t+1:t+H})$ conditional on \mathcal{I}_t . The terminal cost $V(\cdot)$ encodes resilience goals beyond the horizon, such as backlog clearance, state recovery, or returning to a nominal operating mode.

Receding-horizon implementation. Model Predictive Control (MPC) computes an optimal sequence $u_{t:t+H-1}^*$ conditioned on \mathcal{I}_t , applies only the first action u_t^* , and then re-solves the optimization at $t+1$ with updated state (x_{t+1}, q_{t+1}) and information \mathcal{I}_{t+1} . By combining (3.1)–(3.2) with rolling-horizon design, MPC provides a mode-aware and stochastic framework for predictive planning that adapts continually to new observations and regime switches.

Risk-aware variants. When resilience must account for rare but severe events, the expectation in (3.3) can be replaced by a risk measure [220, 225]. Examples include minimizing Conditional Value-at-Risk (CVaR),

$$\min \text{CVaR}_\alpha \left(\sum_{\tau=t}^{t+H-1} \ell(x_\tau, u_\tau, q_\tau) + c(u_\tau, q_\tau) + V(x_{t+H}, q_{t+H}) \middle| \mathcal{I}_t \right),$$

imposing chance constraints such as

$$\mathbb{P}[g(x_\tau, u_\tau, q_\tau) \leq 0 \text{ for all } \tau \mid \mathcal{I}_t] \geq 1 - \varepsilon,$$

or adopting distributionally robust formulations,

$$\sup_{\mathbb{P} \in \mathcal{P}} \mathbb{E}_{\mathbb{P}} \left[\sum_{\tau=t}^{t+H-1} \ell(x_\tau, u_\tau, q_\tau) + c(u_\tau, q_\tau) + V(x_{t+H}, q_{t+H}) \right],$$

where \mathcal{P} is an ambiguity set around the nominal disturbance distribution. Such variants pro-

vide additional protection against tail risks, model uncertainty, and adversarial manipulation of disturbance distributions [150, 197].

Optimal Fallback Switching for Deterministic Systems. Consider a hybrid LQ setting with mode-dependent dynamics and costs. Let $q \in \{0, 1\}$ denote modes (e.g., 0 = abnormal/degraded, 1 = safe). The discrete-time dynamics and mode update are

$$x_{t+1} = A_{q_t} x_t + B u_t^c, \quad (3.4)$$

$$q_{t+1} = \max\{q_t, u_t^m\}, \quad u_t^m \in \{0, 1\}, \quad (3.5)$$

with continuous control $u_t^c \in \mathbb{R}^m$ and switching action u_t^m . We take $q_t = 0$ at time t (currently abnormal), and allow a one-shot switch to $q = 1$ (safe). Let the horizon be $H = 2$ (decisions at t and $t+1$), with terminal time $t+2$. Stage and terminal costs are mode-dependent:

$$\ell(x, u, q) = x^\top Q_q x + (u^c)^\top R u^c + s_q, \quad Q_q \succeq 0, \quad R \succ 0, \quad s_q \geq 0, \quad (3.6)$$

$$V(x, q) = x^\top P_q x, \quad P_q \succeq 0, \quad (3.7)$$

and a switching penalty $\lambda \geq 0$ applies when $u_t^m = 1$ and $q_t = 0$:

$$c(u_t, q_t) = \lambda \mathbf{1}\{q_t = 0, u_t^m = 1\}.$$

The safe mode typically has a *service-loss* term $s_1 \geq 0$ (reduced functionality) but better stability/weights (A_1, Q_1, P_1). Let $H = 2$. At time t , choose (u_t^c, u_t^m) and at time $t+1$ choose (u_{t+1}^c, u_{t+1}^m) to minimize

$$\begin{aligned} J = & [x_t^\top Q_0 x_t + (u_t^c)^\top R u_t^c + s_0] + c(u_t, q_t) + \\ & [x_{t+1}^\top Q_{q_{t+1}} x_{t+1} + (u_{t+1}^c)^\top R u_{t+1}^c + s_{q_{t+1}}] + x_{t+2}^\top P_{q_{t+2}} x_{t+2}, \end{aligned} \quad (3.8)$$

subject to the dynamics and $q_{t+1} = \max\{0, u_t^m\}$, $q_{t+2} = \max\{q_{t+1}, u_{t+1}^m\}$. (For clarity, we take perfect estimates; chance constraints can be added via $g(\hat{x}, u, \hat{q}) \leq 0$.)

Define, for any mode $m \in \{0, 1\}$ and terminal weight $P \succeq 0$, the *one-step minimized quadratic coefficient*

$$\Pi(m, P) := Q_m + A_m^\top P A_m - A_m^\top P B (R + B^\top P B)^{-1} B^\top P A_m \succeq 0. \quad (3.9)$$

Then, the stage- $(t+1)$ cost (including terminal) under mode m minimized over u_{t+1}^c is

$$V_{t+1}(x_{t+1}, m) = x_{t+1}^\top \Pi(m, P_m) x_{t+1} + s_m,$$

where P_m is the terminal weight if mode m is active at $t+2$.

If we *commit* at time t to $q_{t+1} = m$ (i.e., $u_t^m = m$), then (3.8) becomes, after minimizing over u_{t+1}^c ,

$$\begin{aligned} J_m(u_t^c) &= x_t^\top Q_0 x_t + (u_t^c)^\top R u_t^c + s_0 + \mathbf{1}\{m=1\}\lambda + \\ &\quad (A_0 x_t + B u_t^c)^\top \Pi(m, P_m) (A_0 x_t + B u_t^c) + s_m. \end{aligned} \quad (3.10)$$

Minimizing this quadratic in u_t^c yields the value

$$J_m^* = x_t^\top \Gamma(m) x_t + s_0 + s_m + \mathbf{1}\{m=1\}\lambda, \quad (3.11)$$

$$\Gamma(m) := Q_0 + A_0^\top \Pi(m, P_m) A_0 - A_0^\top \Pi(m, P_m) B (R + B^\top \Pi(m, P_m) B)^{-1} B^\top \Pi(m, P_m) A_0. \quad (3.12)$$

“*Stay abnormal*” corresponds to $m = 0$; “*switch to safe*” corresponds to $m = 1$. Since s_0 appears in both, the difference is

$$\Delta J := J_1^* - J_0^* = \lambda + (s_1 - s_0) + x_t^\top (\Gamma(1) - \Gamma(0)) x_t. \quad (3.13)$$

Hence, *fallback switching at time t is optimal* iff

$$x_t^\top (\Gamma(0) - \Gamma(1)) x_t > \lambda + (s_1 - s_0). \quad (3.14)$$

The matrices $\Pi(m, P_m)$ in (3.9) summarize the *best achievable one-step-ahead* (stage + terminal) quadratic cost under mode m after optimizing u^c . The matrices $\Gamma(m)$ in (3.12) fold in the current step’s decision at mode 0 and the impact of choosing the next mode m via $\Pi(m, P_m)$. Condition (3.14) is a *general, verifiable* inequality: if safe mode produces a *smaller* quadratic weight (i.e., $\Gamma(1) \prec \Gamma(0)$), then for sufficiently large x_t the LHS exceeds the (fixed) penalty $\lambda + (s_1 - s_0)$, making the switch optimal.

For the scalar case with $B = 1$, $R = \alpha > 0$, $A_0 = a_0$, $A_1 = a_1$, and terminal weights $P_m = p_m \geq 0$, one computes

$$\Pi(m, p_m) = Q_m + \frac{\alpha p_m a_m^2}{\alpha + p_m}, \quad \Gamma(m) = Q_0 + \frac{\alpha \Pi(m, p_m) a_0^2}{\alpha + \Pi(m, p_m)}.$$

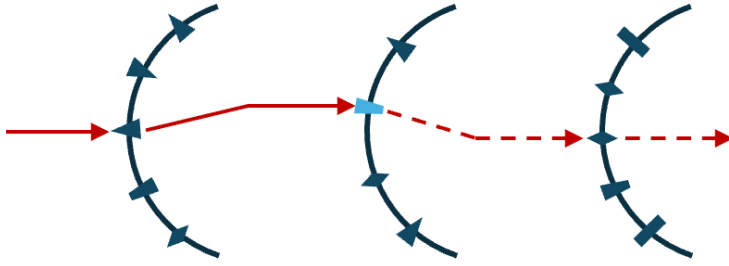


Figure 3.3: **Moving Target Defense (MTD): concept and timing.** The dark blue arcs depict successive *configuration shells*, which are sets of exposure states $\mathcal{A}(t)$ reachable under a fixed setup (e.g., static SBA/IP maps, fixed slice placement, fixed spectrum band). The solid red trajectory shows an attacker’s progress when the surface is *static*. Blue diamonds mark *MTD reconfiguration epochs* at which a control input u_t is applied (port/IP randomization at the service layer, slice migration/reshuffling in orchestration, or spectrum hopping in the RAN). After each u_t , the attack surface $\mathcal{A}(t)$ is mapped to a new shell by the dynamics $\mathcal{A}(t+1) = g(\mathcal{A}(t), u_t)$, forcing the adversary onto the dashed red trajectory (lost progress and renewed reconnaissance). In the moving-horizon formulation (3.16), the defender chooses a sequence of randomized configurations $f_{t+1:t+H}$ that (i) reduce *stage risk* $\mathbb{E}_{c \sim f} \hat{r}_t(c, \mathcal{A}_t)$, (ii) limit churn via the KL trust region, and (iii) shape the surface away from undesirable regions, yielding softmax/mirror-descent updates for f .

Then the switching condition (3.14) becomes

$$|x_t| > \sqrt{\frac{\lambda + (s_1 - s_0)}{a_0^2 \alpha \left(\frac{\Pi(0, p_0)}{\alpha + \Pi(0, p_0)} - \frac{\Pi(1, p_1)}{\alpha + \Pi(1, p_1)} \right)}}.$$

Thus, by *designing* a_1 (more contractive dynamics in safe mode), and/or choosing Q_1, p_1 (smaller state penalties in safe mode) so that

$$\frac{\Pi(0, p_0)}{\alpha + \Pi(0, p_0)} > \frac{\Pi(1, p_1)}{\alpha + \Pi(1, p_1)},$$

one guarantees a finite *state threshold* beyond which fallback switching is optimal. Larger λ or s_1 shift the threshold upward; more stabilizing a_1 or milder Q_1, p_1 shift it downward.

3.1.2 Moving Target Defense.

Moving Target Defense (MTD) is a cornerstone strategy for achieving *responsive resilience*, in which the system actively adapts its configuration to deny adversaries a stable attack surface. Unlike static fault-tolerance mechanisms, which rely on redundancy to absorb disruptions, MTD embodies agility: it reshapes the attack surface in response to evolving threats, thereby

closing the loop between adversarial activity and defensive adaptation.

A fundamental challenge in cyber defense lies in the asymmetry between attacker and defender [87, 227]. Defenders must maintain large, complex, and often static infrastructures, while attackers can patiently probe for vulnerabilities and strike at a time of their choosing. This imbalance, often described as the *fortification bias* phenomenon, implies that defenders must succeed every time, but an attacker needs to succeed only once. MTD offers a paradigm-shifting approach to redress this imbalance. Rather than presenting a fixed and predictable target, MTD dynamically alters the system’s configuration to inject uncertainty, increase attacker workload, and reduce the dwell time of intrusions. By “shifting the ground” under adversaries, MTD denies them the stability required for reconnaissance or exploitation campaigns and thus exemplifies the principle of responsive resilience: defensive actions that adaptively respond to adversarial behavior in real time.

From a control-theoretic perspective, MTD can be modeled as a control input that modifies the system’s exposure to adversarial actions. Within the OODA loop, MTD actions are triggered in the *Decide* phase and implemented in the *Act* phase, directly feeding back into the *Observe* stage as adversaries react to the shifting environment. In the context of 5G and beyond networks, MTD strategies span multiple layers:

1. *Service and interface layer*: port/IP randomization for Service-Based Architecture (SBA) and Multi-access Edge Computing (MEC) endpoints, disrupting adversarial scanning and lateral movement;
2. *Slicing and orchestration layer*: migration or reshuffling of network slices across distributed edge clouds, creating mobility in resource placement that obscures attacker targeting;
3. *Radio layer*: spectrum hopping and frequency agility at the radio access level, preventing jamming or eavesdropping from stabilizing on fixed channels.

Fig. 3.3 illustrates this principle. The blue arcs represent successive *configuration shells*, distinct realizations of the network attack surface. The solid red line depicts an attacker’s trajectory when the system is static, enabling steady progress toward compromise. In contrast, the dashed red line shows how MTD periodically disrupts this trajectory: each blue diamond corresponds to a reconfiguration input u_t that shifts the system to a new configuration shell. This action erases reconnaissance progress, forcing the adversary to restart adaptation and greatly increasing their operational cost.

Formally, the evolution of the attack surface under MTD is modeled as

$$\mathcal{A}(t+1) = g(\mathcal{A}(t), u_t), \quad (3.15)$$

where u_t denotes the MTD action at time t . This controlled nonstationarity has two main effects: (i) it increases the cost and uncertainty for the attacker, who must repeatedly adjust to a changing system, and (ii) it provides the defender with a mechanism to contain natural faults by introducing diversity and compartmentalization into the infrastructure.

In practice, effective MTD design requires careful balancing. Excessive reconfiguration can degrade service quality, consume resources, or create instability, while insufficient reconfiguration may fail to deter adversaries. Hence, MTD must be framed as a decision-making problem that explicitly weighs risk reduction against operational cost and service-level constraints. This naturally motivates receding-horizon (model predictive) formulations, where the defender selects MTD actions not only to reduce immediate risk but also with foresight into their downstream effects on the evolving attack surface.

Moving-Horizon MTD The MTD problem can be cast in the same receding-horizon framework as the stochastic hybrid MPC formulation in (3.3), (3.1), and (3.2). For clarity, we focus on a simplified setting where the hybrid state (x_t, q_t) is reduced to an *attack-surface state* \mathcal{A}_t that evolves under randomized configuration choices.

The disruption mode q_t can still be introduced when needed. For example, in *network slicing*, q_t may encode whether a slice is operating normally or has been degraded by an unknown vulnerability. Each slicing configuration is associated with a distinct set of vulnerabilities. When q_t indicates that a slice has entered an unanticipated adversarial regime resulting in irreparable performance degradation, the controller must fall back to safe default operations, such as reverting to a pre-validated configuration, freezing migrations, or pinning flows to redundant macro-cells. These fallback strategies guarantee service continuity, although with reduced efficiency, and serve as a safety net when predictive optimization cannot ensure resilience.

In the nominal case considered here, we omit explicit mode switching and illustrate how configuration control mitigates nondisruptive uncertainties or adversarial patterns that fall within known classes. For example, in network slicing, the MTD mechanism may randomize spectrum-band assignments, migrate virtual network functions across MEC nodes, or shuffle port/IP mappings at the SBA service mesh level. Such reconfigurations alter the adversary's observation-to-action mapping, increasing reconnaissance costs and reducing the effective lifetime of exploits.

Let \mathcal{C} denote the finite set of admissible MTD configurations (e.g., IP/port maps, slice placements, spectrum bands). At each stage $t+k$, the defender selects a distribution $f_{t+k} \in \Delta(\mathcal{C})$. A configuration $c \sim f_{t+k}$ is then drawn, which induces the realized control action u_{t+k} ; f_{t+k} is the randomized decision variable while u_{t+k} is the concrete control applied to

the system. The attack-surface dynamics evolve according to

$$\mathcal{A}_{t+k+1} = g(\mathcal{A}_{t+k}, u_{t+k}),$$

in parallel with the general network dynamics (3.1)–(3.2). In this way, the notation $(f_{t+k}, \mathcal{A}_{t+k})$ is simply an MTD-specific instance of the hybrid system (x_t, q_t) with control u_t .

The moving-horizon optimization problem is

$$\min_{\{f_{t+1}, \dots, f_{t+H}\}} \mathbb{E} \left[\sum_{k=0}^{H-1} \left(\underbrace{\hat{r}_{t+k}(c, \mathcal{A}_{t+k})}_{\text{stage risk}} + \underbrace{\varepsilon D_{\text{KL}}(f_{t+k+1} \parallel f_{t+k})}_{\text{switching regularization}} + \underbrace{\alpha \psi(\mathcal{A}_{t+k})}_{\text{surface shaping}} \right) \mid \mathcal{I}_t \right], \quad (3.16)$$

subject to QoS and safety constraints,

$$\Phi_j(f_{t+k+1}, \mathcal{A}_{t+k}) \leq 0, \quad h(x_{t+k}, q_{t+k}) \geq 0, \quad \forall k = 0, \dots, H-1,$$

where Φ_j encode service constraints (e.g., URLLC deadlines, SBA queue limits), and $h(\cdot, \cdot)$ is a barrier-function condition ensuring (x_t, q_t) remains in the safe set. The expectation accounts for stochastic realizations of both adversarial and natural disturbances.

Detailed solution structure. For each stage k , if \mathcal{A}_{t+k} is fixed, the subproblem in (3.16) reduces to

$$J(f_{t+k+1}) = \sum_c f_{t+k+1}(c) \hat{r}_{t+k}(c, \mathcal{A}_{t+k}) + \varepsilon D_{\text{KL}}(f_{t+k+1} \parallel f_{t+k}), \quad f_{t+k+1} \in \Delta(\mathcal{C}).$$

This convex program admits the closed-form softmax update

$$f_{t+k+1}^*(c) = \frac{f_{t+k}(c) \exp(-\hat{r}_{t+k}(c)/\varepsilon)}{\sum_{c'} f_{t+k}(c') \exp(-\hat{r}_{t+k}(c')/\varepsilon)}.$$

Thus f_{t+k+1}^* exponentially tilts f_{t+k} toward lower-risk configurations. Small ε yields aggressive switching (close to $\arg \min \hat{r}$), while large ε preserves inertia, ensuring smoother transitions. With additional QoS/resource constraints, the update generalizes to an exponential-family form with dual multipliers λ , analogous to constrained MPC.

Horizon coupling and look-ahead. As in stochastic MPC, horizon coupling means that today's randomized distribution f_{t+k+1} influences not only immediate stage risk but also the downstream attack-surface state \mathcal{A}_{t+k+1} . First-order conditions show that the optimal distribution retains the exponential-family form but incorporates an additional *look-ahead*

term:

$$f_{t+k+1}^*(c) \propto f_{t+k}^*(c) \exp\left(-\frac{1}{\varepsilon}[\hat{r}_{t+k}(c, \mathcal{A}_{t+k}) + \lambda_{t+k}^\top \phi(c) + Q_{t+k}^{\text{ctg}}(c)]\right),$$

where $Q_{t+k}^{\text{ctg}}(c)$ denotes the downstream cost-to-go derivative. The term $\phi(c)$ represents a vector of *resource and QoS features* associated with configuration c , such as migration overhead, added latency, signaling cost, or power consumption. Incorporating $\lambda_{t+k}^\top \phi(c)$ ensures that randomized reconfiguration respects system-level constraints: large values of $\phi(c)$ for certain costly operations (e.g., live migration of a VNF across MEC nodes) increase the effective cost of selecting c , while smaller values (e.g., shuffling IP/port mappings) make such actions more favorable. The multipliers λ_{t+k} act as shadow prices that balance resilience benefits against operational budgets, aligning MTD decisions with network slicing QoS guarantees.

This structure tilts decisions not only against current risk \hat{r}_{t+k} but also against long-term exposure (Q_{t+k}^{ctg}) and resource costs ($\lambda_{t+k}^\top \phi(c)$), paralleling how MPC balances stage costs with terminal objectives.

When $H = 1$ or when Q^{ctg} is negligible, the update reduces to the one-step softmax rule. For $H > 1$, foresight prevents myopic selection of seemingly safe configurations that generate vulnerabilities or exhaust resources later. Thus, moving-horizon MTD is a direct instantiation of receding-horizon control: an online, adaptive defense that continually re-optimizes in light of new state information (\mathcal{A}_t) while shaping both immediate and future resilience outcomes.

3.2 Dynamic Game Foundation

Cyber resilience in 5G networks is not merely about robustness against random faults; it fundamentally involves *adversarial behavior*. Attackers are intelligent, adaptive agents who observe the system, learn its vulnerabilities, and strategically decide how to maximize disruption. Defenders, in turn, must anticipate these maneuvers while balancing trade-offs between performance, security, and operational cost.

Game theory provides a natural framework for such interactions. It models the network as a strategic environment in which multiple players (attackers and defenders) repeatedly interact, shaping each other's payoffs. This perspective captures how resilience mechanisms, such as MTD, slice migration, SDN rerouting, and spectrum hopping, perform not only against average case failures, but under *equilibrium-driven adversarial conditions*. In this sense, game theory embeds resilience into a predictive framework, enabling the design of defense strategies that remain robust against both stochastic disturbances and intelligent adversaries [150, 88].

3.2.1 Model Definition

We model attacker–defender interactions in 5G as a discounted stochastic game

$$\Gamma = (\mathcal{S}, \mathcal{E}, \mathcal{R}, P, \{u_A, u_D\}, \beta, \mathcal{I}),$$

where time evolves as $t = 0, 1, 2, \dots$, and $\beta \in (0, 1)$ is the discount factor. The players are the attacker A and the defender D .

In general, the state at time t can include both the continuous network state x_t and the discrete disruption mode q_t . The variable x_t may represent the operational condition of the network, such as slice queue lengths, URLLC latency, MEC workload, SINR, or backhaul utilization. Alternatively, x_t may capture the configuration of the exposed attack surface, such as the placement of slices across edge clouds or the allocation of spectrum resources. The disruption mode q_t encodes the regime in which the system is operating (e.g., normal, degraded, under attack, or in failure), allowing the game to capture both performance evolution and adversarial regime switching.

Dynamic attacker and defender actions (slice migration example). At each time step t , the attacker and defender select actions simultaneously from their respective sets, conditioned on the current state $s_t = (p_t, \mathcal{A}_t)$. Here, p_t denotes the network performance state (e.g., slice queue lengths, URLLC latency, MEC workload, SINR, or backhaul utilization), while \mathcal{A}_t describes the exposed attack surface, such as the current placement of slices across MEC nodes.

The attacker’s admissible set $\mathcal{E}(s_t)$ depends on the exposed placement \mathcal{A}_t and typically includes

$$\mathcal{E}(s_t) = \{\text{idle}, \text{flood}(j), \text{probe}(j), \text{jam}(b), \text{multi}(S)\}.$$

Here, `idle` represents no attack, `flood`(j) injects adversarial workload into the service-based interface of the slice hosted on MEC node j , `probe`(j) performs low-rate reconnaissance on a slice at node j , `jam`(b) targets a frequency band b relied upon by a slice, and `multi`(S) distributes simultaneous low-rate attacks across a subset of nodes S . For example, if the slice is deployed at MEC node j^* , then choosing `flood`(j^*) directly creates congestion and queue buildup at that node, raising latency and packet loss for URLLC flows. Probing actions may cause little immediate damage but yield information about slice placement or migration patterns.

The defender’s admissible set $\mathcal{R}(s_t)$ represents feasible resilience controls given the current

resource and latency constraints:

$$\mathcal{R}(s_t) = \{\text{stay}, \text{migrate}(j \rightarrow j'), \text{scale_up}(j), \text{scale_down}(j), \text{balance}(j, j')\}.$$

The action `stay` keeps the slice at its current location. The action `migrate`($j \rightarrow j'$) moves a slice from node j to a new node j' , reducing exposure to targeted floods at the cost of signaling overhead and temporary disruption. The action `scale_up`(j) allocates additional processing resources at node j to absorb increased load, while `scale_down`(j) releases excess resources when demand or attack intensity diminishes. Finally, `balance`(j, j') splits the workload across multiple MEC nodes, lowering the risk of localized congestion at the price of synchronization and coordination costs.

To illustrate, suppose the slice is currently hosted at node j^* . If the attacker selects `flood`(j^*), the defender may respond with `stay`, which leaves the slice vulnerable to growing congestion, or with `migrate`($j^* \rightarrow j'$), which restores service continuity after a temporary migration delay but incurs overhead. Alternatively, the defender may opt for `scale_up`(j^*), which increases local service rate and mitigates flooding at the expense of additional resources. Over time, this interplay generates an adaptive cycle: the attacker redirects load toward the current slice placement, while the defender mitigates damage through migration, scaling, or balancing actions across the edge cloud. The resulting dynamics of (p_t, \mathcal{A}_t) thus embody an arms race between targeted flooding and strategic slice migration.

The system state evolves according to a controlled stochastic kernel,

$$s_{t+1} \sim P(\cdot \mid s_t, e_t, r_t),$$

which decomposes into two components:

$$\begin{cases} p_{t+1} = f(p_t, r_t, w(e_t), \xi_t), \\ \mathcal{A}_{t+1} = g(\mathcal{A}_t, u(r_t)). \end{cases}$$

The first component describes the evolution of network performance p_{t+1} under the influence of the defender's control r_t , the disturbance generated by the attacker's exploit $w(e_t)$, and natural exogenous shocks ξ_t such as fiber cuts or sudden power outages. The second component governs the evolution of the exposed attack surface \mathcal{A}_{t+1} , which depends directly on the migration or reconfiguration choices $u(r_t)$ embedded in the defender's resilience action.

To make this concrete, consider the slice queueing dynamics. If x_t^q denotes the queue

length of a slice, then its evolution can be written as

$$x_{t+1}^q = x_t^q + \lambda_t^0 + \lambda_t^q(e_t) - \mu(r_t),$$

where λ_t^0 is the legitimate user arrival rate, $\lambda_t^q(e_t)$ represents the adversarial injection rate induced by a targeted flood (parameterized by the attacker's escalation level e_t), and $\mu(r_t)$ is the service rate determined by the defender's control action r_t (e.g., migration or scaling).

When the defender migrates the slice to a less congested MEC node, $\mu(r_t)$ may increase due to newly available processing capacity, though the migration itself can incur a temporary service penalty during the handoff. Conversely, when the attacker escalates the exploit, $\lambda_t^q(e_t)$ rises, creating additional stress and potentially forcing the defender into costly reallocations.

The coupled dynamics therefore capture the arms race between attacker-induced load on the slice and defender-initiated adaptations through migration or scaling.

Each stage of the game generates immediate rewards and costs for both players. The function $\ell(x_t, e_t, r_t)$ quantifies the instantaneous network loss, which may manifest as missed URLLC deadlines, excessive queue lengths, or temporary service degradation during slice migration. The defender additionally incurs an operational cost $c_D(r_t)$, reflecting overhead from migration, scaling, or load balancing operations. Likewise, the attacker incurs a cost $c_A(e_t)$, corresponding to resources consumed in sustaining a flood or in mounting a probe.

For clarity, we consider the zero-sum formulation, in which the defender's payoff is

$$u_D(s_t, e_t, r_t) = -\ell(x_t, e_t, r_t) - c_D(r_t),$$

and the attacker's payoff is simply its negative,

$$u_A(s_t, e_t, r_t) = -u_D(s_t, e_t, r_t).$$

This structure encodes the adversarial tension: every increment of network damage or defensive overhead is a gain for the attacker and a loss for the defender. In practice, one may also relax this to a general-sum setting in which both players suffer from external factors, such as collateral service degradation or false alarms.

The cumulative discounted payoff of player $i \in \{A, D\}$ under a strategy profile $\pi = (\pi_A, \pi_D)$ is defined as

$$J_i^\pi(s_0) = \mathbb{E}^\pi \left[\sum_{t=0}^{\infty} \beta^t u_i(s_t, e_t, r_t) \mid s_0 \right],$$

where the expectation accounts for the stochastic evolution of the system and the randomized strategies of both players. The discount factor $\beta \in (0, 1)$ emphasizes near-term consequences

but still incorporates the long-run impact of repeated attacker–defender interactions. In the slice migration example, this captures the fact that immediate disruptions—such as transient queue buildup during a flood—must be balanced against the longer-term costs of repeated migrations, resource reallocations, and strategic adaptation over time.

The information structure \mathcal{I} specifies what each player observes at each stage of the game. This is a central aspect of 5G slice defense, since both attacker and defender typically operate under uncertainty and must make strategic decisions based on incomplete or imperfect information.

In the simplest setting of a complete-information or Markov game, both players observe the full state $s_t = (p_t, \mathcal{A}_t)$. The attacker knows exactly where slices are deployed across the MEC nodes, and the defender has perfect visibility into which slice is under attack and how the network is performing. This scenario corresponds to an idealized case of perfect monitoring. While useful as a baseline for analysis, it is rarely realistic in practice, since neither attackers nor defenders enjoy such full transparency in real 5G networks.

A more realistic framework is that of Bayesian, or incomplete-information, games. Here each player i is endowed with a private type $\theta_i \in \Theta_i$, drawn from a prior $\mathbb{P}(\theta_A, \theta_D)$. The type captures hidden attributes such as the attacker’s skill level or the defender’s resource budget for migrations. Instead of directly observing the state, players receive noisy signals o_t through an observation kernel $O(o_t | s_t)$ and must maintain beliefs μ_t about the joint state and the hidden types. In the slice setting, this means an attacker may be uncertain whether a visible slice is a genuine service or a honeypot, while a defender may be unsure whether a spike in traffic is the result of an adversarial flood or a benign user flash crowd. Strategies in this environment are therefore belief-dependent: a cautious defender may choose to migrate only when the posterior probability of attack is sufficiently high, whereas a bold attacker may probe slices to update its own belief about whether the target is real or decoy.

The most general case is captured by partially observable stochastic games (POSGs) [228, 229, 230, 231], where both players only have filtered access to the state. In this setting, not only are private types hidden, but the state itself is not fully observable. Encrypted traffic may obscure adversarial flows, and limited monitoring may create blind spots where probing and reconnaissance cannot be immediately detected. Both attacker and defender must therefore maintain belief states over hidden variables and adapt strategies dynamically as new observations arrive.

Continuing the slice migration example, consider an attacker with high skill level ($\theta_A = \text{skilled}$). Such an adversary can quickly detect slice migrations and redirect flooding toward the new location, while a low-skilled attacker is slower to adapt and may waste resources attacking an old MEC node. On the defender side, the budget type θ_D determines whether

frequent migrations are affordable. A defender with ample resources can migrate aggressively in response to observed anomalies, while a resource-constrained defender must be more selective. In both cases, beliefs play a crucial role: the attacker forms beliefs about the defender's migration policy, while the defender forms beliefs about whether congestion is adversarial or the result of legitimate user demand. The equilibrium outcome depends not just on the physical dynamics of slice migration, but on how information is revealed, processed, and acted upon under uncertainty.

3.2.2 Resilience as an equilibrium property

Within the dynamic game framework, resilience corresponds to the defender's ability to implement a policy π_D that ensures bounded network loss ℓ and recovery of the performance state x_t under worst-case attacker strategies π_A . In other words, resilience is not defined only by the robustness of the system in response to random shocks, but by the equilibrium outcome of the strategic interaction between attacker and defender.

To make this precise, recall that a *strategy* for player $i \in \{A, D\}$ is a mapping π_i from the observed history (or belief state, under incomplete information) to a probability distribution over actions. A pair of strategies $\pi = (\pi_A, \pi_D)$ induces a stochastic process $\{s_t\}$ through the transition kernel P . The performance of a strategy profile is measured by the cumulative discounted payoff

$$J_i^\pi(s_0) = \mathbb{E}^\pi \left[\sum_{t=0}^{\infty} \beta^t u_i(s_t, e_t, r_t) \middle| s_0 \right].$$

A fundamental equilibrium notion is the *Nash equilibrium* [232]. A strategy profile $\pi^* = (\pi_A^*, \pi_D^*)$ is a Nash equilibrium if neither player can improve their expected payoff by deviating unilaterally, i.e.,

$$J_A^{(\pi_A^*, \pi_D^*)}(s) \geq J_A^{(\pi_A, \pi_D^*)}(s), \quad J_D^{(\pi_A^*, \pi_D^*)}(s) \geq J_D^{(\pi_A^*, \pi_D)}(s),$$

for all states $s \in \mathcal{S}$ and all admissible alternative strategies π_A, π_D . In dynamic games, one often considers refinements such as *Markov perfect equilibrium* [233], where strategies depend only on the current state, or *Perfect Bayesian equilibrium* [234], where strategies depend on beliefs in incomplete-information settings.

Resilience can then be understood as a property of the equilibrium value function $V^*(s)$ of the defender, defined by

$$V^*(s) = J_D^{\pi^*}(s),$$

where π^* is an equilibrium strategy profile. The system is resilient if

$$-V^*(s) \leq \bar{L}, \quad \forall s \in \mathcal{S},$$

for some acceptable threshold \bar{L} that encodes performance and service-level guarantees. This inequality states that at equilibrium, where the attacker has no incentive to reduce pressure and the defender has no incentive to over- or under-react—the long-run loss remains bounded within tolerable levels.

In the slice migration example, equilibrium captures the stable operating point of the repeated attacker–defender interaction. A powerful attacker may repeatedly flood whichever MEC node currently hosts a slice, while the defender weighs whether to stay, migrate, or scale resources. If the defender migrates too frequently, service degrades due to excessive handoff costs; if the defender rarely migrates, the attacker succeeds in maintaining prolonged congestion. At equilibrium, the defender’s policy π_D^* specifies the optimal balance, such as migrating only when queue lengths exceed a critical threshold, while the attacker’s policy π_A^* specifies the intensity and frequency of floods consistent with maximizing disruption under this defense. The resulting equilibrium value function predicts the average long-run loss to the network.

By interpreting resilience as an equilibrium property, one obtains both a normative and predictive perspective. Normatively, equilibrium analysis provides a benchmark for the best achievable defense under rational adaptation of the attacker. Predictively, if one can compute or approximate the equilibrium strategies and values, one can forecast how resilient the system will remain under sustained adversarial campaigns and repeated natural disturbances. Thus, equilibrium is not only a mathematical solution concept, but also a quantitative measure of the defender’s ability to maintain service quality in the face of strategic and persistent attacks.

3.2.3 Equilibrium Solution Via Dynamic Programming

Game-theoretic models of resilience in 5G networks ultimately require solution concepts that predict the outcome of attacker–defender interactions. Because these interactions unfold over time and depend on evolving network states, equilibrium notions must capture both the dynamic nature of play and the information structure available to each participant. Dynamic programming plays a central role, as equilibrium computation is typically reduced to recursive value functions or belief updates. In this subsection, we provide a rigorous account of Markov perfect equilibrium, Bayesian and epistemic equilibria, and signaling games, highlighting their relevance to resilience analysis.

Markov perfect equilibrium (MPE). In dynamic stochastic games, players repeatedly act in response to the current state of the system. A *Markov strategy* for player $i \in \{A, D\}$ is defined as a mapping

$$\pi_i : \mathcal{S} \longrightarrow \Delta(\mathcal{A}_i),$$

which prescribes a probability distribution over actions based only on the present state $s \in \mathcal{S}$. This restriction to memoryless strategies is particularly natural in large-scale 5G systems, where keeping track of full action histories is computationally infeasible and unnecessary for optimality in discounted settings.

In the zero-sum case with finite state and action spaces, the defender's equilibrium value function $V(s)$ satisfies the *Shapley equation* [235]:

$$V(s) = \min_{r \in \mathcal{R}(s)} \max_{e \in \mathcal{E}(s)} \left\{ u_D(s, e, r) + \beta \mathbb{E}[V(s') \mid s, e, r] \right\},$$

where $\beta \in (0, 1)$ is the discount factor. The minimization reflects the defender's objective to minimize loss, while the maximization represents the attacker's goal of maximizing disruption. The recursive structure encodes the trade-off between immediate costs and future consequences, allowing resilience strategies to be optimized over time.

Shapley's classical result guarantees that for any finite discounted zero-sum stochastic game [236, 237], there exists a stationary Markov strategy profile (π_A^*, π_D^*) that forms an equilibrium, and that the associated value function $V(s)$ is unique. In general-sum games, the definition extends to a *Markov perfect equilibrium*, a stationary profile (π_A^*, π_D^*) such that each player's value function $V_i(s)$ satisfies its own Bellman optimality condition given the opponent's policy:

$$V_i(s) = \mathbb{E}[u_i(s, e, r) + \beta V_i(s') \mid e \sim \pi_A^*(s), r \sim \pi_D^*(s)], \quad \pi_i^*(s) \in \arg \max_{\pi_i} V_i(s).$$

While existence of MPE is guaranteed in finite discounted games, uniqueness of equilibrium strategies is not, and multiple equilibria may yield different resilience outcomes in practice.

Bayesian and epistemic equilibria. In realistic 5G networks, players rarely have complete knowledge of the environment or of each other's capabilities. Attackers may be uncertain about whether a given slice is genuine or a honeypot, while defenders may lack clarity about the attacker's type, for instance, whether the adversary is an unsophisticated botnet operator, a financially motivated cybercriminal, or a nation-state actor with advanced resources. To capture such uncertainties, one must move beyond complete-information games and employ *Bayesian games* [238], where players hold private information about their own

characteristics, called *types*.

Formally, let $\theta_A \in \Theta_A$ denote the attacker's type and $\theta_D \in \Theta_D$ the defender's type. The pair (θ_A, θ_D) is drawn from a common prior distribution $p \in \Delta(\Theta_A \times \Theta_D)$. Types influence payoffs and feasible actions: a high-skill attacker may have access to advanced jamming techniques, while a low-skill attacker may only generate simple floods. Similarly, a resource-rich defender may afford dynamic slice migration, whereas a constrained defender may rely only on throttling.

A *strategy* for player $i \in \{A, D\}$ is a mapping

$$\sigma_i : \mathcal{H}_t \times \Theta_i \longrightarrow \Delta(\mathcal{A}_i),$$

where \mathcal{H}_t denotes the public history of play up to stage t , and θ_i is the player's private type. Thus, strategies are type-dependent: players condition their actions on what they know privately about themselves.

Because types are unobserved by the opponent, players form and update beliefs over the possible types of the other side. Let $\mu_t(\theta_j | h_t)$ be the defender's (or attacker's) belief about the other player's type θ_j , conditional on the history $h_t \in \mathcal{H}_t$. Beliefs evolve through Bayes' rule whenever the history h_t occurs with positive probability under the players' strategies. If $O(o_t | s_t)$ is the observation kernel describing how observable signals o_t arise from the true state s_t , then the posterior distribution satisfies

$$\mu_{t+1}(\theta_j | h_t, o_t) = \frac{\mu_t(\theta_j | h_t) O(o_t | s_t, \theta_j)}{\sum_{\theta'_j} \mu_t(\theta'_j | h_t) O(o_t | s_t, \theta'_j)},$$

whenever the denominator is nonzero. This recursive update reflects how defenders in 5G adjust their threat models in real time by combining prior expectations with newly observed measurement (e.g., abnormal signaling rates or jamming patterns).

A central solution concept is the *Perfect Bayesian Equilibrium (PBE)* [234]. A PBE is a triple $(\sigma_A^*, \sigma_D^*, \mu^*)$ consisting of attacker and defender strategies and a system of beliefs such that:

- (i) *Sequential rationality*. At every history h_t that arises with positive probability under (σ_A^*, σ_D^*) , each player's strategy is optimal given their beliefs. Formally, for each player i ,

$$\sigma_i^*(\cdot | h_t, \theta_i) \in \arg \max_{\sigma_i} \mathbb{E} \left[\sum_{k=0}^{\infty} \beta^k u_i(s_{t+k}, e_{t+k}, r_{t+k}) \mid h_t, \theta_i, \sigma_j^*, \mu^* \right].$$

- (ii) *Belief consistency*. Beliefs μ^* are updated from the prior p using Bayes' rule whenever

possible, given the equilibrium strategies. On equilibrium paths, beliefs coincide with Bayesian posteriors; off equilibrium paths, beliefs are assigned in a way consistent with the spirit of rational inference.

The PBE concept generalizes Nash equilibrium by requiring not only that strategies are mutual best responses, but also that beliefs are internally consistent with observed actions. This refinement is essential in resilience analysis: a defender deploying honeypots must consider how attackers update their beliefs upon observing suspicious slice behaviors, and whether these beliefs lead attackers to avoid, engage, or ignore the decoys.

An alternative but equivalent framework is provided by *epistemic game theory* [239]. Instead of focusing directly on type distributions, epistemic models describe what players know and believe through *information partitions*. Each player's information is represented by a partition of the state space: the player knows which partition cell they are in, but not which exact state. Aumann (1976) formalized the notion of *common knowledge* as information that is not only known by each player, but also known to be known, and so on recursively. When combined with a common prior over states, epistemic models are equivalent to Harsanyi's Bayesian games.

3.2.4 Equilibria and dynamic programming.

Equilibrium analysis in dynamic games is inherently multistage, since players repeatedly interact over time and the outcome of each stage influences future opportunities and payoffs. At each stage $t = 0, 1, 2, \dots$, the system resides in a state $s_t \in \mathcal{S}$, and players simultaneously select actions $a_t = (a_t^1, \dots, a_t^N) \in \mathcal{A}^1 \times \dots \times \mathcal{A}^N$. The state evolves according to a controlled transition kernel

$$s_{t+1} \sim P(\cdot \mid s_t, a_t),$$

and each player i accrues a stage payoff $u^i(s_t, a_t)$. The infinite-horizon discounted return of player i is

$$J^i(s_0, \sigma) = \mathbb{E} \left[\sum_{t=0}^{\infty} \gamma^t u^i(s_t, a_t) \mid s_0, \sigma \right],$$

where $\sigma = (\sigma^1, \dots, \sigma^N)$ is a profile of stationary strategies and $\gamma \in (0, 1)$ is the discount factor.

The multistage structure implies that equilibrium computations are inherently recursive: each player's optimal strategy today depends on the expected continuation value of future states, which in turn depend on the strategies of others. This recursive interdependence is the essence of the connection between dynamic programming and equilibrium analysis.

Zero-sum discounted stochastic games. In the two-player zero-sum case ($u^1 = -u^2$), Shapley's celebrated recursion generalizes the Bellman equation. Let $V(s)$ denote the value function for the maximizing player. Then

$$V(s) = \max_{\sigma^1(\cdot|s)} \min_{\sigma^2(\cdot|s)} \left\{ \mathbb{E}_{a \sim \sigma^1 \times \sigma^2} [u^1(s, a)] + \gamma \sum_{s' \in \mathcal{S}} P(s' | s, a) V(s') \right\}.$$

This operator is a γ -contraction on the space of bounded functions, so repeated iteration converges to the unique fixed point $V^*(s)$. Computationally, this suggests a value iteration scheme:

$$V_{k+1}(s) = \max_{\sigma^1} \min_{\sigma^2} \left\{ \mathbb{E}[u^1(s, a)] + \gamma \sum_{s'} P(s' | s, a) V_k(s') \right\},$$

which converges at rate $O(\gamma^k)$. The equilibrium strategies $(\sigma^{1*}, \sigma^{2*})$ are obtained by solving the stage game defined by the right-hand side at each state.

General-sum stochastic games. When payoffs are not strictly opposed, each player i seeks to maximize their own return. The value function for player i satisfies the Bellman recursion

$$V^i(s) = \max_{\sigma^i(\cdot|s)} \mathbb{E}_{a \sim \sigma^i \times \sigma^{-i}} \left[u^i(s, a) + \gamma \sum_{s'} P(s' | s, a) V^i(s') \right].$$

Unlike the zero-sum case, these equations are coupled across players: the optimality condition for σ^i depends on σ^{-i} , and vice versa. A profile of stationary strategies $\sigma^* = (\sigma^{1*}, \dots, \sigma^{N*})$ is a *Markov Perfect Equilibrium (MPE)* if the Bellman recursion for each player is simultaneously satisfied.

The existence of an MPE in finite-state, finite-action discounted stochastic games is guaranteed, but uniqueness is not. Computation typically requires iterative fixed-point algorithms (e.g., policy iteration, Newton–Kantorovich methods, or reinforcement learning approximations). Complexity grows sharply with the number of players, as solving the stage game at each iteration involves computing Nash equilibria of finite normal-form games.

Bayesian dynamic games. When players have private types $\theta_i \in \Theta_i$, the effective state includes not only physical conditions but also beliefs about types. Let $\mu_t \in \Delta(\Theta)$ denote the public belief distribution over type profiles $\theta = (\theta_1, \dots, \theta_N)$. Given public history h_t , players update beliefs using Bayes' rule. The dynamic programming recursion is now expressed in the belief space:

$$V^i(\mu) = \max_{\sigma^i(\cdot|\mu)} \mathbb{E}_{\theta \sim \mu, a \sim \sigma^i \times \sigma^{-i}} \left[u^i(\theta, a) + \gamma \sum_{\mu'} P(\mu' | \mu, a) V^i(\mu') \right],$$

where $P(\mu' \mid \mu, a)$ is the transition kernel over beliefs induced by Bayes' rule. Equilibria of such Bayesian dynamic games refine Perfect Bayesian Equilibrium to the infinite-horizon setting, requiring consistency of strategies and beliefs at every stage.

Computationally, belief spaces are continuous and high-dimensional, so approximate dynamic programming or point-based value iteration (adapted from POMDP methods) is often necessary. This highlights the intrinsic difficulty of incomplete-information dynamic games compared to fully observed ones.

3.3 Learning as the Foundation

Game-theoretic modeling provides a rigorous language for analyzing adversarial interactions, but its practical effectiveness is constrained by uncertainties in both model structure and parameters. Threat models rarely capture the full spectrum of adversarial behavior, especially in the presence of zero-day exploits or highly adaptive attackers. Even if models are initially accurate, adversaries may evolve faster than the models can be updated. Furthermore, aleatoric uncertainties in payoffs, admissible action sets, common priors, and network dynamics introduce further mismatches between prescriptive models and operational realities.

Learning emerges as the essential complement to game and control theory. By continuously adapting policies based on feedback, refining beliefs, and recalibrating models, learning enables defenders to sustain resilience in nonstationary and uncertain environments. In this sense, learning is not an afterthought but the foundational layer that operationalizes resilience. It transforms equilibrium analysis from a static prediction into a dynamic process of adaptation, recovery, and stability.

3.3.1 Learning dynamics in games

Learning in games provides a mathematical framework to describe how players iteratively adjust strategies over repeated interactions [240, 241]. Let $\pi_i^k \in \Delta(\mathcal{A}_i)$ denote the mixed strategy of player $i \in \{A, D\}$ at stage k , where $\Delta(\mathcal{A}_i)$ is the simplex over the action set. Suppose the defender receives a payoff u_D^k at stage k , generated from the stochastic dynamics of the network, and updates its policy according to

$$\pi_D^{k+1} = \pi_D^k + \lambda^k (F_D(I_D^k, \pi_D^k) + M_D^k).$$

Here λ^k is the learning rate, I_D^k is the defender's feedback (such as local queue lengths, delays, or alerts), F_D is the deterministic update term encoding the learning rule, and M_D^k is a martingale-difference noise term capturing randomness in observations. The attacker updates π_A^k analogously.

This recursion belongs to the class of stochastic approximation algorithms. Under standard conditions on step sizes ($\lambda^k \rightarrow 0$ with $\sum_k \lambda^k = \infty$) and boundedness of noise, the asymptotic behavior of $\{\pi_A^k, \pi_D^k\}$ can be studied via the associated mean-field ODE:

$$\dot{\pi}_i = F_i(\pi_i, \pi_{-i}), \quad i \in \{A, D\}.$$

Equilibria of this ODE correspond to Nash or Stackelberg equilibria of the underlying game. The key question is whether the equilibria are stable: if small deviations caused by shocks or adversarial perturbations are corrected by the learning dynamics, then the system converges back toward equilibrium. Lyapunov analysis provides the mathematical tool to certify this stability.

3.3.2 Resilience control as a learning process

Resilience should not be understood only as the asymptotic convergence to equilibrium, but as the ability of the learning process itself to adapt, recover, and stabilize performance in the presence of disturbances. Formally, let $V^*(s)$ denote the defender's equilibrium value function under the limiting strategy profile $\pi^* = (\pi_A^*, \pi_D^*)$. The system is said to be *resilient* if the learning trajectories (π_A^k, π_D^k) ensure both bounded long-run losses and effective short-run recovery whenever disruptions occur.

Suppose there exists a Lyapunov function $L(\pi_A, \pi_D) \geq 0$ such that along the trajectories of the learning process,

$$\dot{L}(\pi_A, \pi_D) \leq -\alpha(\ell(x_t, e_t, r_t) - \bar{L}),$$

for some $\alpha > 0$, where $\ell(x_t, e_t, r_t)$ is the instantaneous loss and \bar{L} is a performance threshold. This inequality implies that whenever loss exceeds acceptable levels, the adaptive process acts to reduce it. Resilience here is not a fixed robustness property but a dynamic guarantee: the learning system continuously monitors, adapts, and recovers, ensuring that even under repeated adversarial shocks or random faults, the process is driven back toward safe operation.

Thus, resilience is inherently a *learning process*. The system does not simply resist attacks; it observes deviations, updates strategies, and recovers performance in real time. This aligns resilience with the asymptotic stability of equilibria while also emphasizing transient

adaptation and recovery.

3.3.3 Feedback structures and observability

The convergence and quality of learning dynamics depend critically on the information structure. In complete-information settings, where both players observe the full state and payoffs, learning rules such as fictitious play or regret minimization can converge to equilibrium under broad conditions. In realistic cyber-defense scenarios, however, feedback is local, noisy, and often delayed.

For example, a defender may only observe local queue lengths and slice performance, not the attacker’s action directly. Conversely, the attacker may infer migration policies indirectly through probing rather than observing them outright. Formally, if I_i^k denotes the local signal available to player i , then the update rule depends on conditional expectations $\mathbb{E}[u_i | I_i^k]$ rather than exact utilities. Stability in such decentralized settings typically requires monotonicity or a potential structure in the induced ODE, ensuring that distributed learning rules do not diverge or cycle.

This feedback limitation makes conjectural learning particularly relevant: defenders and attackers both form forecasts about the opponent’s strategy, update them based on local signals, and adapt accordingly. The accuracy and adaptability of these conjectures directly influence resilience.

3.3.4 Reinforcement and Meta-Learning

Reinforcement learning (RL) arises when agents update strategies directly from payoff signals without relying on explicit models of system dynamics or adversary behavior. In the context of resilience, the defender faces a sequential decision problem: at each state s_t , actions a_t correspond to mitigation mechanisms such as workload migration, resource scaling, slice balancing, or spectrum reassignment. The environment responds stochastically due to both adversarial disturbances and natural faults, generating a new state s_{t+1} and payoff u_t . The defender updates its value estimates through experience, gradually improving policy quality.

A canonical update rule is the Q -learning recursion,

$$Q_{t+1}(s, a) = (1 - \alpha_t) Q_t(s, a) + \alpha_t \left(u_t + \beta \max_{a'} Q_t(s', a') \right), \quad (3.17)$$

where α_t is a decaying learning rate and β the discount factor. This update allows the defender to learn effective resilience policies online even when attacker strategies are unknown or non-stationary. For instance, if an adversary launches jamming bursts intermittently, RL

enables the defender to discover spectrum-hopping patterns that maximize service continuity while minimizing unnecessary overhead.

Meta-Learning. Classical RL optimizes for a single environment, but cyber adversaries evolve, and novel exploits continuously emerge. Meta-learning extends RL by training across a distribution of tasks (attack scenarios), producing a meta-policy that encodes adaptation strategies rather than fixed responses. In practice, the meta-policy is parameterized by θ , which is updated in two loops: an *inner loop* that adapts to a specific task (e.g., denial-of-service against MEC nodes), and an *outer loop* that optimizes θ across tasks to enable rapid adaptation. Formally, the outer update takes the form

$$\theta \leftarrow \theta - \gamma \nabla_{\theta} \mathbb{E}_{\mathcal{T} \sim p(\mathcal{T})} [\mathcal{L}_{\mathcal{T}}(\theta - \eta \nabla_{\theta} \mathcal{L}_{\mathcal{T}}(\theta))],$$

where \mathcal{T} indexes attack tasks, $\mathcal{L}_{\mathcal{T}}$ is the loss for task \mathcal{T} , and (η, γ) are step sizes. This Model-Agnostic Meta-Learning (MAML) formulation [242, 243, 244] is particularly suited to resilience, as it equips defenders to handle zero-day exploits with minimal retraining, critical in environments where reaction time directly impacts service-level compliance.

Conjectural Online Learning. In asymmetric-information settings, defenders must anticipate attacker strategies while updating their own. Conjectural Online Learning (COL) generalizes RL by incorporating forecasts of opponent behavior into the learning loop [178, 192]. Architectures such as forecaster–actor–critic models maintain beliefs μ_t about attacker actions, update them as evidence accumulates, and adapt policies accordingly. Concretely, the defender maintains:

- a *forecaster* that predicts the attacker’s next action distribution given past observations,
- an *actor* that selects a mitigation action a_t based on both current state and forecasts,
- a *critic* that evaluates outcomes to refine value estimates and update beliefs.

This creates a closed-loop adaptation scheme where resilience is maintained not only against known attack models but also against adaptive and persistent adversaries who themselves learn over time.

3.3.5 Toward Predictive Resilience

The integration of RL, meta-learning, and conjectural online adaptation highlights that resilience can be both *predicted* and *designed*. Specifically, resilience corresponds to the ability

of learning dynamics to converge toward equilibria that sustain bounded loss while satisfying service-level guarantees. If trajectories of (s_t, a_t) remain within a basin of attraction of resilient equilibria, disruptions are contained; if they cycle or diverge, resilience collapses even if equilibria exist in principle.

Equilibria and Learning Dynamics. In a slice-mitigation example, the defender learns a threshold-based migration rule: when load exceeds a critical level due to adversarial flooding, workloads are shifted to backup MEC nodes. If the attacker stabilizes at a sustainable level of flooding intensity, the system converges to a stable equilibrium characterized by a steady-state value function $V^*(s)$ satisfying the Bellman equation

$$V^*(s) = \max_{a \in \mathcal{A}} \left(u(s, a) + \beta \mathbb{E}[V^*(s') \mid s, a] \right).$$

Here, $V^*(s)$ serves both as a predictive metric of resilience and as a design target.

Basins of Attraction. The resilience of a system depends not only on the equilibria but also on whether learning-driven trajectories converge into them. For example, policies that yield oscillatory migration patterns (frequent switching of slices) may technically satisfy SLA thresholds on average but erode resilience due to instability and wasted resources. Designing reward shaping, step-size schedules, and regularization terms ensures convergence into stable equilibria rather than into pathological cycles [225, 88].

Predictive Implications. Resilience is therefore defined not simply by static metrics (e.g., MTTR, downtime) but by the dynamical properties of learning. Predictive resilience analysis asks: given a learning architecture (RL, meta-learning, COL) and an adversarial strategy space, does the joint adaptation process converge, recover after perturbations, and sustain service guarantees? By embedding resilience objectives into the learning dynamics, networks can be designed to self-stabilize under uncertainty, thereby making resilience a controllable and verifiable property of next-generation infrastructures.

3.4 Network-Theoretic Foundation

The resilience of complex communication infrastructures is intrinsically shaped by the structural and spatial organization of their connectivity. Network science provides a rigorous mathematical language to describe, analyze, and quantify these interconnections and their influence on the ability of a system to maintain functionality under failures or distur-

bances [245]. This section presents the foundational concepts underlying network connectivity, spatial geometry, percolation, and propagation, which together form the analytical basis for resilience modeling.

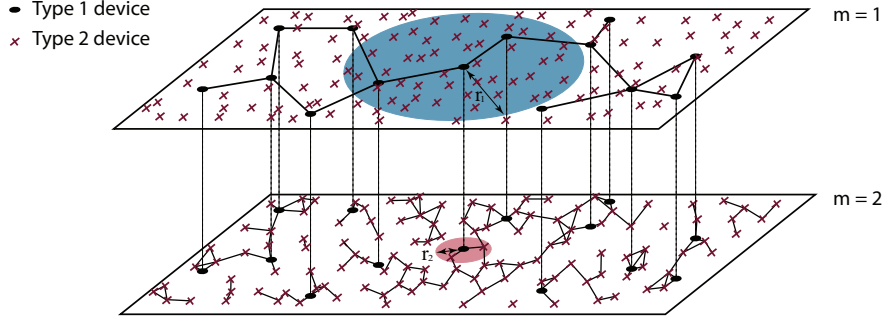


Figure 3.4: Device connectivity across heterogeneous network devices with a different communication range.

Foundations of Network Connectivity

Let a network be represented as a graph $\mathcal{G} = (\mathcal{V}, \mathcal{E})$, where \mathcal{V} is the set of nodes and \mathcal{E} is the set of links between them. The local connectivity of the graph is characterized by the degree distribution $P(k)$, which defines the probability that a randomly selected node has k connections. The global structure of \mathcal{G} determines how efficiently information or failures can propagate.

In the classical Erdős–Rényi (ER) random graph [246], each pair of nodes is connected independently with probability p , producing a binomial degree distribution that approaches a Poisson law for large networks. Although mathematically tractable, the ER model assumes homogeneous connectivity, which seldom reflects the irregular and heterogeneous structures observed in real communication systems.

Empirical studies have demonstrated that many natural and engineered networks, including the Internet and social interaction graphs, exhibit heavy-tailed degree distributions that follow a power law,

$$P(k) \sim k^{-\gamma}, \quad 2 < \gamma < 3.$$

Such *scale-free* networks emerge from growth and preferential attachment mechanisms and possess a small number of highly connected hubs [247]. This topology improves efficiency and fault tolerance against random failures yet increases vulnerability to targeted attacks on hubs. Structural robustness can be quantitatively evaluated using spectral metrics such as the algebraic connectivity $\lambda_2(L)$ of the Laplacian matrix, which measures global cohesion, and the spectral radius $\rho(A)$ of the adjacency matrix, which determines the potential for

rapid diffusion of perturbations.

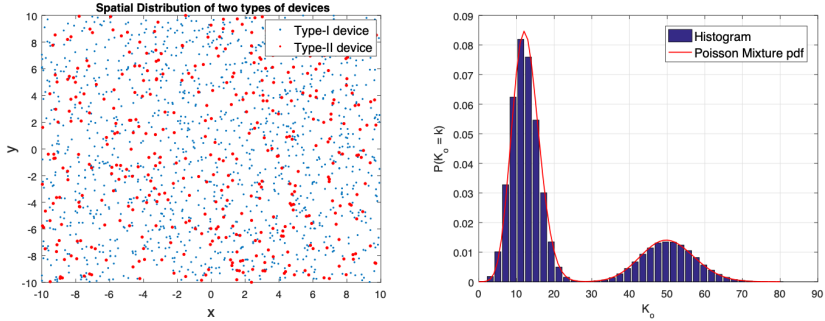


Figure 3.5: Degree distribution of network with two type of devices scattered uniformly in space.

Spatial Embedding and Random Geometric Networks

While abstract topological models reveal structural heterogeneity, real communication infrastructures are spatially embedded and constrained by physical proximity, propagation, and interference. Spatial randomness is commonly captured using the homogeneous Poisson point process (PPP) [248],

$$\Phi = \{x_i\}_{i \geq 1} \subset \mathbb{R}^2, \quad x_i \sim \text{PPP}(\lambda),$$

where λ denotes the node density in nodes per unit area. Two nodes x_i and x_j are connected if $\|x_i - x_j\| \leq r$, where r represents the communication range. The resulting random geometric graph (RGG) [249] exhibits a Poisson degree distribution

$$\mathbb{P}[K = k] = e^{-\lambda\pi r^2} \frac{(\lambda\pi r^2)^k}{k!}, \quad \mathbb{E}[K] = \lambda\pi r^2.$$

This spatial model establishes a direct correspondence between physical deployment parameters (λ, r) and network connectivity. As the density λ or range r increases, the network transitions from a fragmented topology to a fully connected one. This phase transition is described by percolation theory.

Percolation and Structural Transitions

Percolation theory provides the mathematical framework to study the emergence of large-scale connectivity as links or nodes are randomly added or removed [250]. Let p denote the probability that a link or node is functional. A critical value p_c marks the percolation threshold that separates disconnected and connected regimes. For $p < p_c$, the network

consists of isolated clusters of limited size; for $p > p_c$, a macroscopic connected component spans the system, enabling long-range communication or cascading influence. In random geometric networks, p_c depends on the product $\lambda\pi r^2$, which represents the expected number of neighbors per node. The percolation transition thus reflects a geometric phase change controlled by deployment density and communication range, providing an interpretable link between physical layout and resilience.

In the context of communication systems, operating well above the percolation threshold ensures redundant paths and fault tolerance. Conversely, systems near the critical regime are sensitive to small perturbations and therefore exhibit fragile connectivity. Percolation theory thereby formalizes the notion of *structural resilience*, where connectivity and reachability are preserved despite random disruptions.

Dynamic Processes and Propagation Models

Structural connectivity defines the potential for interaction, but resilience also depends on how dynamic processes evolve over the network. Information dissemination, congestion, cascading failures, and cyber threats can all be modeled as state transitions among interacting nodes [251]. Let $x_i(t)$ denote the state of node i at time t . A general state-space representation is given by

$$\frac{dx_i(t)}{dt} = \sum_j a_{ij} f(x_i(t), x_j(t)),$$

where a_{ij} are elements of the adjacency matrix A and $f(\cdot)$ specifies the interaction dynamics. Epidemic-inspired formulations provide an intuitive basis for these interactions. In the susceptible–infected–susceptible (SIS) model [252], the rate of change of the infected fraction in the population is

$$\frac{dI(t)}{dt} = \beta(1 - I(t))\Theta(t) - \mu I(t),$$

where β is the transmission rate, μ the recovery rate, and $\Theta(t)$ the probability that a randomly selected neighbor is infected. This abstraction applies not only to malware propagation but also to the diffusion of information or overload within a networked infrastructure.

Linearization around equilibrium yields a stability condition governed by the spectral radius $\rho(A)$. The process remains subcritical, and disturbances dissipate if the effective ratio $\beta/\mu < 1/\rho(A)$, whereas supercritical dynamics ($\beta/\mu > 1/\rho(A)$) lead to self-sustaining propagation. This threshold provides a direct connection between structural properties and dynamic stability.

Equilibrium Analysis and Design Interpretation

The equilibrium of the propagation process characterizes the steady-state composition of network states, such as the proportion of active, inactive, or compromised nodes, as functions of structural and dynamical parameters. At equilibrium, the condition

$$\mathcal{R}_0 = \frac{\beta \mathbb{E}[K]}{\mu} < 1$$

ensures that the system remains resilient, with perturbations decaying to zero [226, 253]. Here \mathcal{R}_0 represents the effective reproduction number, which integrates both topological and temporal effects. The threshold $\mathcal{R}_0 = 1$ delineates the boundary between stability and systemic propagation. This framework leads to an equilibrium-centric view of network design: resilience can be engineered by adjusting controllable parameters such as density λ , communication range r , and recovery rate μ to ensure that the equilibrium remains within the subcritical regime.

Chapter 4

Cyber Risk Assessment for NextG Networks

Risk assessment techniques are foundational to designing and maintaining resilient next-generation networks. The complexity, heterogeneity, and programmability of 5G infrastructures require dynamic and multifaceted approaches to evaluating threat exposure and system vulnerabilities. This chapter outlines four major approaches used in practice and research: adversarial exercises (blue/red teaming), digital twins and simulation environments, game-theoretic modeling, and supply chain risk analysis.

4.1 Probabilistic Risk Assessment with Digital Twins

Probabilistic Risk Assessment (PRA) provides a principled framework for quantifying the likelihood and consequences of disruptive events in complex infrastructures [254, 255]. Unlike classical reliability analysis, which assumes deterministic failures or component-level probabilities, PRA explicitly accounts for uncertainty by assigning probabilities to a family of disruption scenarios and evaluating their systemic effects. This probabilistic treatment is particularly critical in 5G/NextG networks, where virtualization, disaggregation, and open programmability create broad and interdependent attack surfaces.

Let $\mathcal{Q} = \{q^{(1)}, q^{(2)}, \dots, q^{(m)}\}$ denote the set of disruptive scenarios, each occurring with probability $p(q^{(i)})$. A scenario $q^{(i)}$ may represent, for example, a fronthaul jamming attack, a CU software exploit, or simultaneous slice-level faults. For a given defense policy π , the resilience loss under scenario $q^{(i)}$ is denoted by $L^{(q^{(i)})}(\pi)$. PRA then evaluates the expected resilience loss

$$\mathbb{E}[L(\pi)] = \sum_{i=1}^m p(q^{(i)}) L^{(q^{(i)})}(\pi), \quad (4.1)$$

and may further assess higher-order risk measures such as variance or Conditional Value-at-Risk (CVaR) [256]. These provide operators with insights into which scenarios dominate risk, which investments in resilience yield the largest marginal benefit, and how combinations of hazards can amplify fragility.

Within the digital-twin dynamics of Chapter 3, disruptions evolve in time according to (3.2), where q_t describes the temporal evolution of disruptions within the system at time t , while $q^{(i)}$ is used as a scenario label in PRA. This distinction allows us to integrate PRA’s probabilistic scenario analysis with Chapter 3’s dynamic models.

Digital twins (DTs) complement PRA by simulating the impact of scenarios $q^{(i)}$ on time-evolving network dynamics. A DT maintains a synchronized network state \hat{x}_t mirroring the real state x_t and generates synthetic measurements \hat{y}_t that align with observed outputs y_t . PRA provides probabilities over scenarios, while DTs instantiate these scenarios in realistic 5G dynamics, enabling operators to explore “what-if” conditions without endangering live systems.

4.1.1 State–Space View and Twin Synchronization

Digital twins (DTs) augment PRA by embedding disruption scenarios into the hybrid dynamics introduced in Chapter 3. While PRA quantifies risks at the level of probabilities, DTs instantiate them within a stochastic state–space model that mirrors live 5G networks. The real network is written as

$$x_{t+1} = f(x_t, u_t, w_t, \xi_t, q_t), \quad (4.2)$$

where x_t is the network state, u_t is the control action generated by the policy π , w_t denotes adversarial inputs (e.g., jamming, API abuse), ξ_t is the natural disturbance (e.g., traffic bursts, random failures), and q_t is the disruption process describing abnormal operating modes. In this section we treat w_t as fixed by the scenario, so PRA evaluates how different possible trajectories of q_t affect resilience. More generally, disruptions evolve dynamically according to

$$q_{t+1} = \phi(q_t, x_t, u_t, w_t, \xi_t), \quad (4.3)$$

so adversarial, environmental, and control factors jointly shape future disruptions.

The DT runs in parallel as a surrogate model,

$$\hat{x}_{t+1} = \hat{f}(\hat{x}_t, u_t, \hat{w}_t, \xi_t, q_t), \quad (4.4)$$

driven by the same controls u_t and by replayed or simulated attacks \hat{w}_t . Synchronization is

quantified by

$$e_t = \|x_t - \hat{x}_t\|, \quad \mathcal{F}_T = 1 - \frac{1}{T} \sum_{t=1}^T \frac{e_t}{e_{\max}}, \quad (4.5)$$

where $\mathcal{F}_T \in [0, 1]$ is a normalized fidelity score. High values of \mathcal{F}_T indicate that the twin closely captures the evolution of the real network, ensuring that the PRA results remain representative of the 5G dynamics.

Scenario-Driven Trajectory Evaluation. Let $\mathcal{Q} = \{q^{(1)}, \dots, q^{(m)}\}$ denote the disruption *scenarios* (labels) with probabilities $p(q^{(i)})$. A scenario $q^{(i)}$ specifies a fixed adversarial input path $w_{0:T-1}^{(i)}$, initial conditions $(x_0^{(i)}, q_0^{(i)})$, and, when feedback evolution is enabled, the disruption law $\phi^{(i)}$ used in (4.3). Given a policy $u_t = \pi(\hat{x}_t)$, the twin rolls out

$$\hat{x}_{t+1}^{(i)} = \hat{f}\left(\hat{x}_t^{(i)}, \pi(\hat{x}_t^{(i)}), \hat{w}_t^{(i)}, \xi_t, q_t\right),$$

producing a trajectory $\{\hat{x}_t^{(i)}\}_{t=0}^T$ for the scenario $q^{(i)}$. (When feedback evolution is used, q_t is propagated via $q_{t+1} = \phi^{(i)}(q_t, \hat{x}_t^{(i)}, \pi(\hat{x}_t^{(i)}), \hat{w}_t^{(i)}, \xi_t)$.)

Resilience Quantification from Trajectories. Let $h : \mathbb{R}^n \rightarrow \mathbb{R}$ map the state to a scalar *measurement* (e.g., slice latency, URLLC reliability, throughput). Define the normalized shortfall and cumulative loss in a window $[t_f, t_r]$:

$$\hat{Q}_t^{(i)} = h(\hat{x}_t^{(i)}), \quad s_t^{(i)}(\pi) = 1 - \frac{\hat{Q}_t^{(i)}}{\hat{Q}_{\max}}, \quad L^{(q^{(i)})}(\pi) = \sum_{t=t_f}^{t_r} s_t^{(i)}(\pi). \quad (4.6)$$

Two complementary summaries are often reported:

$$M^{(q^{(i)})}(\pi) = \max_{t \in [t_f, t_r]} s_t^{(i)}(\pi) \quad (\text{maximum drop}),$$

$$D^{(q^{(i)})}(\pi) = s_{t_r}^{(i)}(\pi) \quad (\text{residual deficit}).$$

For availability-style evaluation with threshold Q_{\min} :

$$T_d^{(q^{(i)})}(\pi) = \sum_{t=t_f}^{t_r} \mathbf{1}\left\{ \hat{Q}_t^{(i)} < Q_{\min} \right\}.$$

Monte Carlo over Natural Disturbances. To account for randomness in ξ_t , draw N i.i.d. samples $\{\xi_{0:T-1}^{(i,k)}\}_{k=1}^N$ and average the losses:

$$\widehat{\mathbb{E}}_{\xi}[L^{(q^{(i)})}(\pi)] = \frac{1}{N} \sum_{k=1}^N L^{(q^{(i)})}, \xi^{(i,k)}(\pi), \quad (4.7)$$

$$\widehat{\text{Var}}_{\xi}[L^{(q^{(i)})}(\pi)] = \frac{1}{N-1} \sum_{k=1}^N \left(L^{(q^{(i)})}, \xi^{(i,k)}(\pi) - \widehat{\mathbb{E}}_{\xi}[L^{(q^{(i)})}] \right)^2. \quad (4.8)$$

Aggregation across Scenarios. PRA combines per-scenario statistics using the scenario probabilities:

$$\begin{aligned} \mathbb{E}[L(\pi)] &= \sum_{i=1}^m p(q^{(i)}) \mathbb{E}_{\xi}[L^{(q^{(i)})}(\pi)], \\ \text{CVaR}_{\alpha}[L(\pi)] &= \min_{\eta} \left\{ \eta + \frac{1}{1-\alpha} \mathbb{E}[(L(\pi) - \eta)_+] \right\}. \end{aligned} \quad (4.9)$$

These quantities assess how resilient the system is, on average and in the tail, across the set of scenarios \mathcal{Q} .

In URLLC, $h(x_t)$ might return deadline-meeting reliability; shortfalls $s_t^{(i)}$ then capture reliability dips during fronthaul jamming plus CU overload. In eMBB, $h(x_t)$ can be throughput; the same pipeline quantifies drops and recovery after the transport-layer congestion. Because the twin uses the same policy $u_t = \pi(\hat{x}_t)$ as the real network and maintains high synchronization fidelity, the resulting metrics $L^{(q^{(i)})}, M^{(q^{(i)})}, D^{(q^{(i)})}, T_d^{(q^{(i)})}$ provide actionable evidence about how *state* x_t evolves under each scenario and how robust the system is across the mixture defined by $p(q^{(i)})$.

4.2 Strategic Risk Assessment

Strategic risk assessment assesses resilience against *adaptive* adversaries who plan, coordinate and optimize their actions. It extends the framework of PRA by replacing exogenous scenario probabilities with adversarial decision-making. Whereas PRA quantifies expected loss across random disruptions, strategic risk asks:

What is the performance degradation when attacker and defender both act strategically?

In 5G/NextG networks, this formulation is crucial: adversaries can investigate vulnerabilities, adapt to defenses, and optimize their disruption strategies over time.

Formally, we embed the attacker-defender interaction in the same hybrid dynamics as Chapter 3, but with w_t (attacker actions) chosen strategically rather than probabilistically.

4.2.1 Red–Blue Teaming as a Game

The network evolves according to (3.1) and (3.2), where u_t the defender’s action, w_t the attacker’s action. Both sides choose actions via policies π_b and π_r , possibly under partial observations (as in Chapter 3).

Let $h : \mathbb{R}^n \rightarrow \mathbb{R}$ be a scalar performance measure (e.g., URLLC reliability, eMBB throughput), normalized by $Q_{\max} > 0$. The defender seeks to preserve performance. Define the stage loss

$$\ell_b(x, u) = 1 - \frac{h(x)}{Q_{\max}} + c_b(u),$$

where $c_b(u)$ is the operational cost of defense (e.g., scaling or rerouting overhead). The defender minimizes cumulative loss

$$L_b(\pi_b, \pi_r) = \sum_{t=t_f}^{t_r} \ell_b(x_t, u_t). \quad (4.10)$$

The adversary may pursue a different objective from simply maximizing L_b . For instance, it may wish to maximize disruption subject to resource constraints or balance stealth with impact. Define the stage utility

$$u_r(x, w) = \alpha \left(1 - \frac{h(x)}{Q_{\max}} \right) - c_r(w),$$

where $\alpha \geq 0$ weights the attacker’s preference for disruption and $c_r(w)$ is the cost of the attack effort (for example, power for jamming, risk of detection). The attacker maximizes cumulative utility

$$L_r(\pi_b, \pi_r) = \sum_{t=t_f}^{t_r} u_r(x_t, w_t). \quad (4.11)$$

This formulation admits both *zero-sum* (when $L_r = -L_b$ and costs align) and *general-sum* (when attacker’s goal differs) structures.

Strategic risk formalizes resilience evaluation when the attacker and the defender act strategically rather than randomly [257, 258]. Let Π_b and Π_r denote the sets of admissible defender and attacker policies, respectively. Each policy profile $(\pi_b, \pi_r) \in \Pi_b \times \Pi_r$ induces a stochastic trajectory $\{x_t\}$ through the dynamics of Eq. (3.1), and corresponding performance metrics such as the cumulative defender loss $L_b(\pi_b, \pi_r)$ and attacker utility $L_r(\pi_b, \pi_r)$.

Definition (Strategic Risk). The *strategic risk* of a system under the policy profile (π_b, π_r) is the vector

$$\mathcal{R}(\pi_b, \pi_r) = \left(\mathbb{E}[L_b(\pi_b, \pi_r)], \mathbb{E}[L_r(\pi_b, \pi_r)] \right),$$

where expectations are taken over exogenous uncertainties ξ_t (and possibly over randomized strategies). The strategic risk profile of the system is the set

$$\mathcal{R}^* = \{ \mathcal{R}(\pi_b^*, \pi_r^*) \mid (\pi_b^*, \pi_r^*) \text{ arises from a chosen solution concept} \}.$$

The choice of solution concept, robust min–max or game-theoretic equilibrium, determines how u_t and w_t are generated and thus how resilience is assessed.

1) Robust Worst-Case Risk. The conservative approach assumes that the attacker will always choose the most damaging policy, regardless of its actual incentives. The defender’s task is therefore to minimize the maximum possible expected loss:

$$V_{\text{robust}} = \inf_{\pi_b \in \Pi_b} \sup_{\pi_r \in \Pi_r} \mathbb{E}[L_b(\pi_b, \pi_r)]. \quad (4.12)$$

This formulation guarantees a performance bound under the most harmful rational adversary. The quantity V_{robust} defines a resilience *floor*: the defender can always ensure that its expected loss does not exceed this value, no matter how the attacker behaves.

2) Equilibrium Strategic Risk. When attacker and defender pursue distinct objectives, a more balanced formulation evaluates risk under equilibrium play. A policy pair (π_b^*, π_r^*) is a Nash equilibrium if neither side can improve its expected outcome by deviating:

$$\mathbb{E}[L_b(\pi_b^*, \pi_r^*)] \leq \mathbb{E}[L_b(\pi_b, \pi_r^*)] \quad \forall \pi_b \in \Pi_b, \quad \mathbb{E}[L_r(\pi_b^*, \pi_r^*)] \geq \mathbb{E}[L_r(\pi_b^*, \pi_r)] \quad \forall \pi_r \in \Pi_r. \quad (4.13)$$

In sequential settings, a Stackelberg equilibrium may be more suitable: the defender pre-commits to a policy, and the attacker best-responds.

At equilibrium, the outcomes

$$V_b^{\text{eq}} = \mathbb{E}[L_b(\pi_b^*, \pi_r^*)], \quad V_r^{\text{eq}} = \mathbb{E}[L_r(\pi_b^*, \pi_r^*)]$$

jointly characterize the system’s *strategic risk profile*. These equilibrium values are less conservative than the robust bound but more realistic when adversaries and defenders adapt strategically within operational constraints.

The **robust** approach secures the system against the most harmful adversary, providing guarantees even when the attacker’s incentives are unknown. The **equilibrium** approach captures the likely outcome of a rational contest where both sides adapt and optimize with their own cost–benefit tradeoffs.

Both perspectives are valuable. Robust risk highlights the system’s guaranteed resilience floor, while equilibrium risk provides insight into performance degradation in realistic adversarial environments. Together, they define the spectrum of *strategic risk* faced by 5G/NextG networks.

4.2.2 Integration with Digital Twins

Once the attacker and defender strategies (u_t^*, w_t^*) have been determined, either from the robust solution (4.12) or from the equilibrium solution (4.13), these actions are treated as fixed inputs to the digital twin. The twin then evolves according to

$$\widehat{x}_{t+1} = \widehat{f}(\widehat{x}_t, u_t^*, w_t^*, \xi_t, q_t), \quad (4.14)$$

where ξ_t captures random disturbances and q_t evolves according to the disruption dynamics.

In this way, the game specifies the adversarial strategies, while the digital twin simulates how the system responds under uncertainty. This two-stage procedure—first solving the game, then simulating the residual uncertainty—ensures that resilience is assessed under adversarially realistic conditions, consistent with the hybrid modeling foundations of Chapter 3.

4.2.3 Evaluating Resilience Metrics

Trajectory generation. For each scenario $q^{(i)}$ with initialization $(x_0^{(i)}, q_0^{(i)})$, the DT generates a trajectory $\{\widehat{x}_t^{(i)}\}_{t=0}^T$ by rolling out Eq. (4.14). Monte Carlo draws of ξ_t provide multiple realizations for each scenario, enabling statistical evaluation.

Metric computation. From the simulated state, define

$$\widehat{Q}_t = h(\widehat{x}_t), \quad s_t = 1 - \frac{\widehat{Q}_t}{Q_{\max}}.$$

These shortfalls produce the following resilience metrics:

$$L = \sum_{t=t_f}^{t_r} s_t \text{ (cumulative loss)}, \quad M = \max_{t \in [t_f, t_r]} s_t \text{ (maximum drop)},$$

$$D = s_{t_r} \text{ (residual deficit)}, \quad T_d = \sum_{t=t_f}^{t_r} \mathbf{1}\{\hat{Q}_t < Q_{\min}\} \text{ (downtime)}.$$

Aggregating across samples gives estimates of $\mathbb{E}[L]$, $\text{Var}[L]$, and tail measures such as CVaR_α .

Synchronization. To validate fidelity, the DT is run with the same defender policy u_t^* as in the live system and the fixed attacker action w_t^* . The synchronization error

$$e_t = \|x_t - \hat{x}_t\|, \quad \mathcal{F}_T = 1 - \frac{1}{T} \sum_{t=1}^T \frac{e_t}{e_{\max}},$$

quantifies how closely the twin tracks reality, with $\mathcal{F}_T \approx 1$ indicating high accuracy.

4.2.4 Insights from the Game to DT Pipeline

The integration of game-theoretic solutions with digital twin simulations provides several important insights into system resilience. First, it delivers *worst-case guarantees*. By solving the underlying game before simulation, the attacker's actions w_t^* are chosen to be adversarially optimal, either under the robust formulation or at equilibrium. The defender's actions u_t^* are similarly determined by the solution concept. When these actions are held fixed and rolled out in the digital twin, the resulting resilience metrics represent conservative yet decision-relevant estimates. This ensures that the outcomes reflect realistic adversarial behavior rather than arbitrary scenario design.

Second, the approach highlights *scenario sensitivity*. With the strategic actions (u_t^*, w_t^*) fixed by the game, the digital twin isolates the effects of disruption laws $q^{(i)}$ and natural disturbances ξ_t . By varying these elements across simulations, operators can observe how different attack–disturbance combinations shape degradation and recovery patterns. This makes it possible to identify not only worst-case impacts, but also the range of plausible system responses across diverse operating conditions.

Third, the pipeline supports *policy refinement*. If the simulated outcomes, measured by cumulative loss L , maximum drop M , residual deficit D , or downtime T_d , exceed acceptable thresholds, the defender can adjust its policy π_b and re-solve the game in either the robust or equilibrium framework. The updated strategies are then tested again in the digital twin.

This iterative cycle of solving, simulating, and refining closes the loop between theoretical analysis, policy design, and practical validation.

4.3 Network Analytics for Risk Analysis

Next generation communication infrastructures such as 5G and beyond cellular networks are assembled from many interacting hardware and software components that are procured and operated through complex supply and service chains. A quantitative treatment of cyber risk in such systems benefits from the machinery of reliability theory, where a system is represented as an interconnection of components and a structure function maps component states to system success or failure. In the present context, component states capture the success or failure of security relevant events such as compromise of a network function, exploitation of an interface, or malicious behaviour of a supplier, and the top event corresponds to violation of a specified security property of the network.

Attack Tree and System Graph Representation

A natural entry point is the attack tree representation of a high level compromise scenario. An attack tree is a rooted directed acyclic graph whose root encodes a system level goal such as loss of integrity of the core network or compromise of the slice orchestrator. Internal nodes represent intermediate attack goals and are connected to their children through logical relations of type AND or OR. A child set that is connected to its parent through an AND relation must all be achieved to fulfil the parent goal, whereas an OR relation means that any one of the children suffices. Leaves represent atomic attack steps such as exploitation of a protocol vulnerability in a baseband unit, insertion of malicious code in a virtualized network function, or misuse of a management application programming interface in the service based architecture. An illustrative example of an attack tree is shown in Fig. 4.1.

In order to connect these logical constructions to concrete assets, the attack tree is coupled with a system graph that represents the components and suppliers of the network. Let \mathcal{C} denote the set of components and \mathcal{S} the set of suppliers. A system graph is a directed graph

$$SG = (\mathcal{C} \cup \mathcal{S}, \mathcal{E}),$$

where edges in \mathcal{E} capture functional or supply dependencies among components and suppliers. For example, an edge from a cloud platform supplier to a user plane function indicates that the correct and trustworthy operation of the function depends on that platform. The decomposition of complex components into subcomponents yields a hierarchical system graph

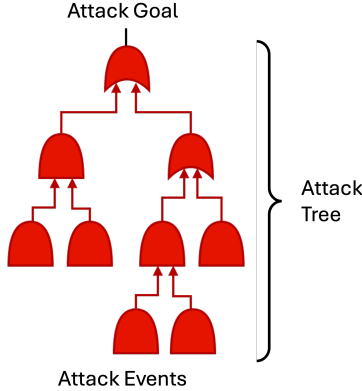


Figure 4.1: Schematic representation of an attack tree capturing the hierarchical decomposition of a high level compromise objective into intermediate goals and atomic attack steps. AND and OR relations encode the logical structure of adversarial progress, providing a foundation for quantitative evaluation of system level security risk in next generation networks.

that exposes the internal structure of network elements such as base stations, distributed units, and core functions. Atomic attack steps in the attack tree are mapped to nodes or edges in this system graph. This mapping creates a bridge from logical attack paths to the concrete elements of a fifth generation or next generation network and its supply chain.

Structure Function and Minimal Cut Sets

Reliability theory represents the behaviour of a coherent system through a structure function. In the risk context, each node v in the system graph is associated with a binary state variable $X_v \in \{0, 1\}$, where $X_v = 1$ denotes that the node is uncompromised and $X_v = 0$ denotes that it has failed from a security perspective. A structure function

$$\varphi : \{0, 1\}^{|\mathcal{C} \cup \mathcal{S}|} \rightarrow \{0, 1\}$$

maps the vector $x = (x_v)_{v \in \mathcal{C} \cup \mathcal{S}}$ to a system level indicator that equals one if the network preserves the specified security property and zero if the adverse event occurs. The function φ is induced by the AND and OR relations in the attack tree and by the logical dependencies in the system graph. For example, if the security of the core network depends on the integrity of the access and control planes through an AND relation, then the corresponding component states appear as a logical conjunction in φ .

A central concept in reliability theory is the minimal cut set [259]. A cut set w is a set of nodes whose simultaneous failure guarantees system failure, that is $\varphi(x) = 0$ whenever $x_v = 0$ for all $v \in w$. A minimal cut set is a cut set that contains no proper subset that is itself a cut set. The family of all minimal cut sets is denoted by \mathcal{W} . In the network

security setting, a minimal cut set describes a smallest combination of components and suppliers whose compromise suffices to realise the top level attack goal. For instance, the set containing a particular cloud infrastructure supplier and a specific authentication service may constitute a minimal cut if their joint compromise always implies loss of trust in the control plane.

Minimal cut sets connect the logical description of attack scenarios to a quantitative measure of risk. Let $r_v \in [0, 1]$ denote the probability that node v is successfully attacked or behaves maliciously during the time horizon of interest. The vector of node level risk values is $r = (r_v)_{v \in \mathcal{C} \cup \mathcal{S}}$. Under the standard assumption that attacks on different nodes are conditionally independent given r , the probability that all nodes in a minimal cut set w fail is $\prod_{v \in w} r_v$, and the probability that at least one minimal cut set fails is

$$R(r) = 1 - \prod_{w \in \mathcal{W}} \left(1 - \prod_{v \in w} r_v \right). \quad (4.15)$$

The quantity $R(r)$ is the systemic risk function. It represents the probability that the adverse security event occurs through at least one minimal combination of component and supplier failures. In a 5G network, $R(r)$ can encode events such as joint compromise of the user plane and an orchestrator, or simultaneous manipulation of a radio unit and its management interface, as long as the corresponding minimal cut sets are enumerated.

In practice, direct computation of all minimal cut sets can be challenging for large networks. Algorithms such as *Method of Obtaining CUT Sets (MOCUS)* and other fault tree based procedures are used to obtain \mathcal{W} from the attack tree and system graph while handling general AND and OR logic [260]. Once \mathcal{W} is available, the systemic risk function in (4.15) provides a compact summary of how individual node risks combine into a network level metric.

Importance Measures from Reliability Theory

The systemic risk function is the starting point for prioritizing defensive actions. Reliability theory offers a family of importance measures that quantify how sensitive the system risk is to the risk of individual nodes [261]. These measures are particularly useful in complex next generation architectures where intuitive criticality rankings may be misleading due to nontrivial logical structure.

Consider first the improvement potential of node i . One interprets improvement as a reduction of its compromise probability from its current value r_i to a lower value, conceptually to zero for maximal improvement. Let s_i^0 denote the current vector of node risks and s_i^1 the

hypothetical vector after hardening node i , defined as

$$s_i^0 = (r_1, \dots, r_i, \dots, r_N), \quad s_i^1 = (r_1, \dots, 0, \dots, r_N), \quad (4.16)$$

where N is the number of nodes and only the i th entry is changed. The improvement potential of node i is then

$$\text{IP}_i = R(s_i^0) - R(s_i^1). \quad (4.17)$$

This is the reduction in systemic risk that would be achieved if node i could be made perfectly secure while leaving all other node risks unchanged. In a 5G network, IP_i measures the benefit of fully hardening a particular base station vendor, virtualized network function, or cloud platform.

A complementary and widely used measure is the Birnbaum importance [262]. In reliability theory the Birnbaum importance of node i is the partial derivative of the system failure probability with respect to the failure probability of that node. Translating to the risk notation above, one defines

$$\text{BI}_i = \frac{\partial R(r)}{\partial r_i}, \quad (4.18)$$

evaluated at the nominal risk vector r . This derivative can be interpreted as the probability that node i is critical for system failure, meaning that changing its state from secure to compromised toggles the state of the system while all other node states are fixed. For coherent systems, the Birnbaum importance is nonnegative and can be computed without explicit differentiation by evaluating the systemic risk function at two auxiliary vectors that differ only in the value of r_i . A common choice is

$$s_i^0 = (0, r_{-i}), \quad s_i^1 = (1, r_{-i}), \quad (4.19)$$

where r_{-i} collects the risks of all nodes other than i . The Birnbaum importance is then

$$\text{BI}_i = R(s_i^1) - R(s_i^0). \quad (4.20)$$

Nodes with large Birnbaum importance are those whose risk has the strongest marginal effect on the overall network risk and therefore represent structurally critical components or suppliers.

For decision making it is often helpful to combine structural importance with the inherent

risk of a node. A risk importance measure [263, 264] can be defined as

$$\text{RI}_i = r_i \text{BI}_i, \quad (4.21)$$

which assigns high values to nodes that are both structurally significant and presently risky. In a next generation network this measure highlights, for instance, suppliers that control components belonging to many minimal cut sets and that are currently assessed to have elevated compromise probabilities. Optimization formulations that reduce the sum of risk importance values across the system can then be used to select mitigation actions that approximately minimize the systemic risk without explicitly recomputing the full function (4.15) for every candidate configuration [80].

4.4 Agentic AI and Large Language Models for Risk Assessment

NextG networks, particularly those built on 5G and evolving toward 6G, exhibit unprecedented scale, heterogeneity, and interdependence across the control, data, and management planes. Virtualization, cloud–edge integration, and software-defined programmability create immense flexibility but also enlarge the attack surface and introduce complex, cross-domain vulnerabilities. Traditional static or rule-based defenses, designed for isolated and predictable infrastructures, are inadequate for this environment.

To achieve resilience as defined in Fig. 2.1, network defense must become adaptive, proactive, and continually learning. This requires *agentic artificial intelligence (AI)* coupled with *large language models (LLMs)*, enabling cyber defense to be conducted by distributed, goal-directed agents that perceive, reason, act, and learn across layers [265].

4.4.1 What is Agentic AI?

Agentic AI denotes AI systems that operate not as passive predictors but as autonomous decision-makers that perceive, reason, act, and learn in dynamic environments. Unlike conventional models that only provide point predictions, an agentic system is endowed with the capability to engage continuously with its environment and adapt to evolving conditions.

The first of its core functions is **perception**, whereby the system collects heterogeneous signals that reveal different facets of its operational domain. These may include radio spectrum measurements that capture wireless interference patterns, SDN controller logs that expose network-level events, or cloud workload metrics that reflect computational demand

and congestion. Such observations provide the raw material from which the system builds an understanding of the state of the world.

Building on perception, agentic AI performs **reasoning and planning**. At this stage, the system maintains beliefs about hidden network states, denoted x_t , and adversarial types, represented by q_t . These beliefs serve as the basis for projecting possible future trajectories of the system and anticipating adversarial strategies. Through this predictive reasoning, the agent formulates control policies that balance performance and resilience.

The function of **action** translates plans into concrete interventions. These interventions are expressed as defender actions $u_t \in \mathcal{A}_b$, such as reconfiguring network slices, scaling computational resources, or deploying deception mechanisms. The adversary chooses counter-actions $w_t \in \mathcal{A}_r$. Together, these actions drive the network dynamics:

$$x_{t+1} \sim P(x_{t+1} \mid x_t, u_t, w_t, \xi_t, q_t),$$

where ξ_t represents natural disturbances and q_t captures disruption modes. In this way, the agent does not merely adapt to the environment but actively shapes its evolution.

Finally, **learning** enables the agent to refine its strategies over time. By updating its policy parameters ϕ through mappings of the form

$$\pi_b^\phi : (\mathcal{O}_t, h_t) \mapsto \Delta(\mathcal{A}_b),$$

the system adapts its decision rules based on accumulated observations \mathcal{O}_t and historical context h_t . Performance outcomes $y_t = g(x_t)$ and resilience metrics such as (M, L, D) serve as feedback signals, guiding the agent toward improved choices in subsequent episodes.

Through this cycle of perception, reasoning, action, and learning, agentic AI embodies a closed-loop intelligence that is continuously evolving, capable of operating autonomously in adversarial and uncertain environments.

4.4.2 What are Large Language Models (LLMs)?

Large Language Models (LLMs) are foundation models trained on massive corpora of natural language and code. Their distinctive power lies in their ability to generalize and to perform reasoning across diverse contexts. For example, an LLM can parse unstructured threat intelligence reports and extract the underlying indicators of compromise, translate highly technical specifications such as 3GPP standards into operational guidelines, generate plausible hypotheses about attacker behavior, and produce human-interpretable explanations of otherwise opaque system dynamics. In this sense, LLMs extend beyond the role of

a language interface; they provide a flexible substrate for reasoning across modalities and domains.

Formally, an LLM can be described as a parameterized mapping

$$f_\theta : \mathcal{X} \longrightarrow \Delta(\mathcal{Y}),$$

where \mathcal{X} denotes the space of input tokens (text, code, measurement, or symbolic prompts), \mathcal{Y} represents the output vocabulary, and $\Delta(\mathcal{Y})$ is the probability simplex over possible next tokens. Through training on large-scale data, the parameters θ capture statistical regularities that give rise to emergent capabilities such as chain-of-thought reasoning, analogical inference, and instruction following. What distinguishes LLMs in the context of agentic AI is not only their predictive accuracy but also their capacity to embed domain knowledge and contextual constraints into probabilistic reasoning over extended sequences.

Within an agentic AI ecosystem, LLMs serve as the *cognitive glue* that binds together heterogeneous agents. They are capable of normalizing and interpreting measurement drawn from domains as varied as the Core network, the Transport layer, the RAN, MEC, and end-user devices. This capacity allows disparate signals to be expressed in a unified representation that can be acted upon. Building on this integration, LLMs can generate structured action plans or machine-enforceable policies from high-level operator intent, effectively translating human guidance into control directives for automated agents. They can also assume adversarial perspectives by simulating attacker reasoning and role-playing red-team strategies, thereby providing a means to stress-test defenses before real incidents occur. At the same time, their generative capabilities enable them to facilitate communication and coordination across distributed agents: they can summarize evolving conditions in natural language, highlight anomalies, and convert low-level measurement into actionable insights.

Together, these functions make LLMs more than passive text processors. They become strategic orchestrators that bridge human operators and autonomous agents, providing both interpretability and adaptability. In this role, they enable the distributed components of next-generation networks to cooperate coherently, ensuring that the larger agentic system can anticipate threats, coordinate countermeasures, and maintain resilience under adversarial pressure.

4.4.3 Distributed Agent Roles in NextG

In large-scale heterogeneous networks, resilience emerges not from any single safeguard but from the coordinated effort of distributed agents embedded across architectural domains. Each type of agent contributes different capabilities, aligned with the threat points high-

lighted in Fig. 1.1 and the cross-layer interactions shown in Fig. 4.1. Together, they enable resilience as a dynamic property that is continuously maintained across prevention, response, and adaptation cycles.

Core Orchestration Agents. These agents oversee SDN controllers, NFV orchestrators, and slice lifecycle managers. They enforce isolation policies across tenants, manage instantiations of virtualized functions, and coordinate recovery after disruptions. Their responsibilities include mitigating denial-of-service or misconfiguration attacks against the Core (threat points 3–4) while sustaining service continuity across slices.

Transport Agents. Transport-layer agents monitor the state of backhaul and fronthaul links (threat point 4), collecting measurement on throughput, latency, and packet integrity. They implement anomaly detection for routing manipulation or link sabotage, and dynamically reconfigure paths and bandwidth allocations to maintain service quality despite congestion or disruption.

RAN Agents. RAN-level agents control the disaggregated elements of the radio access network: RUs, DUs, and CUs (threat points 5–7). They implement fast countermeasures such as adaptive power control, beam steering, frequency hopping, and cross-cell coordination to counter jamming, spoofing, and rogue base stations. Integrated with RAN Intelligent Controllers (RICs), these agents leverage xApps/rApps for near-real-time optimization.

Edge/MEC Agents. At the network edge, MEC agents orchestrate computation, caching, and application placement for URLLC and mMTC services. They guard against resource exhaustion and poisoning attacks by monitoring workload integrity, enforcing isolation, and migrating critical applications to alternative edge or cloud sites when under duress.

Digital Twin (DT) Agents. A dedicated class of agents maintains and synchronizes digital twin environments for probabilistic risk assessment and ‘what if’ stress testing. DT agents track system status, calibrate models with live measurement, and simulate adversarial scenarios. Their output informs operational decisions such as resource reallocation, slice reconfiguration, or defensive posture adjustments.

Analytics and Measurement Agents. These agents specialize in collecting, aggregating, and interpreting data across domains. They perform metric evaluation (latency, availability, resilience indices), anomaly detection, and log analysis. By quantifying disruptions

and recovery trajectories, they provide the evidence base for both automated decision-making and retrospective learning.

Sense-Making and Policy Agents. These agents bridge raw analytics with high-level defensive logic. They synthesize heterogeneous data streams, infer causal relationships between events, and generate policy updates. Their outputs guide both local orchestration agents (e.g., traffic shaping, isolation) and global strategies (e.g., zero-trust enforcement, prioritization of URLLC slices).

Strategic LLM Agents. Operating across all layers, strategic LLM agents integrate measurement o_t , incident logs Y_t , external threat intelligence \mathcal{D} , and DT outputs. They reason about cross-domain interdependencies, simulate attacker–defender strategies, and produce human-interpretable recommendations. By aligning tactical agent responses with global resilience goals, they serve as the cognitive glue of the ecosystem.

The interplay of these roles transforms heterogeneity into resilience: DT and measurement agents provide a predictive foundation; transport, RAN, and MEC agents deliver rapid, localized reactions; policy and LLM agents ensure coherence across layers. Together, they enable NextG networks to anticipate, withstand, and adapt to disruptions in an integrated and measurable way.

4.4.4 Agentic AI Workflow Across Resilience Stages

The agentic AI workflow unfolds as a dynamic and recursive cycle aligned with the three resilience stages.

Proactive phase. Agents leverage reasoning (e.g., through LLMs) to scan for known vulnerabilities, model potential attacker strategies $w \in \mathcal{A}_r$, and design preventive measures. For instance, a Core orchestration agent may, based on LLM-curated threat intelligence, proactively enforce stricter authentication rules at the SBA interface (threat point 2) or pre-provision redundant UPFs (threat point 3). Formally, this corresponds to selecting an initial defender policy π_b^ϕ that minimizes the prior expectation of resilience loss:

$$\phi^* = \arg \min_{\phi \in \Phi} \mathbb{E}_{w \sim \mu_0} \left[\sum_{t=0}^T C_t \cdot \left(1 - \frac{Q_t}{Q_{\max}} \right) \right],$$

where μ_0 encodes the prior distribution over attacker strategies and $Q_t = h(x_t)$ is a performance measurement (e.g., reliability or throughput).

Responsive phase. During disruptions ($t_f \leq t \leq t_r$), local agents act on real-time observations. For example, a RAN agent may detect SINR degradation at threat point 5 and trigger frequency hopping, while a Transport agent dynamically reroutes traffic around a severed fiber link at point 4. A strategic reasoning agent (powered by LLMs) can mediate across these layers, interpreting multi-modal measurement, hypothesizing about adversary behavior, and suggesting coordinated responses. This aligns with the decision-making stage of the OODA loop:

$$u_t \sim \pi_b^\phi(o_t, h_t), \quad x_{t+1} = f(x_t, u_t, w_t, \xi_t, q_t).$$

Retrospective phase. After stabilization ($t > t_r$), retrospective agents perform forensic analysis, update threat models, and retrain detection or control policies. Large language models can transform raw audit trails, incident reports, and cross-layer traces into structured insights. For example, they can extract causal chains of attack actions, identify recurring misconfigurations $\mu(x_t)$, and quantify residual performance deficits D . These insights feed back into proactive planning by updating μ_0 and refining π_b^ϕ , thereby closing the resilience loop.

4.4.5 Integration Across Mechanisms in Large-Scale Contexts

The systemic interdependencies of NextG networks magnify both the promise and the challenge of agentic resilience. If proactive mechanisms were flawless, responsive and retrospective layers would be redundant. However, the inevitability of unknown vulnerabilities and adaptive adversaries ensures that such perfection is unattainable. Conversely, relying solely on responsive or retrospective mechanisms would be prohibitively expensive, as operators would continually absorb high losses L and large maximum drops M before recovery.

For example, in a dense urban environment, a sophisticated adversary could simultaneously exploit a misconfigured cloud API (threat point 2) and launch a coordinated jamming attack on multiple RAN interfaces (threat points 5–7). A purely proactive defense may block known API vulnerabilities but fail against novel jamming patterns. A purely responsive defense may detect the jamming but expend substantial resources on real-time countermeasures. Only by integrating proactive segmentation, responsive adaptation (e.g., dynamic spectrum hopping), and retrospective learning can the system both contain immediate impact and reduce future exposure.

Therefore, resilience in NextG networks must be treated as an *integrated, multi-agent, and quantitatively optimized process*. Control theory provides temporal stability guarantees, game theory captures the strategic dynamics of red–blue interactions, learning theory

supports adaptive policy refinement across episodes, and network theory models the cross-domain interdependencies illustrated in Fig. 2.1. When coupled with LLM-based cognitive agents for reasoning, explanation, and strategy generation, this integrated approach ensures that resilience is not merely reactive but becomes a first-class, evolving property of next-generation communication infrastructures.

Chapter 5

Resilient System Designs

Chapter 5 focuses on the design of resilient networked systems by translating the principles developed in earlier chapters into concrete control and orchestration mechanisms. The emphasis is on how resilience can be explicitly engineered into softwarized 5G and O RAN architectures through adaptive resource management rather than treated as an implicit byproduct of over-provisioning or redundancy.

Through a set of representative case studies, the chapter examines trust aware optimization, risk aware edge cloud orchestration, learning based slice management, and LLM driven control as complementary approaches for sustaining performance under uncertainty and adversarial conditions. Collectively, these examples illustrate how resilience emerges from the tight coupling of performance objectives, security awareness, and adaptive decision making across multiple timescales.

5.1 Trust-Aware Resource Management for Resilient Network Slicing

The work of [266] provides a comprehensive demonstration of resilience in 5G mobile edge networks through a trust-aware resource management framework. The central motivation stems from the vulnerability of mobile edge computing (MEC) systems, which expose a significantly enlarged attack surface by bringing computation closer to end users. These MEC nodes, despite enabling ultra-reliable low-latency communication (URLLC), are resource-limited and can be rapidly overwhelmed under denial-of-service (DoS) or distributed DoS (DDoS) attacks. Conventional defenses, such as coarse-grained access control or anomaly detection based solely on packet loss, often fail to provide the sensitivity or rapid responsiveness required for URLLC. To address this gap, the proposed scheme introduces *trust* as

a first-class system variable, coupling it with distributed optimization techniques to jointly deliver robust security guarantees and efficient service provisioning.

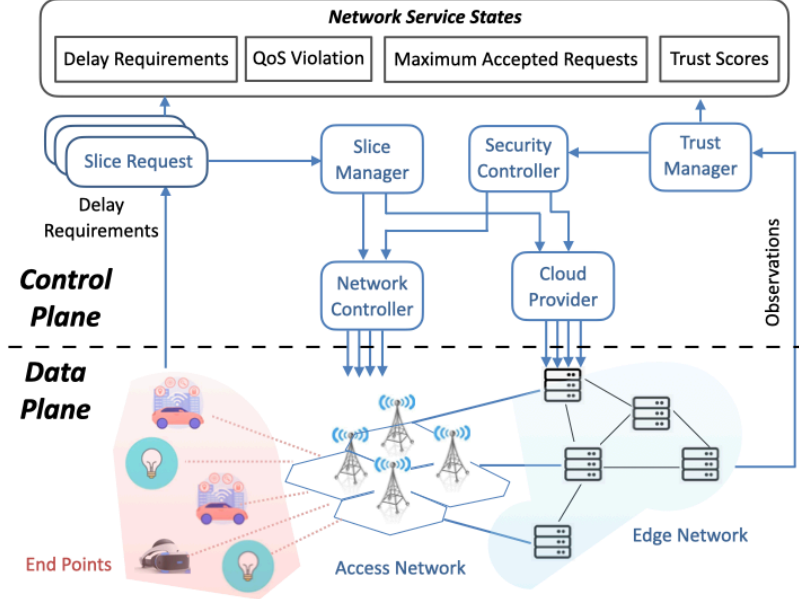


Figure 5.1: System architecture of trust-aware resource management for resilient network slicing. The control plane consists of the slice manager, security controller, trust manager, and network/cloud controllers, which coordinate resource allocation based on trust scores, QoS violations, and delay requirements. The data plane includes endpoints, access networks, and edge networks, where tasks are offloaded and executed.

System Architecture

The network is modeled as a hierarchical tree of MEC nodes, with capacities increasing toward the network core. Each MEC node $m \in M$ possesses finite computing capacity $c_m \in \mathbb{R}_+$ and bandwidth $b_m \in \mathbb{R}_+$. Network slices $n \in N$ represent diverse 5G applications such as enhanced mobile broadband (eMBB), URLLC, and massive machine-type communications (mMTC). Each slice n is characterized by average traffic x_n , processing density ω_n (CPU cycles per bit), and maximum tolerable delay \hat{e}_n .

The end-to-end delay for slice n is modeled as

$$e_n = e_n^{\text{trans}} + e_n^{\text{proc}} + e_n^{\text{prop}}, \quad (5.1)$$

where the transmission delay is

$$e_n^{\text{trans}} = \sum_{m \in p_n} \frac{\alpha_n^m}{b_m}, \quad (5.2)$$

the processing delay is

$$e_n^{\text{proc}} = \sum_{m \in p_n} \frac{\omega_n \alpha_n^m}{\beta_n^m}, \quad (5.3)$$

and e_n^{prop} is the propagation delay over path p_n . Here α_n^m denotes the allocated traffic of slice n on node m , while β_n^m is the allocated CPU capacity.

Trust Management via Bayesian Inference

Trust management provides a quantitative means of excluding compromised nodes from critical routing paths. Each MEC node m maintains a trust score $s_{m,k} \in [0, 1]$ at epoch k . During interval $[kT_{\text{inter}}, (k+1)T_{\text{inter}}]$, node m processes R_m^k requests, of which V_m^k violate QoS requirements. Using Bayesian inference with Beta priors, the posterior trust distribution is

$$f(s_m | o_m^k) \sim \text{Beta}(\theta_k + R_m^k - V_m^k, \gamma_k + \phi V_m^k), \quad (5.4)$$

where ϕ is a penalty factor that accelerates trust decay upon violations. The trust expectation is

$$E_k[S_m] = \frac{\theta_k}{\theta_k + \gamma_k}. \quad (5.5)$$

To capture memory fading, the effective trust score is updated recursively:

$$s_{m,k} = (1 - \epsilon)s_{m,k-1} + \epsilon E_k[S_m], \quad (5.6)$$

with $\epsilon \in (0, 1)$ controlling the weight of recent evidence. This formulation ensures stability for reliable nodes and rapid degradation for compromised nodes.

Trust-Aware Optimization of Slicing

The slicing optimization balances service latency and reliability. Formally, the objective is

$$\min_{\alpha, p} f(\alpha, p) = \eta \sum_{n=1}^N e_n - (1 - \eta) \sum_{n=1}^N \sum_{m \in p_n} s_m, \quad (5.7)$$

where $\eta \in (0, 1)$ is a tradeoff parameter. Constraints include

$$\sum_{n \in N} \alpha_n^m \leq b_m, \quad \forall m \in M, \quad (5.8)$$

$$\sum_{n \in N} \beta_n^m \leq c_m, \quad \forall m \in M, \quad (5.9)$$

$$e_n \leq \hat{e}_n, \quad \forall n \in N. \quad (5.10)$$

This ensures feasible allocations within MEC resource budgets while meeting per-slice QoS requirements.

Distributed ADMM Decomposition

To achieve scalability, we solve the trust-aware slicing problem by ADMM in *scaled* form. Let $\alpha = \{\alpha_n^m\}$ be traffic allocations, $y = \{y_m\}$ the CPU allocations, and $p = \{p_n\}$ the routes. Introduce the consensus constraints

$$x_n = \sum_{m \in p_n} \alpha_n^m, \quad \forall n \in N, \quad (5.11)$$

$$y_m = \sum_{n \in N} q \omega_n \alpha_n^m, \quad \forall m \in M, \quad (5.12)$$

and denote the *scaled* duals by $u = \{u_n\}$ and $v = \{v_m\}$. The scaled augmented objective is

$$\begin{aligned} \mathcal{L}_\rho(p, y, \alpha; u, v) = & f(\alpha, p) \\ & + \frac{\rho}{2} \sum_{n \in N} \left\| x_n - \sum_{m \in p_n} \alpha_n^m + u_n \right\|_2^2 \\ & + \frac{\rho}{2} \sum_{m \in M} \left\| y_m - \sum_{n \in N} q \omega_n \alpha_n^m + v_m \right\|_2^2. \end{aligned} \quad (5.13)$$

At iteration $t = 0, 1, 2, \dots$, with penalty $\rho > 0$, ADMM performs:

(1) Secure routing update (Security Controller): p -step. We use a convex *soft-routing* relaxation. Introduce path-incidence variables $z_{n,m} \in [0, 1]$ with $\sum_{m \in \mathcal{N}(n)} z_{n,m} = 1$

and set $\alpha_n^m = z_{n,m} x_n$.¹ For fixed $(\alpha^t, y^t, u^t, v^t)$, the p -update is

$$\begin{aligned} z^{t+1} \in \arg \min_{z \in \mathcal{Z}} \sum_{n,m} & \left[\eta \left(\frac{z_{n,m} x_n}{b_m} + \frac{\omega_n z_{n,m} x_n}{\beta^{m,t}} \right) - (1 - \eta) s_m \right] \\ & + \frac{\rho}{2} \sum_n \left\| x_n - \sum_m z_{n,m} x_n + u_n^t \right\|_2^2. \end{aligned} \quad (5.14)$$

where $\beta^{m,t}$ is the (fixed) effective CPU available to slice n at node m given y^t (e.g., via proportional sharing $\beta^{m,t} = \frac{y_m^t z_{n,m} x_n}{\sum_{n'} z_{n',m} x_{n'}}$). The problem in (5.14) decomposes across slices and reduces to a shortest-path/flow problem on the layered MEC graph with node weights

$$w_{n,m}^{(t)} = \eta \left(\frac{x_n}{b_m} + \frac{\omega_n x_n}{\beta^{m,t}} \right) - (1 - \eta) s_m + \rho x_n \left(\frac{1}{|\mathcal{N}(n)|} - u_n^t \right),$$

which can be solved by Dijkstra or K -shortest paths.

(2) Resource update (Cloud Provider): y -step. For fixed $(p^{t+1}, \alpha^t, u^t, v^t)$,

$$y^{t+1} \in \arg \min_{0 \leq y_m \leq c_m} \frac{\rho}{2} \sum_{m \in M} \left\| y_m - \sum_n q \omega_n \alpha_n^{m,t} + v_m^t \right\|_2^2. \quad (5.15)$$

This is separable with the closed form projection

$$y_m^{t+1} = \Pi_{[0, c_m]} \left(\sum_n q \omega_n \alpha_n^{m,t} - v_m^t \right), \quad \forall m \in M. \quad (5.16)$$

(3) Traffic update (Network Controller): α -step. For fixed $(p^{t+1}, y^{t+1}, u^t, v^t)$, solve

$$\begin{aligned} \alpha^{t+1} \in \arg \min_{\alpha \geq 0} & \underbrace{\eta \sum_n \sum_{m \in p_n^{t+1}} \frac{\alpha_n^m}{b_m}}_{\text{transmission cost}} + \underbrace{\eta \sum_n \sum_{m \in p_n^{t+1}} \frac{\omega_n \alpha_n^m}{\beta_n^m(y^{t+1})}}_{\text{processing cost}} \\ & + \frac{\rho}{2} \sum_n \left\| x_n - \sum_{m \in p_n^{t+1}} \alpha_n^m + u_n^t \right\|_2^2 \\ & + \frac{\rho}{2} \sum_m \left\| y_m^{t+1} - \sum_n q \omega_n \alpha_n^m + v_m^t \right\|_2^2. \end{aligned} \quad (5.17)$$

¹If discrete routes are required, round to the best path or run a K -shortest enumeration with trust-aware costs.

This is a convex quadratic program. A fast *proximal-gradient with projection* works well:

$$\tilde{\alpha}_n^m = \alpha_n^{m,t} - \tau \nabla_{\alpha_n^m} \tilde{\mathcal{L}}_\rho(p^{t+1}, y^{t+1}, \alpha^t, u^t, v^t), \quad (5.18)$$

$$\alpha_n^{m,t+1} = \Pi_{\Delta(b_m)}(\tilde{\alpha}_n^m), \quad \Delta(b_m) = \{a \geq 0 : \sum_n a_n \leq b_m\}, \quad (5.19)$$

where $\tau > 0$ is a stepsize (e.g., backtracking), $\Pi_{\Delta(b_m)}$ is Euclidean projection onto the (capped) simplex, and $\nabla_{\alpha_n^m} \tilde{\mathcal{L}}_\rho$ is the gradient of (5.17). The simplex projection has an $O(|N| \log |N|)$ closed form via sorting:

$$\alpha_n^{m,t+1} = \max\{\tilde{\alpha}_n^m - \theta_m, 0\}, \quad \text{with } \theta_m \text{ s.t. } \sum_n \max\{\tilde{\alpha}_n^m - \theta_m, 0\} = b_m.$$

(4) Dual ascent (Consensus): u - and v -steps.

$$u_n^{t+1} = u_n^t + \left(x_n - \sum_{m \in p_n^{t+1}} \alpha_n^{m,t+1} \right), \quad \forall n \in N, \quad (5.20)$$

$$v_m^{t+1} = v_m^t + \left(y_m^{t+1} - \sum_{n \in N} q\omega_n \alpha_n^{m,t+1} \right), \quad \forall m \in M. \quad (5.21)$$

Primal/dual residuals and stopping. Define the *primal residual*

$$r^{t+1} = \begin{bmatrix} \{x_n - \sum_{m \in p_n^{t+1}} \alpha_n^{m,t+1}\}_n \\ \{y_m^{t+1} - \sum_n q\omega_n \alpha_n^{m,t+1}\}_m \end{bmatrix},$$

and the *dual residual*

$$s^{t+1} = \rho \begin{bmatrix} \{\sum_{m \in p_n^{t+1}} (\alpha_n^{m,t+1} - \alpha_n^{m,t})\}_n \\ \{\sum_n q\omega_n (\alpha_n^{m,t+1} - \alpha_n^{m,t})\}_m \end{bmatrix}.$$

Terminate when $\|r^{t+1}\|_2 \leq \varepsilon_{\text{pri}}$ and $\|s^{t+1}\|_2 \leq \varepsilon_{\text{dual}}$, with

$$\varepsilon_{\text{pri}} = \sqrt{|N| + |M|} \varepsilon_{\text{abs}} + \varepsilon_{\text{rel}} \max\{\|x\|_2, \|y\|_2\}, \quad (5.22)$$

$$\varepsilon_{\text{dual}} = \sqrt{|N| + |M|} \varepsilon_{\text{abs}} + \varepsilon_{\text{rel}} \rho \|A^\top [u^{t+1}; v^{t+1}]\|_2. \quad (5.23)$$

Penalty adaptation and over-relaxation. To balance residuals, update ρ adaptively:

$$\rho \leftarrow \begin{cases} \tau_{\text{inc}}\rho, & \|r^{t+1}\|_2 > \mu \|s^{t+1}\|_2, \\ \rho/\tau_{\text{inc}}, & \|s^{t+1}\|_2 > \mu \|r^{t+1}\|_2, \quad (\tau_{\text{inc}} \approx 2, \mu \approx 10). \\ \rho, & \text{otherwise,} \end{cases}$$

Empirically, an over-relaxation factor $\gamma \in [1, 1.8]$ improves convergence: replace α^{t+1} in (5.20)–(5.21) by $\tilde{\alpha}^{t+1} = \gamma \alpha^{t+1} + (1 - \gamma)\alpha^t$.

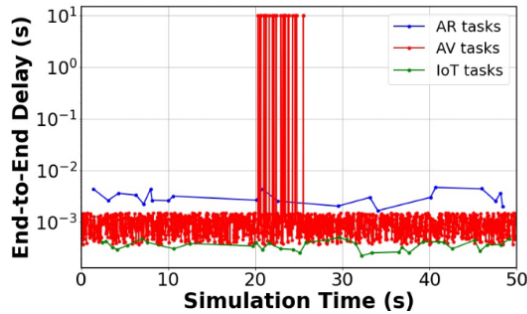
The p -step reduces to shortest paths on the layered MEC graph ($O(|E| \log |V|)$ per slice). The y -step is $O(|M|)$ due to the projection (5.16). The α -step uses per-node simplex projections (5.19), $O(|N| \log |N|)$ per MEC node, and communicates only the local sums in (5.20)–(5.21). Asynchronous or partially synchronous ADMM variants are compatible with this decomposition; each controller needs only neighbor aggregates to proceed, which keeps signaling overhead modest.

If hard, single-path routing is required, solve the relaxed z -problem, pick the maximum-weight path per slice, and reuse the duals (u^t, v^t) to warm-start the next iteration. In practice we observed (i) few ADMM iterations (< 10) to hit the tolerances, and (ii) identical solutions to exact MIP formulations on small topologies, but with orders-of-magnitude speedups.

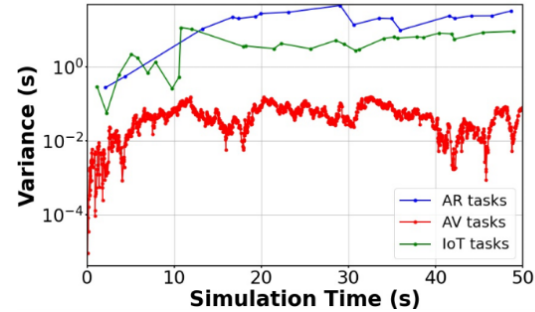
Simulation Results

The proposed framework is validated on the ETSI-MEC simulator [267]. In small-scale simulations (12 MEC nodes, 6 UEs, 3-layer topology), a DDoS attack launched at $t = 20$ s is effectively mitigated. Fig. 5.3a shows that the proposed trust-aware schemes—both end-to-end delay-based and packet-loss-based—consistently achieve faster recovery times than the existing scheme. As the penalty factor ϕ increases, recovery time decreases sharply, with the delay-based scheme converging below 2s at $\phi = 50$. Complementarily, Fig. 5.3b highlights how the average end-to-end delay is reduced under the proposed scheme, reaching sub-0.5s levels compared to approximately 1s under the existing design.

In large-scale simulations (194 MEC hosts, 30 UEs, 4-layer topology), the trust-aware scheme demonstrates scalability. Figures 5.2a and 5.2b illustrate the performance for application-specific slices. Autonomous vehicle (AV) slices experience transient spikes during attack onset at $t = 20$ s, but quickly stabilize due to trust-aware rerouting. Augmented reality (AR) and IoT slices maintain stability throughout, though with higher variance due to looser QoS constraints. Importantly, the variance of the delay of the AV remains consistently below 10^{-1} s after recovery, corroborating the robustness even for latency-critical applications.

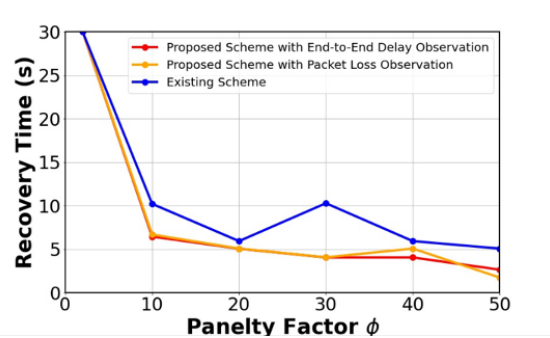


(a) End-to-end delay over simulation time for AR, AV, and IoT tasks. AV tasks exhibit transient delay spikes during attack onset but quickly stabilize due to trust-aware rerouting.

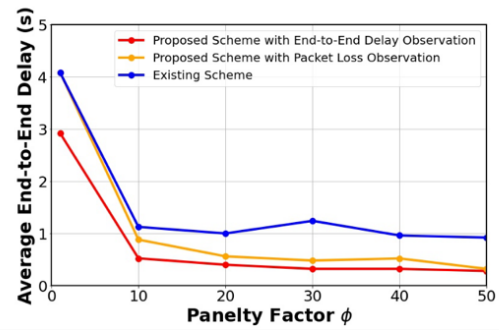


(b) Variance of end-to-end delay across AR, AV, and IoT tasks over simulation time. AV tasks maintain low variance after recovery, confirming robust latency guarantees.

Figure 5.2: Temporal performance of heterogeneous tasks under adversarial conditions. (a) End-to-end delay trajectories. (b) Delay variance evolution.



(a) Recovery time as a function of the penalty factor ϕ . The proposed schemes achieve significantly faster recovery than the existing scheme.



(b) Average end to end delay versus penalty factor ϕ . The proposed schemes consistently reduce delay compared to the existing scheme.

Figure 5.3: Performance comparison under varying penalty factor ϕ . (a) Recovery time. (b) Average end to end delay.

Resilience Implications

The integration of trust into the optimization framework operationalizes resilience along three axes. Proactively, unreliable MEC nodes are excluded from routing paths, reducing the expected resilience loss $\mathbb{E}[L]$. Responsively, real-time updates of s_m adapt resource allocations to mitigate ongoing attacks, lowering the degradation of peak performance M . Retrospectively, forensic trust updates penalize nodes that repeatedly misbehave, thus strength-

ening long-term robustness by reducing residual deficits D . The cumulative resilience loss,

$$L = \sum_{t=t_f}^{t_r} \left(1 - \frac{Q_t}{Q_{\max}} \right), \quad (5.24)$$

is consistently smaller under the trust-aware design compared to baselines. The figures collectively demonstrate that resilience is not only a byproduct of redundancy, but it can be systematically engineered through the coupling of trust dynamics with distributed optimization.

5.2 Risk-Aware Resource Orchestration in Multi-Tier 5G Edge-Cloud Systems

The evolution of 5G networks toward softwarized and virtualized architectures introduces a multi-tier computing substrate that spans the radio edge, mobile edge computing layers, and centralized cloud infrastructures. Applications deployed in these environments increasingly adopt microservices-based designs, where each service is decomposed into a collection of fine-grained computational functions with explicit data dependencies. This decomposition improves modularity and scalability, yet introduces intricate orchestration challenges because the end-to-end behavior of an application depends strongly on the tier in which each function is placed, the amount of compute and network resources it receives, and the coupling among resources across different layers. In addition, the openness of the 5G ecosystem raises the possibility that adversarial or malicious applications may request resources. This creates the need for a resource allocation strategy that jointly evaluates performance objectives and the risk associated with each application. Fig. 5.4 illustrates the orchestration setting based on the work in [268], where the resource orchestrator manages the compute and network resources across levels while accounting for normal and malicious applications.

System Structure and Multi-Tier Execution Model

We consider a set of computing tiers indexed by $n \in \mathcal{N} = \{1, \dots, N\}$. Each level n provides finite computing capacity $C_n \in \mathbb{R}_+$ and finite network capacity $B_n \in \mathbb{R}_+$. The system hosts a set of applications indexed by $m \in \mathcal{M} = \{1, \dots, M\}$, where each application m is represented as a directed acyclic graph (DAG) $G_m = (V_m, E_m)$, with vertices V_m denoting functions (microservices) and directed edges E_m denoting data dependencies. The placement of a function onto a specific tier determines both its baseline execution characteristics and its

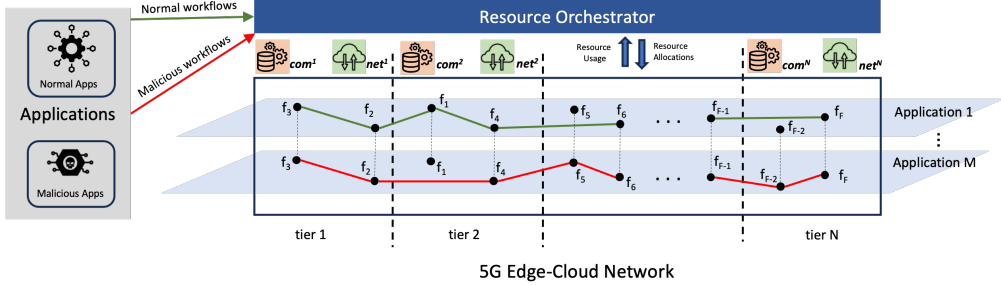


Figure 5.4: Schematic representation of the resource orchestrator managing resources between normal and malicious applications considering the workflows of apps over the set of microservices f_1 through f_m .

contribution to end-to-end latency and accuracy. Lower tiers offer reduced transport delay due to proximity to users, while higher tiers offer greater compute abundance at the expense of longer transport delays. This tradeoff is central to the orchestration problem.

A key characteristic of this setting is the usage of shared functions. A function may appear in multiple application graphs, inducing coupling across workloads. Let I_v denote the aggregate intensity of invocation of the function v induced by all applications. Increased load on shared functions increases contention and affects both latency and accuracy, thereby creating multi-dimensional interactions between compute and network resources that must be modeled explicitly.

5.2.1 Risk Modeling and Application Beliefs

To incorporate security considerations, each application m is associated with a belief value $\pi_m \in [0, 1]$ that quantifies the probability that application m is malicious. These belief values serve as soft risk indicators that modulate orchestration decisions. Rather than enforcing hard exclusions, the orchestrator penalizes resource allocations to high-risk applications through the objective function. This enables continuous risk-aware adaptation and provides robustness under uncertainty.

Latency and Accuracy Representation with Resource Coupling

For each function $v \in V_m$ placed on tier n , let $r_{v,m}^{\text{net}} \geq 0$ and $r_{v,m}^{\text{com}} \geq 0$ denote the allocated network and compute resources. The latency of a function decreases monotonically with the network allocation, while the accuracy increases monotonically with the compute allocation. To reflect coupling due to shared usage, we parameterize the performance of a function by the aggregate intensity of invocation I_v .

We adopt the following tier-dependent models for latency and accuracy:

$$\ell_{v,n}(r_{v,m}^{\text{net}}, I_v) = a_n - b \frac{r_{v,m}^{\text{net}}}{I_v}, \quad (5.25)$$

$$\alpha_{v,n}(r_{v,m}^{\text{com}}, I_v) = a'_n + b' \frac{r_{v,m}^{\text{com}}}{I_v}, \quad (5.26)$$

where a_n captures the tier baseline latency, a'_n captures the tier baseline accuracy, and $b > 0$, $b' > 0$ quantify the marginal effects of network and compute allocations. These models operationalize the principle that contention increases with I_v , requiring additional resources to maintain performance.

Let $x_{v,m}^n \in \{0, 1\}$ indicate whether function $v \in V_m$ is placed on tier n , with $\sum_{n \in \mathcal{N}} x_{v,m}^n = 1$. The application end-to-end latency and accuracy are modeled as

$$L_m = \sum_{v \in V_m} \sum_{n \in \mathcal{N}} x_{v,m}^n \ell_{v,n}(r_{v,m}^{\text{net}}, I_v), \quad (5.27)$$

$$A_m = \sum_{v \in V_m} \sum_{n \in \mathcal{N}} x_{v,m}^n \alpha_{v,n}(r_{v,m}^{\text{com}}, I_v). \quad (5.28)$$

This composition captures how local function performance aggregates across the application workflow, and why critical-path functions dominate the end-to-end delay.

Risk-Aware Optimization Formulation

The orchestrator jointly decides function-to-tier placement and resource allocations while accounting for risk beliefs. Define the effective resource consumption of application m as

$$R_m \triangleq \sum_{v \in V_m} (r_{v,m}^{\text{com}} + r_{v,m}^{\text{net}}). \quad (5.29)$$

Let $\phi(L_m, A_m)$ denote a monotone performance utility that increases with higher accuracy and improves with lower latency. The risk-aware orchestration problem is posed as

$$\min_{x, r, L, A} \sum_{m \in \mathcal{M}} (\theta + \lambda \pi_m) R_m - \kappa \sum_{m \in \mathcal{M}} \phi(L_m, A_m) \quad (5.30)$$

$$\text{s.t. } \sum_{n \in \mathcal{N}} x_{v,m}^n = 1, \quad \forall m \in \mathcal{M}, \quad \forall v \in V_m, \quad (5.31)$$

$$\sum_{m \in \mathcal{M}} \sum_{v \in V_m} r_{v,m}^{\text{com}} x_{v,m}^n \leq C_n, \quad \forall n \in \mathcal{N}, \quad (5.32)$$

$$\sum_{m \in \mathcal{M}} \sum_{v \in V_m} r_{v,m}^{\text{net}} x_{v,m}^n \leq B_n, \quad \forall n \in \mathcal{N}, \quad (5.33)$$

$$L_m \leq \bar{L}_m, \quad A_m \geq \bar{A}_m, \quad \forall m \in \mathcal{M}, \quad (5.34)$$

constraints (5.27) and (5.28) hold for all $m \in \mathcal{M}$.

The weight $(\theta + \lambda \pi_m)$ penalizes resource allocations to high-risk applications. Parameter $\lambda \geq 0$ tunes the sensitivity to risk, while $\kappa > 0$ balances performance utility against resource consumption. The presence of binary placement variables and nonlinear coupling in (5.27) to (5.28) yields a mixed-integer nonlinear program that is NP-hard in general.

Iterative Solution via Decomposition

A practical solution approach adopts a two-step iterative procedure. For fixed performance targets (\bar{L}_m, \bar{A}_m) , the algorithm computes a placement and allocation solution by relaxing tier capacity constraints using Lagrangian multipliers. The achieved performance then informs updated targets, and the process repeats until convergence. This structure enables tractable numerical solutions while preserving the coupled nature of compute and network resources across tiers.

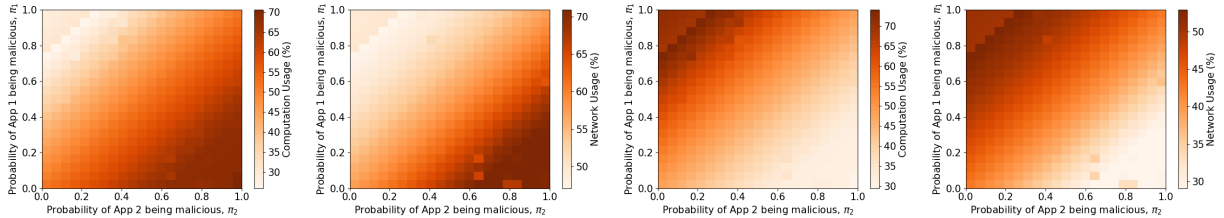
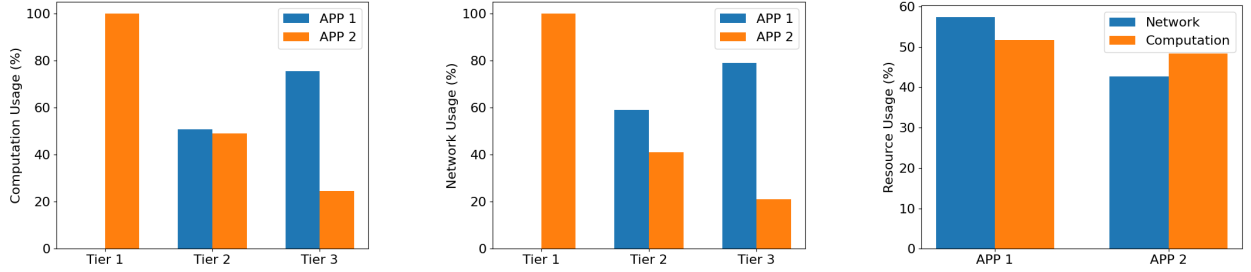


Figure 5.5: Comparative analysis of computational and network usage percentages under varying probabilities of App 1 (π_1) and App 2 (π_2) being malicious. Each subplot represents (from left to right): a) Computational usage of App 1, b) Network usage of App 1, c) Computational usage of App 2, and d) Network usage of App 2.

Fig. 5.5 illustrates how compute and network usage shift as the belief parameters vary



(a) Compute resource usage by tier. (b) Network resource usage by tier. (c) Aggregate resource utilization of App 1 and App 2.

Figure 5.6: Resource utilization analysis across a three-tier architecture for App 1 and App 2. (a) Compute resource usage by tier. (b) Network resource usage by tier. (c) Aggregate resource utilization comparison between applications.

across applications. The results indicate that increasing belief for an application systematically reduces its allocated resources, thereby protecting the infrastructure from resource wastage under elevated risk.

Adaptive Re-Orchestration After Malicious Application Removal

Once an application is identified as malicious and removed from the system, the remaining resources can be reallocated to improve the performance of benign applications. Since function placement decisions have already been determined, the re-orchestration focuses on reallocating compute and network resources within each tier. Let $\mathcal{D} \subset \mathcal{M}$ denote the set of detected malicious applications, and let $\{x_{v,m}^{n*}\}$ be the placement solution obtained before removal. The re-orchestration problem can be written as

$$\min_{r, L, A} \sum_{m \in \mathcal{M} \setminus \mathcal{D}} R_m - \kappa \sum_{m \in \mathcal{M} \setminus \mathcal{D}} \phi(L_m, A_m) \quad (5.35)$$

$$\text{s.t.} \quad \sum_{m \in \mathcal{M} \setminus \mathcal{D}} \sum_{v \in V_m} r_{v,m}^{\text{com}} x_{v,m}^{n*} \leq C_n, \quad \forall n \in \mathcal{N}, \quad (5.36)$$

$$\sum_{m \in \mathcal{M} \setminus \mathcal{D}} \sum_{v \in V_m} r_{v,m}^{\text{net}} x_{v,m}^{n*} \leq B_n, \quad \forall n \in \mathcal{N}, \quad (5.37)$$

$$L_m \leq \bar{L}_m, \quad A_m \geq \bar{A}_m, \quad \forall m \in \mathcal{M} \setminus \mathcal{D}, \quad (5.38)$$

along with the performance definitions in (5.27) and (5.28) with fixed placements $x_{v,m}^{n*}$. Under linear or convex performance utilities, (5.35) to (5.38) reduces to a convex program, enabling rapid recovery after malicious removal. Fig. 5.6 summarizes tier-wise resource utilization and demonstrates improved efficiency after reallocation.

Risk–Performance Tradeoffs and Resource Efficiency

The impact of belief-driven risk awareness on application-level performance is further illustrated in Fig. 5.7. The figure depicts the tradeoff between end-to-end latency and application accuracy as the belief parameters (π_1, π_2) are varied. As the belief associated with an application increases, the orchestrator systematically deprioritizes its resource allocation, resulting in increased latency and reduced accuracy. Conversely, applications with lower belief values benefit from preferential allocation, achieving improved performance. This behavior confirms that the proposed framework does not impose rigid isolation but instead induces a continuous and controllable degradation of performance for high-risk workloads.

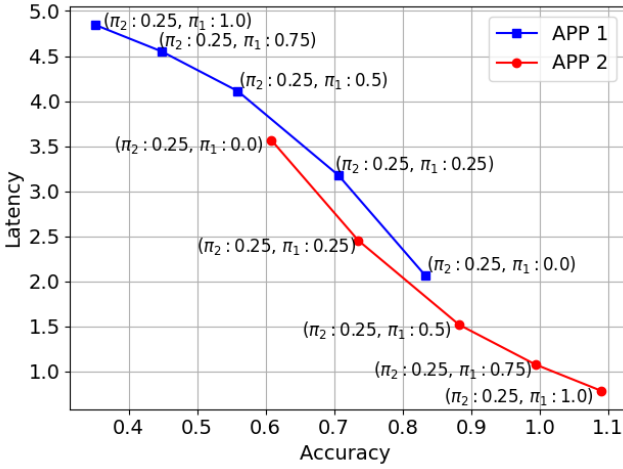


Figure 5.7: Trade-off between latency and accuracy for App 1 and App 2 across varying belief of being malicious (π_2, π_1) . Each data point represents a specific configuration of (π_2, π_1) values.

Fig. 5.8 further elucidates the coupling between resource usage and application performance. Specifically, the figure demonstrates how increasing computation or network resource utilization improves accuracy while reducing latency, albeit with diminishing returns. These curves provide empirical justification for the structure of the utility function $\phi(L_m, A_m)$ in (5.30), and highlight why balanced allocation across compute and network dimensions is essential for efficient orchestration in multi-tier environments.

Finally, Fig. 5.9 quantifies the effect of increasing belief on overall resource efficiency for different values of the weighting parameter λ . As the belief of an application increases, both computation and network efficiency decrease, reflecting the intentional withdrawal of resources from potentially malicious workloads. Larger values of λ amplify this effect, enabling the system operator to tune the aggressiveness of risk mitigation. These results demonstrate that the proposed formulation offers a principled mechanism to trade resource efficiency for security assurance in a controlled and interpretable manner.

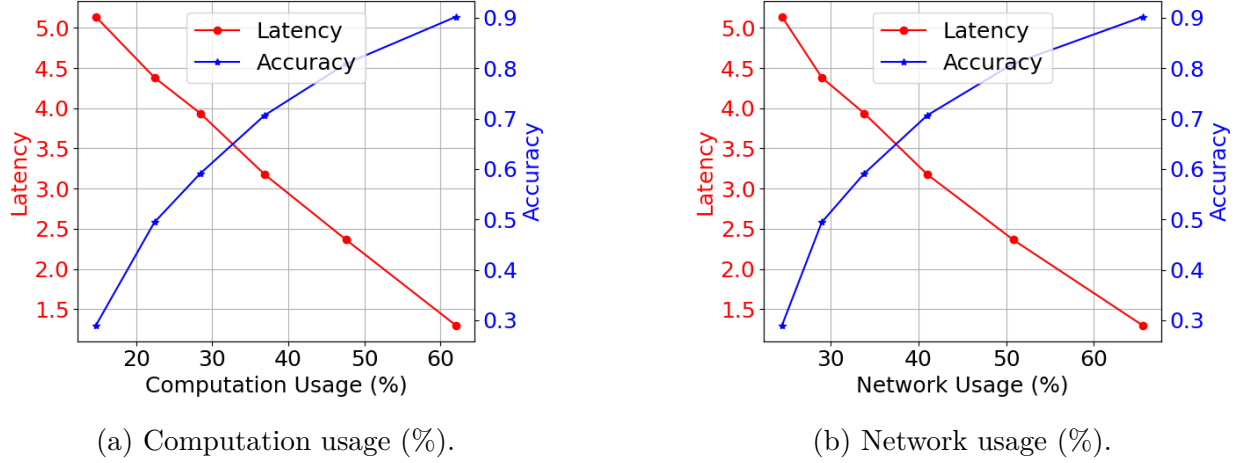


Figure 5.8: Trade-off between system latency (seconds) and application accuracy as a function of resource utilization. (a) Computation usage. (b) Network usage.

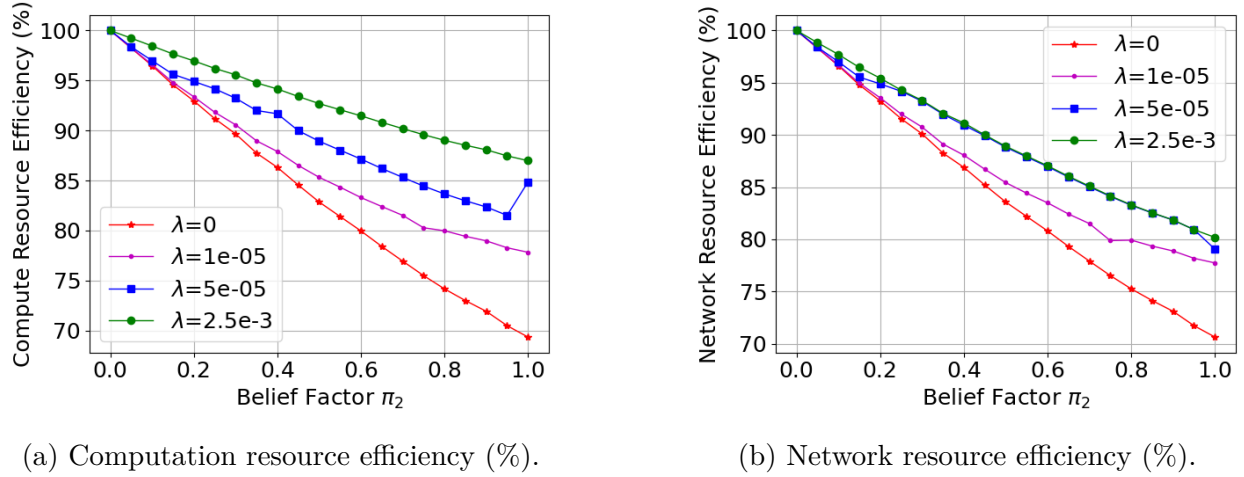
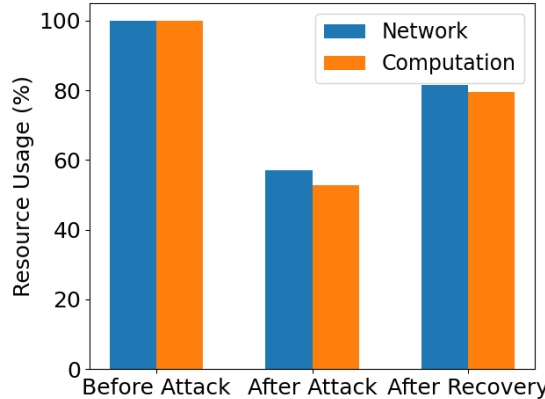
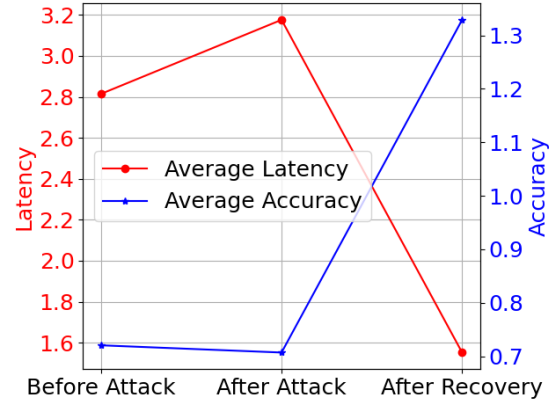


Figure 5.9: Variation of resource efficiency with respect to the belief factor for different λ values. (a) Computation resource efficiency. (b) Network resource efficiency.

Fig. 5.10 illustrates the dynamic resilience behavior of the proposed orchestration framework following the detection and removal of malicious applications. Upon attack detection, the system experiences a transient degradation in performance due to resource contention and belief updates. However, adaptive re-orchestration rapidly reallocates reclaimed compute and network resources to benign applications, resulting in a prompt recovery of system performance. The figure highlights both the recovery speed and the stability of the post-attack operating point, demonstrating the ability of the framework to maintain service continuity under adversarial conditions.



(a) Attack and recovery dynamics over time.



(b) Post-detection performance recovery.

Figure 5.10: Resilience of resource orchestration following the detection of malicious applications. (a) Attack and recovery dynamics. (b) System performance recovery after mitigation.

Resilience Implications

This risk-aware orchestration framework illustrates how resilience can be systematically engineered in softwarized networks by integrating performance requirements with explicit modeling of adversarial risk. Proactively, belief-weighted costs reduce expected wastage by steering allocations away from high-risk applications. Responsively, re-orchestration reallocates reclaimed resources to restore and improve benign performance following malicious removal. In retrospect, belief updates and associated penalties discourage persistent misbehavior and improve long-term robustness. Collectively, these mechanisms demonstrate that resilience in multi-tier 5G systems emerges from the coupling of optimization, risk modeling, and adaptive control.

5.3 Resilient Slice Management through Multi Agent Reinforcement Learning

While optimization-based orchestration provides strong guarantees under quasi-static conditions, slice management in O-RAN environments must operate under highly stochastic traffic arrivals, time-varying channel conditions, and delayed feedback. In particular, URLLC slices impose stringent probabilistic delay constraints that cannot be enforced using static admission thresholds or greedy allocation policies. This motivates a sequential decision-making framework capable of adapting admission and resource allocation decisions over time while explicitly respecting reliability and resource constraints.

To this end, we model resilient slice management as a constrained multi-agent Markov

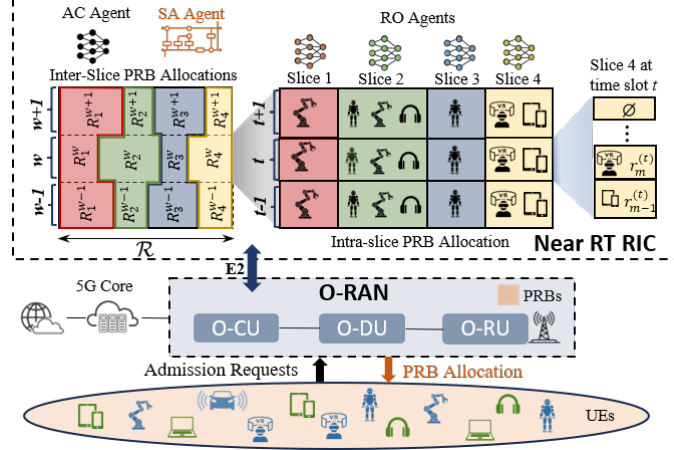


Figure 5.11: Integrated admission control and resource orchestration framework in O-RAN architecture.

decision process (CMDP), where interacting agents learn coordinated policies that jointly control slice admission and resource orchestration within the near-real-time RAN Intelligent Controller (near-RT RIC) [269]. Fig. 5.11 illustrates the integrated slice admission control and resource orchestration architecture implemented within the near-RT RIC. The framework operates across both inter-slice and intra-slice resource allocation layers, enabling coordinated control over physical resource blocks (PRBs) in O-RAN. Admission requests originating from heterogeneous URLLC and eMBB users are first processed by the admission control agent, which regulates slice entry based on current system load and reliability conditions. The admitted slices are then managed by a collection of slice-specific resource orchestration agents that dynamically allocate PRBs across time slots and slices. This hierarchical control structure allows the system to jointly manage slice admission and fine-grained radio resource allocation under shared capacity constraints, while preserving the modularity of O-RAN functional splits across the O-RU, O-DU, and O-CU.

System Model and Time-Slotted Operation

We consider a single gNB serving a set of active user equipments (UEs) over discrete time slots indexed by $t \in \mathbb{N}$. At each time slot, a set of new slice requests arrives according to a stochastic arrival process. Each request belongs to a service class $s \in \mathcal{S}$, where \mathcal{S} includes URLLC and eMBB services.

Let N_t denote the number of active users at time t . The system is constrained by total available bandwidth B_{\max} and total computational capacity C_{\max} . Each active user i is

allocated bandwidth b_i^t and computational resources c_i^t , satisfying

$$\sum_{i=1}^{N_t} b_i^t \leq B_{\max}, \quad \sum_{i=1}^{N_t} c_i^t \leq C_{\max}. \quad (5.39)$$

The instantaneous latency experienced by user i at time t is denoted by D_i^t , which depends on both radio transmission delay and processing delay. For URLLC users, a delay threshold D_{th} is imposed.

CMDP Formulation

The resilient slice management problem is modeled as a CMDP defined by the tuple

$$\mathcal{M} = (\mathcal{N}, \mathcal{S}, \{\mathcal{O}_i\}_{i \in \mathcal{N}}, \{\mathcal{A}_i\}_{i \in \mathcal{N}}, P, \{r_i\}_{i \in \mathcal{N}}, \{c_i\}_{i \in \mathcal{N}}, \gamma),$$

where $\mathcal{N} = \{a, o\}$ denotes the set of agents corresponding to admission control (a) and resource orchestration (o).

The global system state at time t is

$$s_t = (N_t, \mathbf{b}^t, \mathbf{c}^t, \mathbf{h}^t, \boldsymbol{\eta}^t), \quad (5.40)$$

where \mathbf{b}^t and \mathbf{c}^t denote current resource allocations, \mathbf{h}^t represents channel quality indicators, and $\boldsymbol{\eta}^t$ captures historical latency fulfillment statistics.

Each agent observes a partial view of the system. The admission agent observes

$$o_a^t = (N_t, \bar{D}^t, \rho^t), \quad (5.41)$$

where \bar{D}^t is the average URLLC delay and ρ^t denotes current resource utilization. The orchestration agent observes

$$o_o^t = (\mathbf{b}^t, \mathbf{c}^t, \mathbf{h}^t). \quad (5.42)$$

Action Spaces

The admission control agent selects an action

$$a_a^t \in \mathcal{A}_a = \{0, 1, \dots, K\}, \quad (5.43)$$

corresponding to admitting up to K new slice requests at time t . The admitted users are selected based on channel quality ordering.

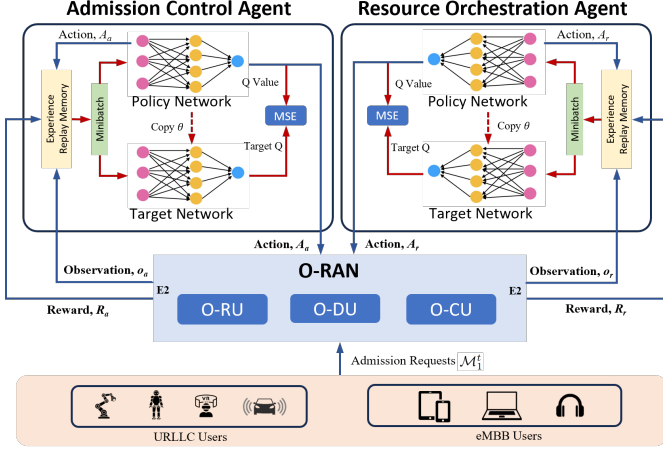


Figure 5.12: Multi-agent reinforcement learning architecture for admission control and resource orchestration in O-RAN.

The resource orchestration agent selects continuous-valued actions

$$a_o^t = \{\Delta b_i^t, \Delta c_i^t\}_{i=1}^{N_t}, \quad (5.44)$$

which adjust per-user bandwidth and computation allocations subject to (5.39).

The internal learning structure of the proposed multi-agent framework is depicted in Fig. 5.12. The admission control agent and the resource orchestration agent operate as independent yet interacting decision-makers, each equipped with a dueling double deep Q-network architecture. At each time step, both agents receive partial observations from the O-RAN environment via the E2 interface, compute their respective actions, and receive delayed reward feedback reflecting latency reliability and energy efficiency outcomes. The admission control agent focuses on regulating the number of incoming slice requests, while the resource orchestration agent adjusts PRB allocations across admitted users and slices. Although trained independently, the agents are coupled through the shared environment dynamics, resulting in non-stationary observations that necessitate robust learning mechanisms such as target networks and experience replay.

Latency Reliability and Energy Efficiency Metrics

For URLLC users, reliability is quantified via the latency fulfillment ratio

$$\mathcal{R}^t = \frac{1}{N_t^{\text{URLLC}}} \sum_{i \in \mathcal{U}_{\text{URLLC}}} \mathbb{I}(D_i^t \leq D_{\text{th}}), \quad (5.45)$$

where $\mathbb{I}(\cdot)$ denotes the indicator function.

Energy efficiency at time t is defined as

$$\mathcal{E}^t = \frac{\sum_{i=1}^{N_t} R_i^t}{\sum_{i=1}^{N_t} (b_i^t + c_i^t)}, \quad (5.46)$$

where R_i^t denotes the achieved throughput.

Reward and Constraint Functions

The admission agent reward is defined as

$$r_a^t = \alpha N_t^{\text{admit}} - \beta (1 - \mathcal{R}^t), \quad (5.47)$$

penalizing reliability violations. The orchestration agent reward is

$$r_o^t = \mu \mathcal{R}^t + \nu \mathcal{E}^t - \xi \sum_{i=1}^{N_t} \mathbb{I}(D_i^t > D_{\text{th}}). \quad (5.48)$$

System-level constraints are enforced via expectation bounds

$$\mathbb{E}[1 - \mathcal{R}^t] \leq \epsilon, \quad \mathbb{E}[\rho^t] \leq \rho_{\text{max}}. \quad (5.49)$$

Learning Objective

Each agent seeks to maximize its expected discounted return

$$\max_{\pi_i} \mathbb{E}_{\pi} \left[\sum_{t=0}^{\infty} \gamma^t r_i^t \right], \quad i \in \{a, o\}, \quad (5.50)$$

subject to constraints (5.49). Policies π_i are parameterized using dueling double deep Q-networks, enabling stable learning under partial observability and nonstationary interactions.

Learning Dynamics and Performance Evaluation

Fig. 5.13 illustrates the evolution of cumulative training rewards for both the admission control agent and the resource orchestration agent under varying admission strategies. The admission control agent converges toward a stable reward profile as it learns to regulate slice admissions in a manner that balances throughput with reliability preservation. In parallel, the resource orchestration agent exhibits a smoother reward trajectory, reflecting its continuous adaptation of PRB allocations in response to admitted load. The joint convergence

behavior confirms that the decentralized learning process stabilizes despite non-stationary interactions between agents, validating the effectiveness of the dueling double deep Q-network architecture in the proposed multi-agent CMDP formulation.

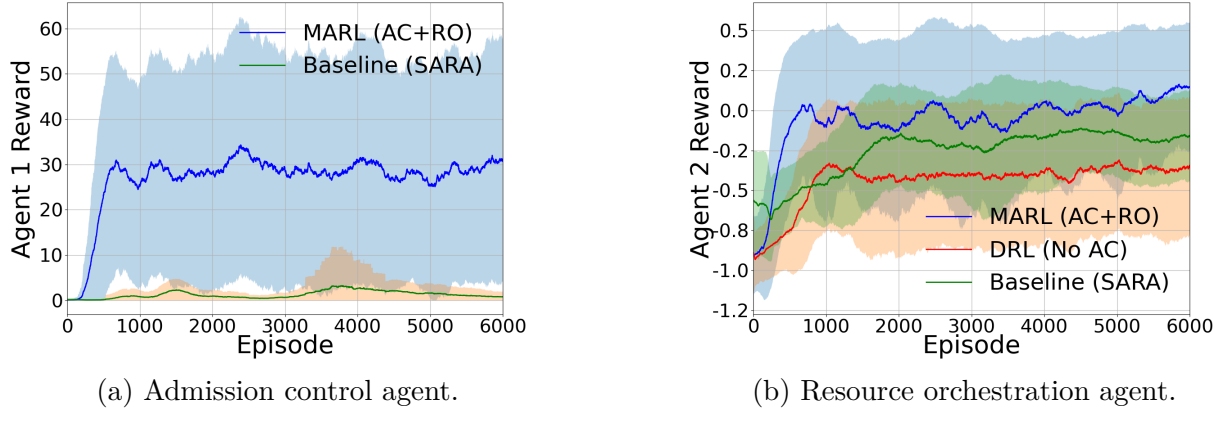


Figure 5.13: Training reward trajectories of the learning based agents under varying admission strategies. (a) Admission control agent. (b) Resource orchestration agent.

The convergence of key reliability and efficiency indicators during training is further illustrated in Fig. 5.14. As learning progresses, the delay violation rate and packet drop rate decrease monotonically, while energy efficiency improves steadily. These trends indicate that the agents progressively internalize the latency reliability constraints encoded in the reward functions and learn to mitigate congestion before violations occur. The simultaneous improvement across all three metrics demonstrates that the learning process does not overfit to a single objective, but instead achieves a balanced operating point consistent with the resilience goals of URLLC slice management.

The end-to-end delay characteristics of admitted slices are analyzed through the empirical complementary cumulative distribution functions shown in Fig. 5.15. For both eMBB and URLLC services, the proposed multi-agent framework yields sharply decaying delay tails, with URLLC traffic exhibiting particularly tight concentration below the latency threshold. This behavior confirms that the learned admission and resource orchestration policies successfully suppress extreme delay events, which are the primary drivers of reliability degradation in time-critical services. The separation between eMBB and URLLC delay distributions further demonstrates effective service differentiation under shared radio and compute resources.

Fig. 5.16 evaluates system performance under varying resource capacities, highlighting the robustness of the learned policies across different operating regimes. As available resources increase, both packet drop rate and delay violation rate decrease, while energy

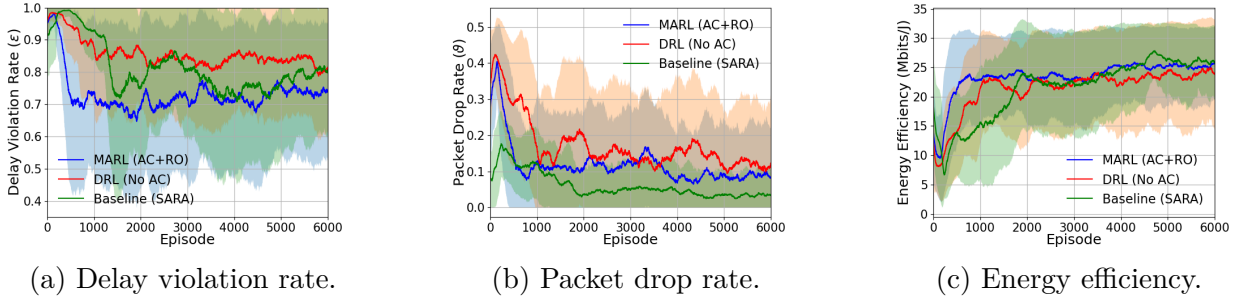


Figure 5.14: Evolution of training performance metrics. (a) Delay violation rate. (b) Packet drop rate. (c) Energy efficiency.

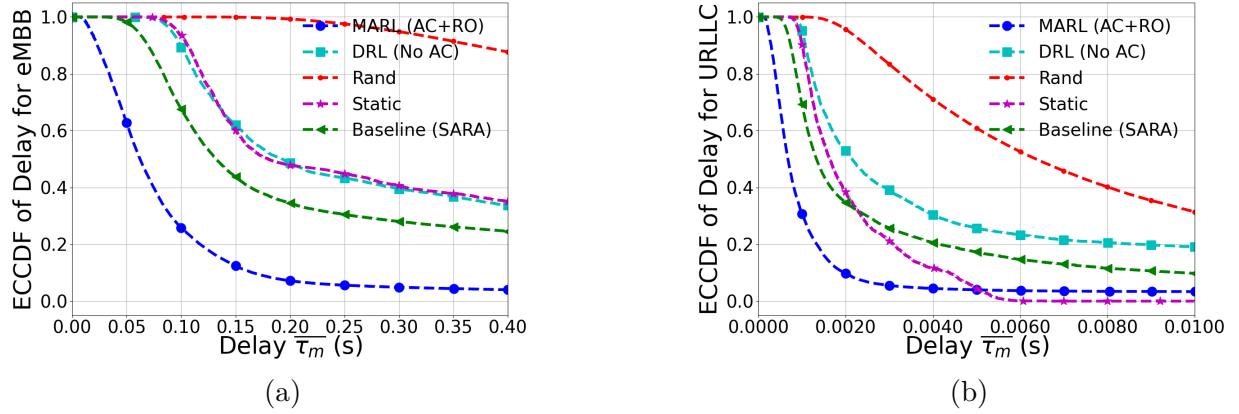


Figure 5.15: ECCDF of delay for admitted slices – (a) eMBB and (b) URLLC.

efficiency and reliability improve correspondingly. Importantly, the framework maintains acceptable reliability even under constrained resource budgets, indicating that the agents learn conservative admission and allocation strategies when capacity is scarce. This adaptability is a key indicator of resilience, as it enables the system to sustain service guarantees under fluctuating infrastructure conditions.

Finally, Fig. 5.17 compares average resource utilization and efficiency achieved by the proposed framework. While resource utilization increases with demand, the corresponding resource efficiency remains high, indicating that additional resources are translated into reliability gains rather than wasted capacity. This behavior reflects the effectiveness of the CMDP constraints in preventing over-allocation and highlights the ability of the multi-agent framework to operate near the Pareto-efficient frontier between utilization and reliability.

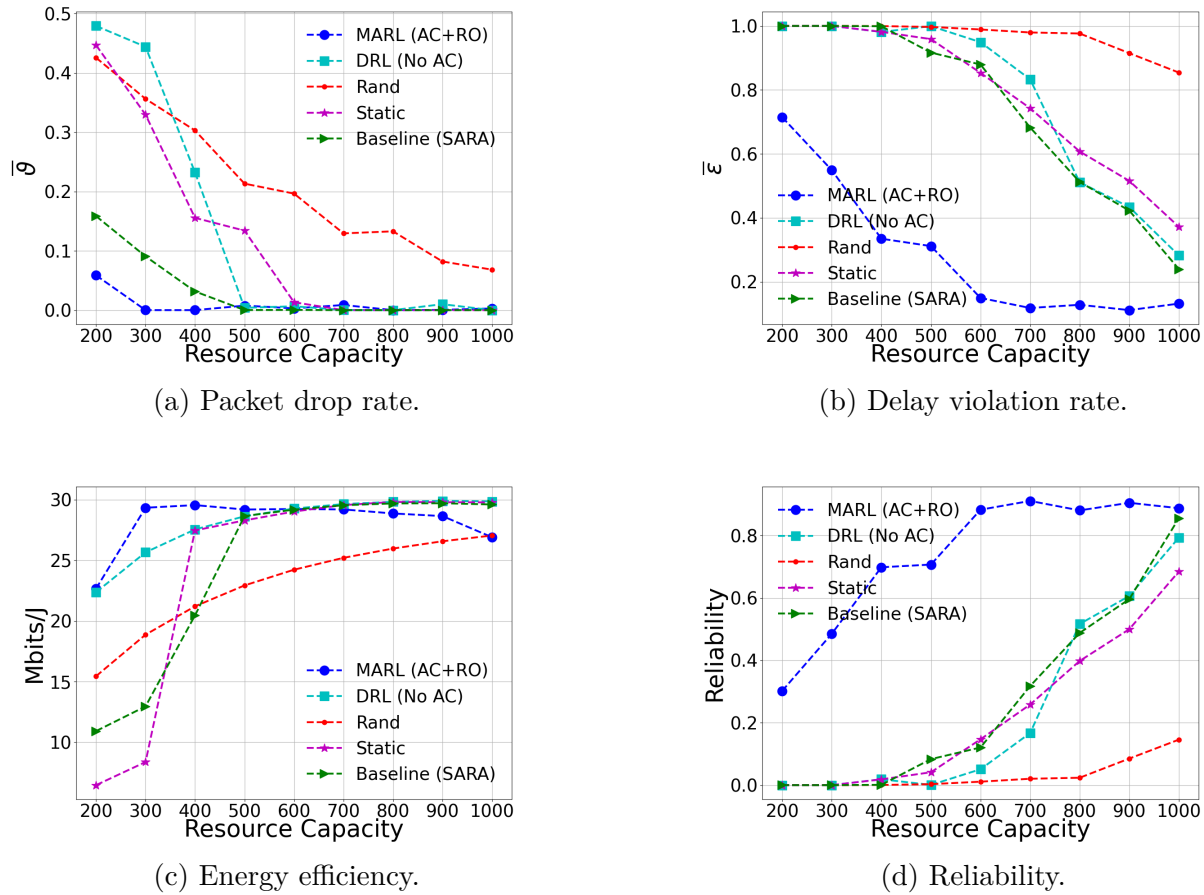


Figure 5.16: Performance metrics across varying resource capacities. (a) Packet drop rate. (b) Delay violation rate. (c) Energy efficiency. (d) Reliability.

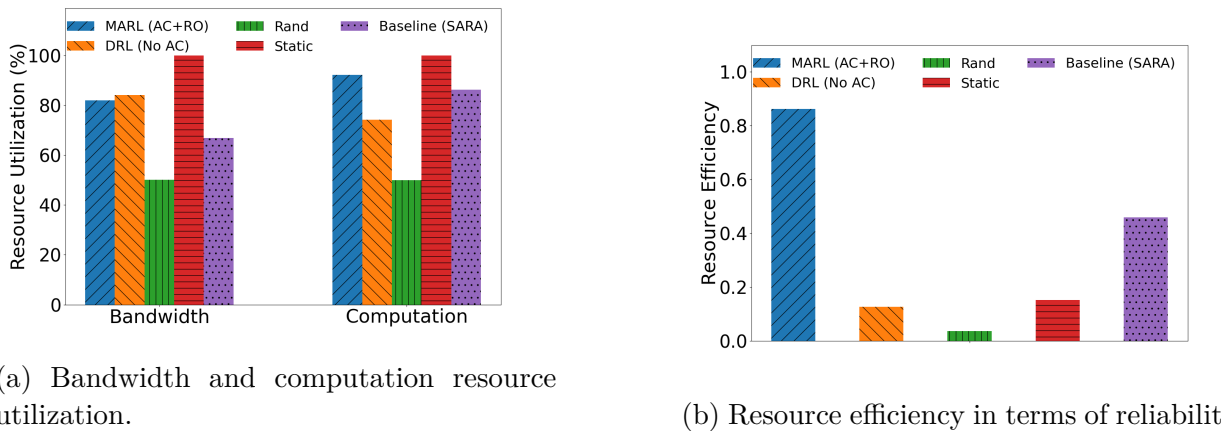


Figure 5.17: Comparison of average resource utilization and efficiency. (a) Bandwidth and computation resource utilization. (b) Resource efficiency measured in terms of reliability.

Resilience Interpretation

From a resilience standpoint, the CMDP formulation enables proactive overload avoidance by internalizing reliability constraints into the learning objective. The admission agent learns to limit arrivals before congestion occurs, while the orchestration agent dynamically reallocates resources to absorb traffic surges and channel degradation. Recovery emerges naturally as agents adapt their policies following transient violations, restoring reliability without explicit reconfiguration. This establishes multi-agent reinforcement learning as a complementary resilience mechanism to the optimization-based orchestration strategies developed earlier in this chapter.

5.4 LLM Driven Resilient Slice Management

While the multi-agent reinforcement learning framework in Section 5.3 enables fine-grained, closed-loop adaptation at near real-time timescales, its performance is inherently bounded by the expressiveness of predefined state representations, reward structures, and training regimes. In contrast, large language models (LLMs) introduce a complementary decision-making paradigm that operates at a higher semantic level, enabling intent-aware, context-driven resilience mechanisms that are not easily captured by conventional optimization or reinforcement learning formulations. In this section, we formalize the role of LLMs as cognitive controllers for resilient slice management and analyze their interaction with the O-RAN control stack.

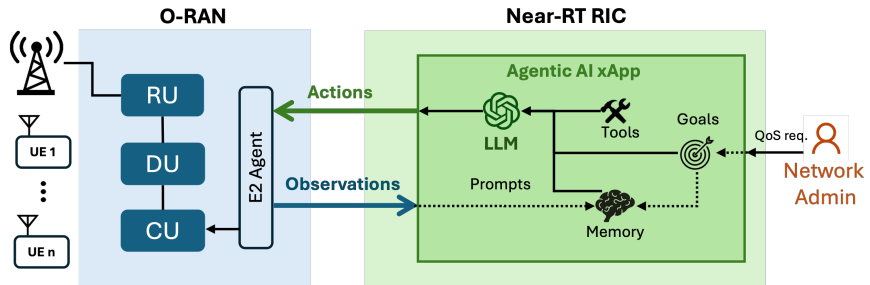


Figure 5.18: O-RAN system with LLM-powered xApp deployed in the near-RT RIC.

Fig. 5.18 illustrates the deployment of the LLM-powered xApp within the near-real-time RIC, where it interfaces with the O-RAN E2 control plane and operates alongside data-driven agents. The LLM observes abstracted slice-level performance summaries, historical control actions, and operator-defined intent constraints, and produces structured control recommendations that guide admission control, inter-slice prioritization, and long-term resource re-balancing.

Intent-to-Policy Mapping Model

Let \mathcal{I}_k denote the intent specification at reconfiguration slot k , expressed as a structured semantic tuple

$$\mathcal{I}_k = \{\mathcal{Q}_k, \mathcal{P}_k, \mathcal{C}_k\}, \quad (5.51)$$

where \mathcal{Q}_k represents slice-level QoS objectives such as latency bounds or reliability targets, \mathcal{P}_k encodes relative slice priorities, and \mathcal{C}_k captures system-level constraints including resource budgets and policy limits. Unlike numeric optimization variables, these components may be expressed in natural language or semi-structured templates and may evolve dynamically over time.

The LLM implements a mapping

$$\Phi_{\text{LLM}} : (\mathcal{I}_k, \mathcal{H}_k) \rightarrow \mathcal{A}_k, \quad (5.52)$$

where \mathcal{H}_k denotes the optimization history and system feedback accumulated up to slot k , and \mathcal{A}_k represents a candidate control action expressed as a slice-level allocation vector or policy adjustment. This mapping is realized through in-context reasoning rather than parameterized policy evaluation, allowing the LLM to generalize beyond previously observed operating points.

The generated action \mathcal{A}_k is subsequently normalized and enforced through the RIC control loop, yielding concrete resource allocations $\{r_k^s\}_{s \in \mathcal{S}}$ that satisfy

$$\sum_{s \in \mathcal{S}} r_k^s \leq R, \quad (5.53)$$

while respecting slice isolation and feasibility constraints.

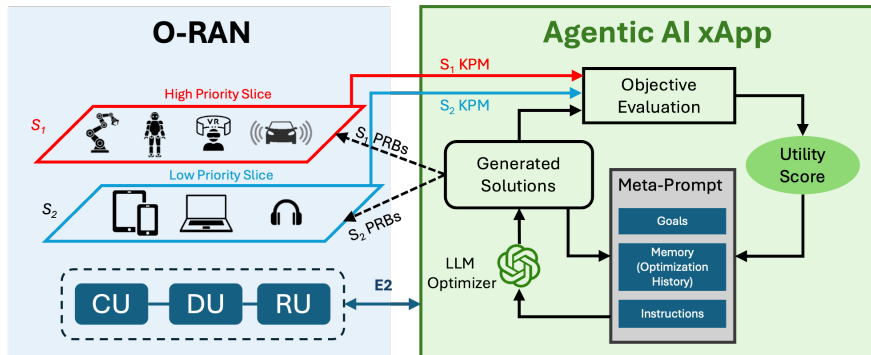


Figure 5.19: LLM-Driven Agentic AI-based resource provisioning framework.

Fig. 5.19 illustrates the LLM-driven agentic AI workflow for intent-aware resource provi-

sioning within the O-RAN architecture. The framework operates by ingesting slice-level key performance measurements (KPMs) from the near real-time RIC via the E2 interface, including latency, reliability, and PRB utilization metrics for both high-priority and low-priority slices. These measurements are processed by an agentic xApp that integrates an LLM-based optimizer with a meta-prompt structure comprising optimization goals, historical memory, and operational instructions. Based on the observed system state and intent constraints, the LLM generates candidate resource allocation solutions, which are subsequently evaluated by an objective function to produce a scalar utility score. The selected solution is then translated into concrete PRB allocation commands and enforced back into the O-RAN control loop.

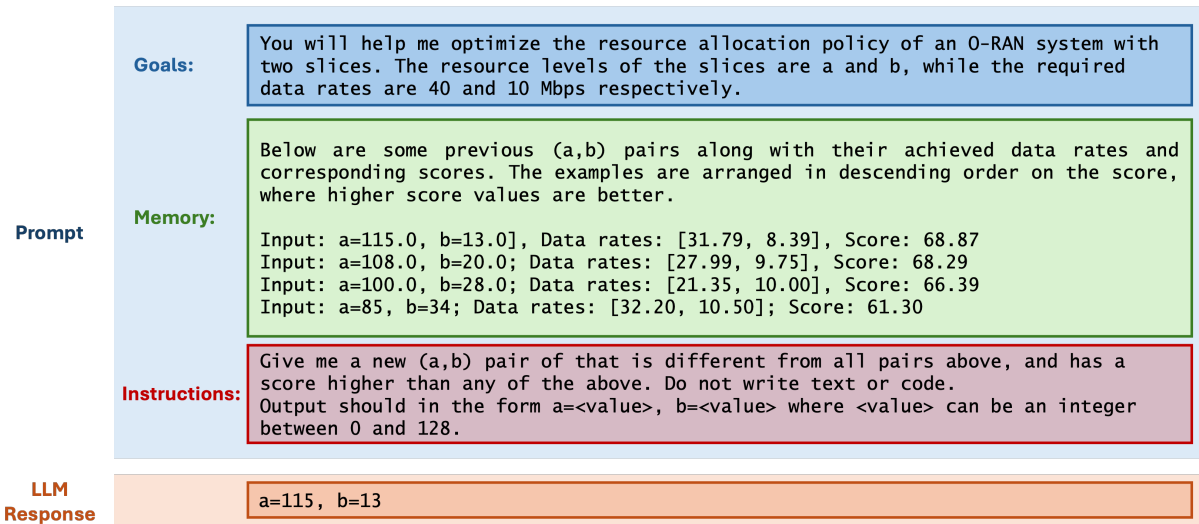


Figure 5.20: Examples of meta-prompt and LLM response for resource orchestration.

Fig. 5.20 provides concrete examples of the meta-prompt structure supplied to the LLM and the corresponding responses generated for resource orchestration. The prompts encode slice-level objectives, priority semantics, and operational constraints together with historical context, while the LLM responses produce structured allocation recommendations that are consistent with these inputs. These examples illustrate how qualitative intent and quantitative system state are jointly embedded into the decision process, bridging the semantic reasoning performed by the LLM with the utility-based evaluation and enforcement mechanisms formalized in the subsequent analysis.

LLM-Guided Resilience Objective

The resilience contribution of the LLM can be formalized through its effect on long-horizon performance stability. Let Θ_k denote the system-wide reliability metric aggregated across

slices at slot k , defined as

$$\Theta_k = \frac{1}{|\mathcal{S}|} \sum_{s \in \mathcal{S}} \frac{1}{|\mathcal{T}_k|} \sum_{t \in \mathcal{T}_k} \theta_s^t, \quad (5.54)$$

where θ_s^t follows the definition in Section 5.3. The LLM-driven controller implicitly seeks to maximize the discounted resilience objective

$$\max_{\{\mathcal{A}_k\}} \mathbb{E} \left[\sum_{k=0}^{\infty} \lambda^k \Theta_k \right], \quad (5.55)$$

with discount factor $\lambda \in (0, 1)$, without requiring an explicit model of state transitions or reward gradients.

This formulation highlights a key distinction from reinforcement learning. Rather than learning a stationary policy, the LLM continuously reinterprets the optimization objective in response to evolving context, thereby enhancing robustness under non-stationary traffic patterns, admission bursts, and slice demand shifts.

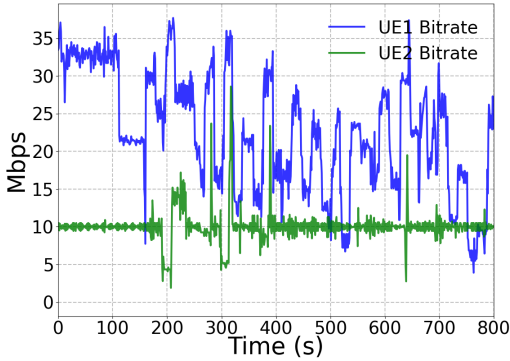
5.4.1 Performance Implications and Observed Gains

The performance of the LLM-driven framework is first evaluated against baseline allocation schemes in Fig. 5.21. Compared to random, equal, and proportional allocation, the LLM-driven approach consistently achieves superior performance by adapting resource distribution based on contextual reasoning rather than instantaneous demand alone. This confirms that intent-aware decision making yields tangible gains over heuristic strategies.

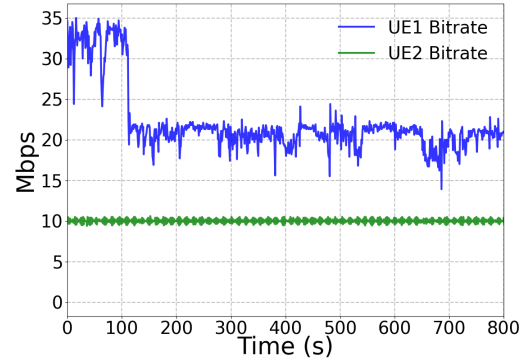
Fig. 5.22 presents a comparative analysis of system utility and reliability. The LLM-driven approach achieves higher instantaneous and average utility while simultaneously improving reliability, indicating that performance gains are achieved without compromising resilience. The reduced variance observed in both metrics reflects improved control stability under LLM-guided operation.

Priority-aware behavior is examined in Fig. 5.23, which shows window-smoothed utility and reliability for two users as the priority factor of UE 1 varies. Increasing priority yields monotonic improvements for UE 1 while inducing graceful degradation for UE 2, demonstrating controlled differentiation rather than abrupt starvation. The long-term effects of priority configuration are further quantified in Fig. 5.24, where time-averaged utility and reliability vary smoothly with the priority factor β_1 , indicating convergence to stable operating points.

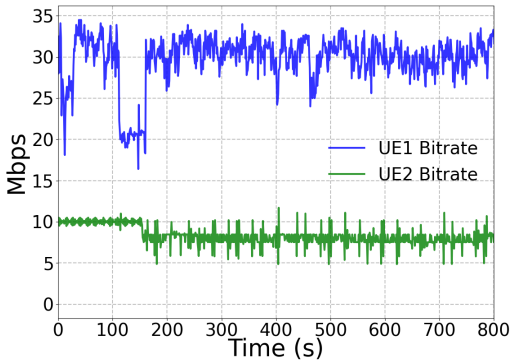
Finally, Fig. 5.25 compares different LLM models. While all evaluated models outperform heuristic baselines, more capable models achieve higher utility and improved reliability



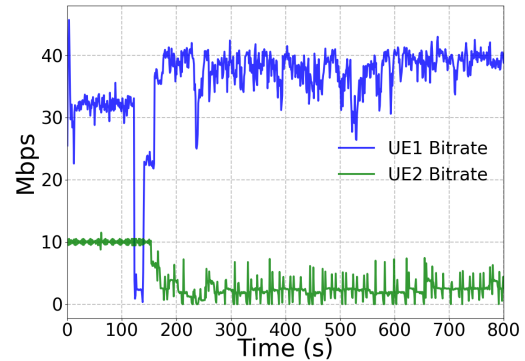
(a) Random allocation.



(b) Equal allocation.



(c) Proportional allocation.



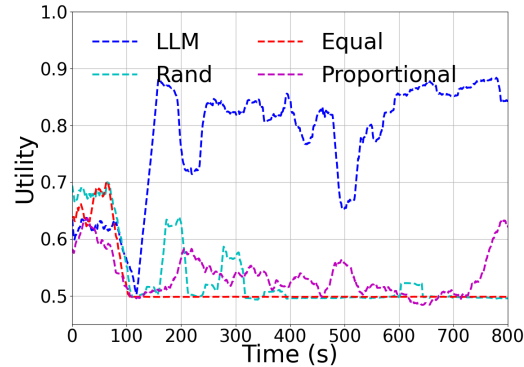
(d) LLM-driven allocation.

Figure 5.21: Comparative results of resource allocation schemes. (a) Random allocation. (b) Equal allocation. (c) Proportional allocation. (d) LLM-driven allocation.

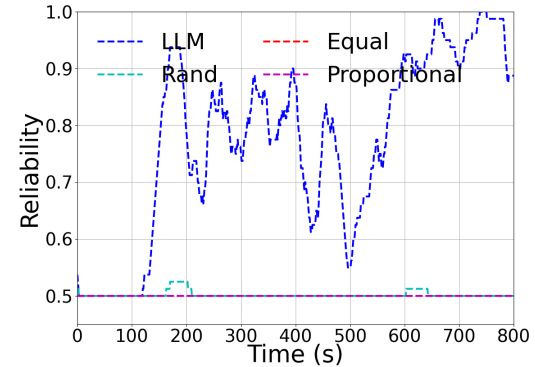
consistency, highlighting the impact of foundation model capacity on control effectiveness.

5.4.2 Discussion

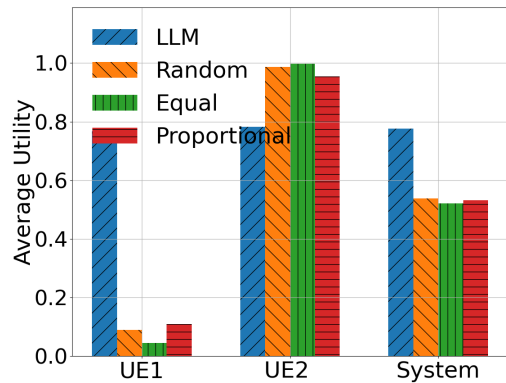
This section demonstrates that LLMs can serve as effective cognitive controllers for resilient slice management by translating intent into quantitative policy guidance. Unlike optimization-based or reinforcement learning approaches that operate on fixed abstractions, LLM-driven control adapts to evolving context, priorities, and operational goals. When integrated with learning-based control layers, LLMs enable a multi-timescale resilience framework that combines semantic reasoning with fast, reactive adaptation, strengthening the robustness and interpretability of O-RAN slice management.



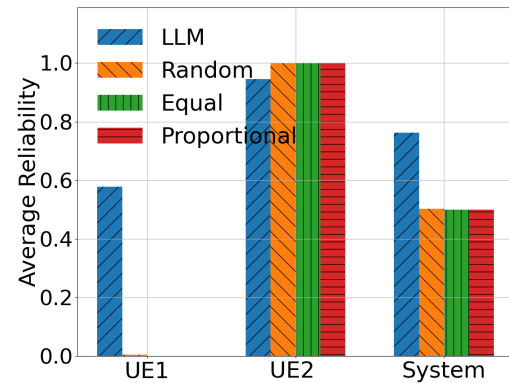
(a) System utility.



(b) System reliability.

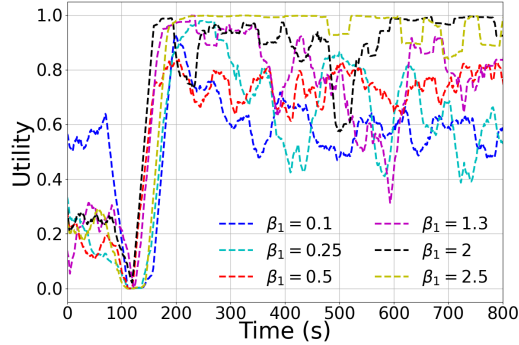


(c) Average utility.

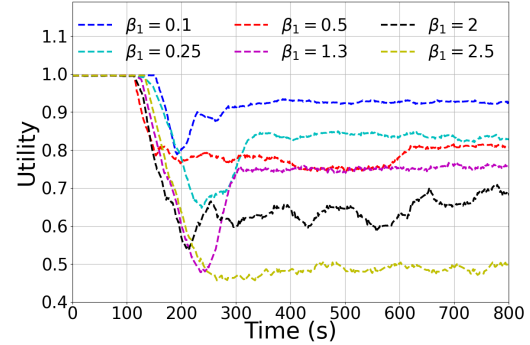


(d) Average reliability.

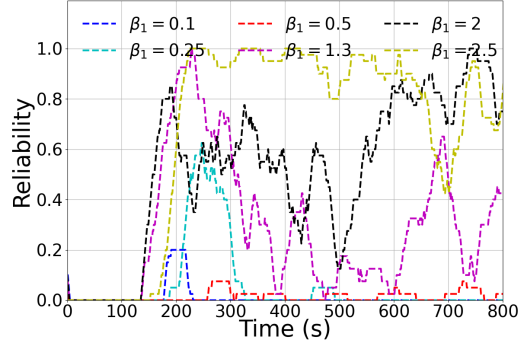
Figure 5.22: Comparative analysis of utility and reliability. (a) System utility. (b) System reliability. (c) Average utility. (d) Average reliability.



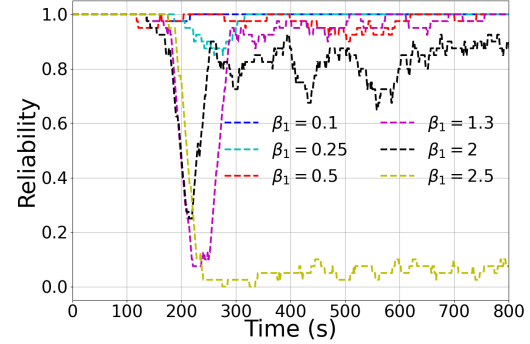
(a) UE 1 utility.



(b) UE 2 utility.

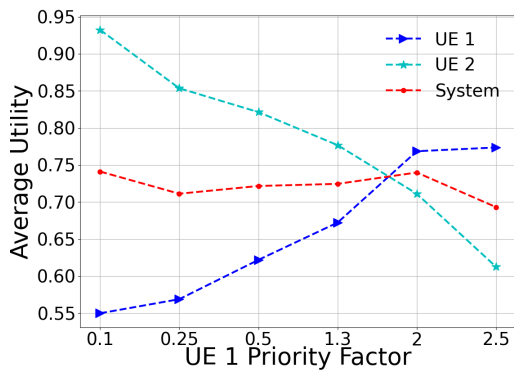


(c) UE 1 reliability.

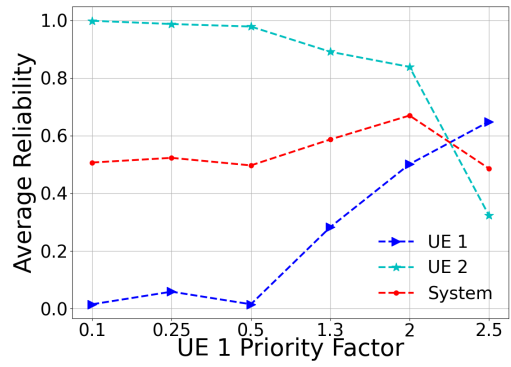


(d) UE 2 reliability.

Figure 5.23: Comparative analysis of window smoothed utility and reliability as functions of the priority factor of UE 1. (a) UE 1 utility. (b) UE 2 utility. (c) UE 1 reliability. (d) UE 2 reliability.

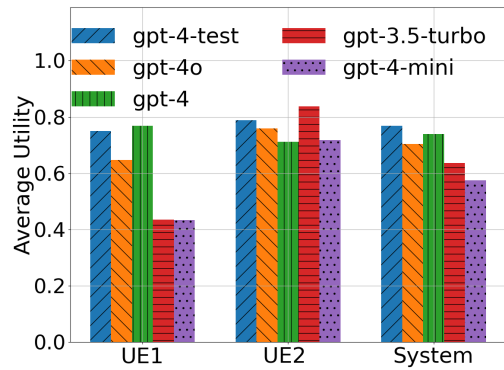


(a) Time-averaged utility.

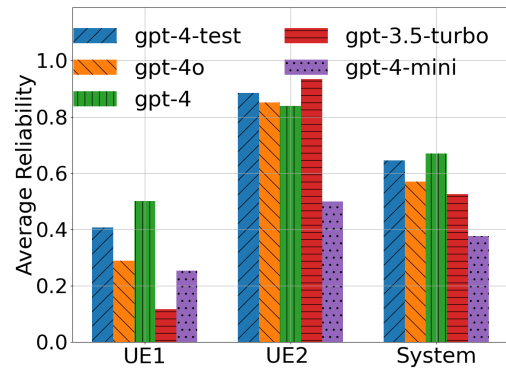


(b) Time-averaged reliability.

Figure 5.24: Comparative analysis of time-averaged utility and reliability as functions of the priority factor β_1 of UE 1. (a) Utility. (b) Reliability.



(a) Time-averaged utility.



(b) Time-averaged reliability.

Figure 5.25: Comparative analysis of time-averaged utility and reliability across different LLM models. (a) Utility. (b) Reliability.

Chapter 6

Concluding Remarks

This article has examined cyber resilience in next-generation (NextG) networks from complementary perspectives spanning threat characterization, theoretical foundations, analytical methodologies, and system-level design paradigms. The chapters are organized to progressively move from problem framing to formalization and finally to actionable design insights. We briefly summarize each chapter before synthesizing the overarching lessons and outlining future directions.

6.1 Summary of the Article

The article begins by characterizing the evolving threat landscape of NextG networks. Unlike legacy telecommunications systems, NextG networks are deeply softwarized, virtualized, and integrated with cloud and edge computing infrastructures. This chapter identifies how architectural innovations—such as SDN, NFV, O-RAN, MEC, and network slicing—expand the attack surface and introduce new classes of cyber, physical, and AI-driven risks. By systematically mapping threats across core, transport, RAN, edge, and cloud domains, the chapter establishes that risks in NextG networks are inherently cross-domain and systemic, motivating the need for resilience-centric rather than perimeter-based security approaches.

Chapter 2 develops a rigorous conceptual foundation for resilience in NextG networks. It distinguishes resilience from robustness, fault tolerance, and reliability, emphasizing resilience as a dynamic, multi-stage capability encompassing preparation, absorption, recovery, and adaptation. The chapter introduces a lifecycle view of resilience (proactive, responsive, and retrospective) and discusses how each stage manifests in 5G and beyond. It also surveys metrics and evaluation approaches that move beyond static availability measures toward time-dependent performance degradation, recovery trajectories, and learning effects, providing a basis for quantitative resilience assessment.

Chapter 3 provides the formal underpinnings necessary for principled resilience engineering. Control theory is used to model stability, disturbance rejection, and recovery under uncertainty. Dynamic and stochastic game theory captures adversarial interactions, incentive misalignment, and strategic behavior among attackers, defenders, and network stakeholders. Learning theory, particularly reinforcement learning and online adaptation—addresses nonstationarity, partial observability, and model uncertainty. Network-theoretic tools illuminate interdependencies and cascading failures. Together, these frameworks establish resilience as an emergent property arising from feedback, strategic reasoning, and learning across interconnected subsystems.

Chapter 4 translates theory into analytical tools for assessing cyber risk. It introduces probabilistic and strategic risk assessment methods, including the use of digital twins to simulate failures, attacks, and recovery processes. The chapter emphasizes that risk in NextG networks is endogenous: adversaries adapt to defenses, and defensive actions reshape attacker incentives. It also highlights the growing role of agentic AI and large language models in automating risk analysis, threat intelligence synthesis, and scenario exploration, while cautioning that these tools themselves must be treated as part of the attack surface.

The final technical chapter focuses on concrete design mechanisms for resilience. Through case studies on trust-aware resource management, risk-aware orchestration in edge–cloud systems, multi-agent reinforcement learning for slice management, and LLM-driven network control, the chapter demonstrates how resilience concepts can be operationalized. These examples illustrate how adaptive control, learning, and strategic reasoning can be embedded into real network management workflows to enable graceful degradation, rapid recovery, and long-term adaptation under uncertainty.

6.2 AI-Enabled Resilience and Vertical-Specific Challenges

While the preceding chapters establish resilience as a systems-level property grounded in control, game theory, and learning, two dimensions merit deeper emphasis when looking toward the future of NextG and beyond: (i) the evolving role of artificial intelligence as an enabler of resilience, and (ii) the increasing importance of domain-specific resilience specifications driven by vertical application requirements.

6.2.1 AI as an Enabler of Resilience

Artificial intelligence, including reinforcement learning and large language models, plays a dual role in NextG resilience. On one hand, AI offers unprecedented capabilities for anticipation, adaptation, and learning across complex, high-dimensional network environments. On the other hand, AI systems themselves introduce new vulnerabilities, uncertainties, and governance challenges that must be explicitly incorporated into resilience design.

From an enabling perspective, AI enhances resilience across all stages of the lifecycle. Proactively, AI can be used to analyze configuration spaces, software supply chains, and historical incident data to identify latent vulnerabilities and misconfigurations before deployment. Learning-based controllers and policy synthesis tools can evaluate resilience trade-offs—such as redundancy versus efficiency or isolation versus utilization—under uncertainty. In responsive settings, AI-driven analytics enable real-time anomaly detection, root-cause inference, and adaptive orchestration across slices, edge nodes, and cloud resources, often at time scales beyond human decision-making. Retrospectively, learning systems can mine forensic data, logs, and performance traces to update detection thresholds, refine control policies, and accelerate patching and recovery processes.

At the same time, the book highlights that AI systems are not passive tools but strategic components of the network. Learning algorithms may operate under partial observability, nonstationarity, or adversarial manipulation, leading to model drift, biased decisions, or emergent behaviors that degrade resilience rather than enhance it. Large language models, when embedded in network management or security workflows, raise additional concerns related to hallucination, prompt manipulation, data leakage, and accountability. As a result, future resilience frameworks must treat AI models as first-class entities whose trustworthiness, robustness, and failure modes are explicitly modeled, monitored, and governed.

This calls for a shift from “AI-assisted resilience” toward resilience-aware AI: AI systems designed with explicit safety margins, uncertainty quantification, and fallback mechanisms, and embedded within hierarchical control structures that preserve human oversight and policy constraints. Formal methods, game-theoretic reasoning, and risk-sensitive learning will be essential to ensure that AI-driven autonomy strengthens, rather than undermines, the resilience of NextG networks.

6.2.2 Vertical Domains and Domain-Specific Resilience Specifications

A second major outlook concerns the growing heterogeneity of vertical application domains that NextG networks are expected to support. Unlike previous generations of mobile net-

works, which were optimized primarily for consumer connectivity, NextG networks serve as foundational infrastructure for safety-critical, mission-critical, and economically critical systems. As a result, resilience can no longer be specified solely at the network level; it must be tailored to the requirements and risk profiles of individual verticals.

Different domains impose fundamentally different resilience specifications. In healthcare applications such as remote surgery or real-time patient monitoring, resilience is tightly coupled to ultra-low latency, bounded jitter, and deterministic recovery guarantees, where even brief disruptions can lead to irreversible harm. In transportation and autonomous mobility, resilience must account for coordinated failures across communication, control, and physical dynamics, with strong requirements on graceful degradation and fail-safe operation. Industrial automation and smart manufacturing emphasize continuity, isolation, and predictability, where resilience failures may propagate through tightly coupled cyber-physical workflows. Energy systems and smart grids demand resilience against cascading failures and coordinated attacks that span cyber and physical layers, often under strict regulatory and safety constraints.

These domain-specific requirements introduce new challenges for resilience engineering. First, resilience metrics must be contextualized: acceptable degradation and recovery times vary dramatically across verticals. Second, cross-domain interdependencies, such as a shared network slice supporting both public safety and commercial services, create complex trade-offs that cannot be resolved through uniform policies. Third, regulatory, legal, and ethical constraints differ across domains, shaping what forms of adaptation or automation are permissible during disruptions.

Addressing these challenges requires vertical-aware resilience design, where network slicing, orchestration, and control policies are explicitly informed by domain semantics, risk tolerance, and mission priorities. Digital twins and simulation-based validation will play a critical role in stress-testing resilience strategies under domain-specific scenarios. Moreover, collaboration between network operators, vertical stakeholders, regulators, and standards bodies will be essential to define resilience benchmarks that are both technically meaningful and societally acceptable.

These two dimensions point toward a future in which resilience is both AI-enabled and context-aware. AI provides the computational and cognitive machinery needed to manage complexity and uncertainty at scale, while vertical-specific requirements ground resilience to real-world consequences and societal impact. The central challenge lies in integrating these perspectives: designing AI-driven networked systems that can adapt intelligently while respecting domain constraints, governance frameworks, and human values.

Bibliography

- [1] X. Lin and N. Lee, “5G and beyond,” *Cham, Switzerland: Springer Nature Switzerland AG*, 2021.
- [2] H. Tataria, M. Shafi, A. F. Molisch, M. Dohler, H. Sjöland, and F. Tufvesson, “6G wireless systems: Vision, requirements, challenges, insights, and opportunities,” *Proceedings of the IEEE*, vol. 109, no. 7, pp. 1166–1199, 2021.
- [3] M. Giordani, M. Polese, M. Mezzavilla, S. Rangan, and M. Zorzi, “Toward 6G networks: Use cases and technologies,” *IEEE communications magazine*, vol. 58, no. 3, pp. 55–61, 2020.
- [4] K. Benzekki, A. El Fergougui, and A. Elbelrhiti Elalaoui, “Software-defined networking (SDN): A survey,” *Security and communication networks*, vol. 9, no. 18, pp. 5803–5833, 2016.
- [5] Z. Zaidi, V. Friderikos, Z. Yousaf, S. Fletcher, M. Dohler, and H. Aghvami, “Will SDN be part of 5G?,” *IEEE Communications Surveys & Tutorials*, vol. 20, no. 4, pp. 3220–3258, 2018.
- [6] H. Hawilo, A. Shami, M. Mirahmadi, and R. Asal, “NFV: state of the art, challenges, and implementation in next generation mobile networks (vEPC),” *IEEE network*, vol. 28, no. 6, pp. 18–26, 2014.
- [7] J. Matias, J. Garay, N. Toledo, J. Unzilla, and E. Jacob, “Toward an SDN-enabled NFV architecture,” *IEEE Communications Magazine*, vol. 53, no. 4, pp. 187–193, 2015.
- [8] A. Garcia-Saavedra and X. Costa-Perez, “O-RAN: Disrupting the virtualized RAN ecosystem,” *IEEE Communications Standards Magazine*, vol. 5, no. 4, pp. 96–103, 2021.

- [9] M. Polese, L. Bonati, S. D'oro, S. Basagni, and T. Melodia, "Understanding O-RAN: Architecture, interfaces, algorithms, security, and research challenges," *IEEE Communications Surveys & Tutorials*, vol. 25, no. 2, pp. 1376–1411, 2023.
- [10] P. Popovski, K. F. Trillingsgaard, O. Simeone, and G. Durisi, "5G wireless network slicing for eMBB, URLLC, and mMTC: A communication-theoretic view," *Ieee Access*, vol. 6, pp. 55765–55779, 2018.
- [11] T. Dragičević, P. Siano, S. Prabaharan, *et al.*, "Future generation 5G wireless networks for smart grid: A comprehensive review," *Energies*, vol. 12, no. 11, p. 2140, 2019.
- [12] H. C. Leligou, T. Zahariadis, L. Sarakis, E. Tsampasis, A. Voulkidis, and T. E. Velivassaki, "Smart grid: a demanding use case for 5G technologies," in *IEEE international conference on pervasive computing and communications workshops (PerCom Wkshps 2018)*, pp. 215–220, IEEE, 2018.
- [13] A. Gohar and G. Nencioni, "The role of 5G technologies in a smart city: The case for intelligent transportation system," *Sustainability*, vol. 13, no. 9, p. 5188, 2021.
- [14] L. Guevara and F. Auat Cheein, "The role of 5G technologies: Challenges in smart cities and intelligent transportation systems," *Sustainability*, vol. 12, no. 16, p. 6469, 2020.
- [15] S. Latif, J. Qadir, S. Farooq, and M. A. Imran, "How 5G wireless (and concomitant technologies) will revolutionize healthcare?," *Future Internet*, vol. 9, no. 4, p. 93, 2017.
- [16] D. H. Devi, K. Duraisamy, A. Armghan, M. Alsharari, K. Aliqab, V. Sorathiya, S. Das, and N. Rashid, "5g technology in healthcare and wearable devices: A review," *Sensors*, vol. 23, no. 5, p. 2519, 2023.
- [17] G. Brown, P. Analyst, and H. Reading, "Ultra-reliable low-latency 5G for industrial automation," *Technol. Rep. Qualcomm*, vol. 2, no. 52065394, pp. 1–11, 2018.
- [18] S. K. Rao and R. Prasad, "Impact of 5G technologies on industry 4.0," *Wireless personal communications*, vol. 100, no. 1, pp. 145–159, 2018.
- [19] I. Ahmad, S. Shahabuddin, T. Kumar, J. Okwuibe, A. Gurtov, and M. Ylianttila, "Security for 5G and beyond," *IEEE Communications Surveys & Tutorials*, vol. 21, no. 4, pp. 3682–3722, 2019.

- [20] J. Groen, S. D’Oro, U. Demir, L. Bonati, D. Villa, M. Polese, T. Melodia, and K. Chowdhury, “Securing O-RAN open interfaces,” *IEEE Transactions on Mobile Computing*, vol. 23, no. 12, pp. 11265–11277, 2024.
- [21] J. Groen, S. D’Oro, U. Demir, L. Bonati, M. Polese, T. Melodia, and K. Chowdhury, “Implementing and evaluating security in O-RAN: Interfaces, intelligence, and platforms,” *IEEE Network*, 2024.
- [22] M. Lyu, J. Farooq, and Q. Zhu, “Mapping cyber threats in the 5G supply chain: Landscape, vulnerabilities, and risk management,” *IEEE Network*, vol. 39, no. 1, pp. 251–260, 2025.
- [23] C. De Alwis, P. Porambage, K. Dev, T. R. Gadekallu, and M. Liyanage, “A survey on network slicing security: Attacks, challenges, solutions and research directions,” *IEEE Communications Surveys & Tutorials*, vol. 26, no. 1, pp. 534–570, 2023.
- [24] A. S. Abdalla and V. Marojevic, “End-to-end O-RAN security architecture, threat surface, coverage, and the case of the open fronthaul,” *IEEE Communications Standards Magazine*, vol. 8, no. 1, pp. 36–43, 2024.
- [25] E. Konstantopoulou, N. Sklavos, and I. Ognjanovic, “Securing public safety mission-critical 5G communications of smart cities,” in *Internet of Everything for Smart City and Smart Healthcare Applications*, pp. 61–74, Springer, 2023.
- [26] J. Suomalainen, J. Julku, M. Vehkaperä, and H. Posti, “Securing public safety communications on commercial and tactical 5G networks: A survey and future research directions,” *IEEE Open Journal of the Communications Society*, vol. 2, pp. 1590–1615, 2021.
- [27] R. Barona and E. M. Anita, “A survey on data breach challenges in cloud computing security: Issues and threats,” in *2017 International conference on circuit, power and computing technologies (ICCPCT)*, pp. 1–8, IEEE, 2017.
- [28] A. Rostami, P. Ohlen, K. Wang, Z. Ghebretensae, B. Skubic, M. Santos, and A. Vidal, “Orchestration of RAN and transport networks for 5G: An SDN approach,” *IEEE Communications Magazine*, vol. 55, no. 4, pp. 64–70, 2017.
- [29] I. Parvez, A. Rahmati, I. Guvenc, A. I. Sarwat, and H. Dai, “A survey on low latency towards 5G: RAN, core network and caching solutions,” *IEEE Communications Surveys & Tutorials*, vol. 20, no. 4, pp. 3098–3130, 2018.

- [30] M. Mahyoub, A. AbdulGhaffar, E. Alalade, E. Ndubisi, and A. Matrawy, “Security analysis of critical 5G interfaces,” *IEEE Communications Surveys & Tutorials*, vol. 26, no. 4, pp. 2382–2410, 2024.
- [31] N. Agrawal and S. Tapaswi, “Defense mechanisms against DDoS attacks in a cloud computing environment: State-of-the-art and research challenges,” *IEEE Communications Surveys & Tutorials*, vol. 21, no. 4, pp. 3769–3795, 2019.
- [32] N. Wehbe, H. A. Alameddine, M. Pourzandi, E. Bou-Harb, and C. Assi, “A security assessment of HTTP/2 usage in 5G service-based architecture,” *IEEE Communications Magazine*, vol. 61, no. 1, pp. 48–54, 2022.
- [33] M. Pearce, S. Zeadally, and R. Hunt, “Virtualization: Issues, security threats, and solutions,” *ACM Comput. Surv. (CSUR)*, vol. 45, no. 2, pp. 1–39, 2013.
- [34] D. H. de Miranda Marques and D. C. G. Valadares, “Radio access network attacks: A comprehensive survey,” *IEEE Internet of Things Journal*, 2025.
- [35] Q. Zhu, S. Rass, B. Dieber, and V. M. Vilches, “Cybersecurity in robotics: Challenges, quantitative modeling, and practice,” *Foundations and Trends in Robotics*, vol. 9, no. 1, pp. 1–129, 2021.
- [36] Y.-T. Yang and Q. Zhu, “Game-theoretic foundations for cyber resilience against deceptive information attacks in intelligent transportation systems,” *arXiv preprint arXiv:2412.04627*, 2024.
- [37] Q. Zhu, “Multilayer cyber-physical security and resilience for smart grid,” in *Smart grid control: overview and research opportunities*, pp. 225–239, Springer, 2018.
- [38] P. Oser, R. W. van der Heijden, S. Lüders, and F. Kargl, “Risk prediction of IoT devices based on vulnerability analysis,” *ACM Transactions on Privacy and Security*, vol. 25, no. 2, pp. 1–36, 2022.
- [39] Y. Zhao, J. Chen, and Q. Zhu, “Integrated cyber-physical resiliency for power grids under IoT-enabled dynamic botnet attacks,” *IEEE Transactions on Control Systems Technology*, vol. 32, no. 5, pp. 1755–1769, 2024.
- [40] J. Pawlick, E. Colbert, and Q. Zhu, “Modeling and analysis of leaky deception using signaling games with evidence,” *IEEE Transactions on Information Forensics and Security*, vol. 14, no. 7, pp. 1871–1886, 2018.

- [41] M. Mohebbi Moghaddam, M. H. Manshaei, and Q. Zhu, “To trust or not: A security signaling game between service provider and client,” in *Decision and Game Theory for Security: 6th International Conference, GameSec 2015, London, UK, November 4-5, 2015, Proceedings* 6, pp. 322–333, Springer, 2015.
- [42] M. Asadi, M. A. J. Jamali, A. Heidari, and N. J. Navimipour, “Botnets unveiled: A comprehensive survey on evolving threats and defense strategies,” *Transactions on Emerging Telecommunications Technologies*, vol. 35, no. 11, p. e5056, 2024.
- [43] Z. Yang, B. Xu, J. M. Zhang, H. J. Kang, J. Shi, J. He, and D. Lo, “Stealthy backdoor attack for code models,” *IEEE Transactions on Software Engineering*, vol. 50, no. 4, pp. 721–741, 2024.
- [44] S. Da Canal, F. Mancini, and G. Bianchi, “5GRecon: Automating 5G network function recognition and misconfiguration troubleshooting,” in *13th IFIP/IEEE International Conference on Performance Evaluation and Modeling in Wired and Wireless Networks (PEMWN 2024)*, pp. 1–6, IEEE, 2024.
- [45] S. Shringarpurale, P. McDaniel, K. Butler, and T. La Porta, “Co-residency attacks on containers are real,” in *Proceedings of the 2020 ACM SIGSAC conference on cloud computing security workshop*, pp. 53–66, 2020.
- [46] M. Suchara, A. Fabrikant, and J. Rexford, “BGP safety with spurious updates,” in *2011 Proceedings IEEE INFOCOM*, pp. 2966–2974, IEEE, 2011.
- [47] P. Garg, “Cloud security posture management: Tools and techniques,” *Available at SSRN 5357921*, 2025.
- [48] L. Williams, G. Benedetti, S. Hamer, R. Paramitha, I. Rahman, M. Tamanna, G. Tys-tahl, N. Zahan, P. Morrison, Y. Acar, *et al.*, “Research directions in software supply chain security,” *ACM Transactions on Software Engineering and Methodology*, vol. 34, no. 5, pp. 1–38, 2025.
- [49] R. Yazdani, M. Resing, and A. Sperotto, “Glossy mirrors: On the role of open resolvers in reflection and amplification DDoS attacks,” in *20th International Conference on Network and Service Management (CNSM 2024)*, pp. 1–9, IEEE, 2024.
- [50] S. Xi, K. Bu, W. Mao, X. Zhang, K. Ren, and X. Ren, “RuleOut forwarding anomalies for SDN,” *IEEE/ACM Transactions on Networking*, vol. 31, no. 1, pp. 395–407, 2022.

- [51] M. Zoure, T. Ahmed, and L. Réveillère, “Network services anomalies in NFV: Survey, taxonomy, and verification methods,” *IEEE Transactions on Network and Service Management*, vol. 19, no. 2, pp. 1567–1584, 2022.
- [52] T. D. Ngoc, B. Teabe, A. Tchana, G. Muller, and D. Hagimont, “Mitigating vulnerability windows with hypervisor transplant,” in *Proceedings of the Sixteenth European Conference on Computer Systems*, pp. 162–177, 2021.
- [53] A. Al-Alaj, R. Krishnan, and R. Sandhu, “SDN-RBAC: An access control model for SDN controller applications,” in *4th International Conference on Computing, Communications and Security (ICCCS 2019)*, pp. 1–8, IEEE, 2019.
- [54] M. Alabbad and R. Khedri, “Dynamic segmentation, configuration, and governance of SDN,” *J. Ubiquitous Syst. Pervasive Networks*, vol. 16, no. 1, pp. 7–22, 2022.
- [55] A. K. Alnaim, “Securing 5G virtual networks: A critical analysis of SDN, NFV, and network slicing security,” *International Journal of Information Security*, pp. 1–21, 2024.
- [56] C. Mas-Machuca, F. Musumeci, P. Vizarreta, D. Pezaros, S. Jouët, M. Tornatore, A. Hmaity, M. Liyanage, A. Gursov, and A. Braeken, “Reliable control and data planes for softwarized networks,” in *Guide to disaster-resilient communication networks*, pp. 243–270, Springer, 2020.
- [57] T. Hayford-Acquah and B. Asante, “Causes of fiber cut and the recommendation to solve the problem,” *IOSR J. Electron. Commun. Eng*, vol. 12, no. 01, pp. 46–64, 2017.
- [58] Y.-C. Tian and J. Gao, “Network security and privacy architecture,” in *Network Analysis and Architecture*, pp. 361–402, Springer, 2023.
- [59] D. Raposo, M. L. Pardal, L. Rodrigues, and M. Correia, “Machete: Multi-path communication for security,” in *2016 IEEE 15th International Symposium on Network Computing and Applications (NCA)*, pp. 60–67, IEEE, 2016.
- [60] V. Lakshmi and S. Azad, “Self-healing networks leverage intelligent protocols enable autonomous fault detection and recovery,” in *International Conference on Intelligent Systems in Computing and Communication*, pp. 317–330, Springer, 2023.
- [61] A. Filali, A. Abouaomar, S. Cherkaoui, A. Kobbane, and M. Guizani, “Multi-access edge computing: A survey,” *IEEE Access*, vol. 8, pp. 197017–197046, 2020.

- [62] B. Balasubramanian, E. S. Daniels, M. Hiltunen, R. Jana, K. Joshi, R. Sivaraj, T. X. Tran, and C. Wang, “RIC: A RAN intelligent controller platform for AI-enabled cellular networks,” *IEEE Internet Computing*, vol. 25, no. 2, pp. 7–17, 2021.
- [63] J.-H. Huang, S.-M. Cheng, R. Kaliski, and C.-F. Hung, “Developing xApps for rogue base station detection in SDR-enabled O-RAN,” in *IEEE Conference on Computer Communications Workshops (INFOCOM WKSHPS 2023)*, pp. 1–6, IEEE, 2023.
- [64] Z. Abou El Houda, H. Moudoud, and B. Brik, “Federated deep reinforcement learning for efficient jamming attack mitigation in O-RAN,” *IEEE Transactions on Vehicular Technology*, vol. 73, no. 7, pp. 9334–9343, 2024.
- [65] C.-F. Hung, Y.-R. Chen, C.-H. Tseng, and S.-M. Cheng, “Security threats to xapps access control and E2 interface in O-RAN,” *IEEE Open Journal of the Communications Society*, vol. 5, pp. 1197–1203, 2024.
- [66] P. Fernando, P. Porambage, M. Liyanage, K. Steenhaut, and A. Braeken, “Securing xApps in Open RAN: A hierarchical approach to authentication and authorisation,” in *IEEE Conference on Communications and Network Security (CNS 2025)*, pp. 1–9, IEEE, 2025.
- [67] S.-M. Cheng, B.-K. Hong, and C.-F. Hung, “Attack detection and mitigation in MEC-enabled 5G networks for AIoT,” *IEEE Internet of Things Magazine*, vol. 5, no. 3, pp. 76–81, 2022.
- [68] T. Li, Y. Pan, and Q. Zhu, “Decision-dominant strategic defense against lateral movement for 5G zero-trust multi-domain networks,” in *Network Security Empowered by Artificial Intelligence*, pp. 25–76, Springer, 2024.
- [69] R. Pietrantuono, M. Ficco, and F. Palmieri, “Testing the resilience of MEC-based IoT applications against resource exhaustion attacks,” *IEEE Transactions on Dependable and Secure Computing*, vol. 21, no. 2, pp. 804–818, 2023.
- [70] T. Yu, V. Sekar, S. Seshan, Y. Agarwal, and C. Xu, “Handling a trillion (unfixable) flaws on a billion devices: Rethinking network security for the internet-of-things,” in *Proceedings of the 14th ACM workshop on hot topics in networks*, pp. 1–7, 2015.
- [71] Y. Wu, J. Wang, Y. Wang, S. Zhai, Z. Li, Y. He, K. Sun, Q. Li, and N. Zhang, “Your firmware has arrived: A study of firmware update vulnerabilities,” in *33rd USENIX Security Symposium (USENIX Security 24)*, pp. 5627–5644, 2024.

- [72] D. Puthal, X. Wu, N. Surya, R. Ranjan, and J. Chen, “SEEN: A selective encryption method to ensure confidentiality for big sensing data streams,” *IEEE Transactions on Big Data*, vol. 5, no. 3, pp. 379–392, 2017.
- [73] T. O. Atalay, S. Maitra, D. Stojadinovic, A. Stavrou, and H. Wang, “An OpenRAN security framework for scalable authentication, authorization, and discovery of xApps with isolated critical services,” *IEEE Transactions on Dependable and Secure Computing*, 2024.
- [74] K. Alam, M. A. Habibi, M. Tammen, D. Krummacker, W. Saad, M. Di Renzo, T. Melodia, X. Costa-Pérez, M. Debbah, A. Dutta, *et al.*, “A comprehensive tutorial and survey of O-RAN: Exploring slicing-aware architecture, deployment options, use cases, and challenges,” *IEEE Communications Surveys & Tutorials*, 2025.
- [75] L. Aversano, M. L. Bernardi, M. Cimitile, R. Pecori, and L. Veltri, “Effective anomaly detection using deep learning in IoT systems,” *Wireless Communications and Mobile Computing*, vol. 2021, no. 1, p. 9054336, 2021.
- [76] M. V. Ngo, Y. H. Pua, T.-L. Le, B. Chen, T. Quek, *et al.*, “AI-driven rApps for reducing radio access network interference in real-world 5G deployment,” in *IEEE Conference on Computer Communications Workshops (INFOCOM WKSHPS 2024)*, pp. 1–2, IEEE, 2024.
- [77] D. Attanayaka, P. Porambage, M. Liyanage, and M. Ylianttila, “Peer-to-peer federated learning based anomaly detection for open radio access networks,” in *IEEE International Conference on Communications (ICC 2023)*, pp. 5464–5470, IEEE, 2023.
- [78] M. Lyu, J. Farooq, and Q. Zhu, “Mapping cyber threats in the 5G supply chain: Landscape, vulnerabilities, and risk management,” *IEEE Netw.*, 2024. early access.
- [79] T. Kieras, J. Farooq, and Q. Zhu, “Iot supply chain security risk analysis and mitigation: Modeling, computations, and software tools,” in *Springer Nature*, 2022.
- [80] T. Kieras, J. Farooq, and Q. Zhu, “I-SCRAM: A framework for IoT supply chain risk analysis and mitigation decisions,” *IEEE Access*, vol. 9, pp. 29827–29840, 2021.
- [81] M. Lyu and J. Farooq, “Zero trust in 5G networks: Principles, challenges, and opportunities,” *Resilience Week (RWS 2024)*, pp. 1–8, 2024.
- [82] S. Lachmund, “Standards driven security assurance for mobile networks,” *Journal of ICT Standardization*, pp. 105–132, 2015.

- [83] C. Benzaïd, T. Taleb, and M. Z. Farooqi, “Trust in 5G and beyond networks,” *IEEE Network*, vol. 35, no. 3, pp. 212–222, 2021.
- [84] R. A. Paskauskas, “A preliminary ontology for 5G network resilience: Hybrid threats, risk reduction, compliance,” in *IEEE International Conference on Cyber Security and Resilience (CSR 2025)*, pp. 490–497, IEEE, 2025.
- [85] A. Alshamrani, S. Myneni, A. Chowdhary, and D. Huang, “A survey on advanced persistent threats: Techniques, solutions, challenges, and research opportunities,” *IEEE Communications Surveys & Tutorials*, vol. 21, no. 2, pp. 1851–1877, 2019.
- [86] Y. Wang, H. Liu, Z. Li, Z. Su, and J. Li, “Combating advanced persistent threats: Challenges and solutions,” *IEEE Network*, vol. 38, no. 6, pp. 324–333, 2024.
- [87] Q. Zhu and S. Rass, “On multi-phase and multi-stage game-theoretic modeling of advanced persistent threats,” *IEEE Access*, vol. 6, pp. 13958–13971, 2018.
- [88] Y. Huang, J. Chen, L. Huang, and Q. Zhu, “Dynamic games for secure and resilient control system design,” *Nat. Sci. Rev.*, vol. 7, no. 7, pp. 1125–1141, 2020.
- [89] S. Khan, I. Kabanov, Y. Hua, and S. Madnick, “A systematic analysis of the capital one data breach: Critical lessons learned,” *ACM Transactions on Privacy and Security*, vol. 26, no. 1, pp. 1–29, 2022.
- [90] Z. Tan, S. P. Parambath, C. Anagnostopoulos, J. Singer, and A. K. Marnerides, “Advanced persistent threats based on supply chain vulnerabilities: Challenges, solutions & future directions,” *IEEE Internet of Things Journal*, 2025.
- [91] I. Palamà, F. Gringoli, G. Bianchi, and N. Belfari-Melazzi, “Imsi catchers in the wild: A real world 4G/5G assessment,” *Computer Networks*, vol. 194, p. 108137, 2021.
- [92] Y.-T. Yang and Q. Zhu, “Toward a multi-echelon cyber warfare theory: A meta-game-theoretic paradigm for defense and dominance,” *arXiv preprint arXiv:2509.08976*, 2025.
- [93] Y.-T. Yang and Q. Zhu, “A multi-resolution dynamic game framework for cross-echelon decision-making in cyber warfare,” in *International Conference on Game Theory and AI for Security*, pp. 335–355, Springer, 2025.
- [94] L. Axon, J. Saunders, P. Esteve-González, J. Carver, W. Dutton, M. Goldsmith, and S. Creese, “Private-public initiatives for cybersecurity: the case of Ukraine,” *Journal of Cyber Policy*, vol. 9, no. 3, pp. 399–422, 2024.

[95] H. Oz, A. Aris, A. Levi, and A. S. Uluagac, “A survey on ransomware: Evolution, taxonomy, and defense solutions,” *ACM Computing Surveys (CSUR)*, vol. 54, no. 11s, pp. 1–37, 2022.

[96] A. Bhardwaj, “Cybercrime, digital terrorism, and 5G paradigm: Attack trends of the new millennium,” in *5G and Fiber Optics Security Technologies for Smart Grid Cyber Defense*, pp. 1–27, IGI Global, 2024.

[97] Y. Zhao, Y. Ge, and Q. Zhu, “Combating ransomware in internet of things: a games-in-games approach for cross-layer cyber defense and security investment,” in *International Conference on Decision and Game Theory for Security*, pp. 208–228, Springer, 2021.

[98] J. Beerman, D. Berent, Z. Falter, and S. Bhunia, “A review of colonial pipeline ransomware attack,” in *2023 IEEE/ACM 23rd International Symposium on Cluster, Cloud and Internet Computing Workshops (CCGridW)*, pp. 8–15, IEEE, 2023.

[99] S. Bhunia, M. Blackert, H. Deal, A. DePero, and A. Patra, “Analyzing the 2021 Kaseya ransomware attack: Combined spearphishing through SonicWall SSLVPN vulnerability,” *IET Information Security*, vol. 2025, no. 1, p. 1655307, 2025.

[100] P. Ranaweera, A. Jurcut, and M. Liyanage, “MEC-enabled 5G use cases: A survey on security vulnerabilities and countermeasures,” *ACM Computing Surveys (CSUR)*, vol. 54, no. 9, pp. 1–37, 2021.

[101] S. Alzahrani, Y. Xiao, and W. Sun, “An analysis of conti ransomware leaked source codes,” *IEEE Access*, vol. 10, pp. 100178–100193, 2022.

[102] G. Moore, Z. Khurshid, T. McDonnell, L. Rogers, and O. Healy, “A resilient workforce: patient safety and the workforce response to a cyber-attack on the ICT systems of the national health service in Ireland,” *BMC Health Services Research*, vol. 23, no. 1, p. 1112, 2023.

[103] G. Tang, Y. Wang, and H. Lu, “Shiftguard: Towards reliable 5G network by optimal backup power allocation,” in *IEEE International Conference on Communications, Control, and Computing Technologies for Smart Grids (SmartGridComm 2020)*, pp. 1–6, IEEE, 2020.

[104] J. Chen and Q. Zhu, “A game-theoretic framework for resilient and distributed generation control of renewable energies in microgrids,” *IEEE Transactions on Smart Grid*, vol. 8, no. 1, pp. 285–295, 2016.

- [105] Q. Zhu, “Multilayer cyber-physical security and resilience for smart grid,” in *Smart grid control: overview and research opportunities*, pp. 225–239, Springer, 2019.
- [106] P. C. Fonseca and E. S. Mota, “A survey on fault management in software-defined networks,” *IEEE Communications Surveys & Tutorials*, vol. 19, no. 4, pp. 2284–2321, 2017.
- [107] Q. Zhu and T. Başar, “Disentangling resilience from robustness: Contextual dualism, interactionism, and game-theoretic paradigms,” *IEEE Control Systems Magazine*, vol. 44, no. 3, pp. 95–103, 2024.
- [108] J. W. Baker, M. Schubert, and M. H. Faber, “On the assessment of robustness,” *Structural safety*, vol. 30, no. 3, pp. 253–267, 2008.
- [109] Y. Benslimen, H. Sedjelmaci, and A.-C. Manenti, “Attacks and failures prediction framework for a collaborative 5G mobile network,” *Computing*, vol. 103, no. 6, pp. 1165–1181, 2021.
- [110] L. De Simone, M. Di Mauro, R. Natella, and F. Postiglione, “Performance and availability challenges in designing resilient 5G architectures,” *IEEE Transactions on Network and Service Management*, vol. 21, no. 5, pp. 5291–5303, 2024.
- [111] G. Windle, “What is resilience? a review and concept analysis,” *Reviews in clinical gerontology*, vol. 21, no. 2, pp. 152–169, 2011.
- [112] T. Taleb, A. Ksentini, and B. Sericola, “On service resilience in cloud-native 5G mobile systems,” *IEEE Journal on Selected Areas in Communications*, vol. 34, no. 3, pp. 483–496, 2016.
- [113] S. Vittal, S. Sarkar, and A. A. Franklin, “Revamping the resilience and high availability of 5G core for 6G ready network slices,” *IEEE Transactions on Network and Service Management*, vol. 21, no. 2, pp. 2287–2302, 2023.
- [114] B. Zhou, Z. Liu, and H. Su, “5G networks enabling cooperative autonomous vehicle localization: A survey,” *IEEE Transactions on Intelligent Transportation Systems*, vol. 25, no. 11, pp. 15291–15313, 2024.
- [115] Y. Ma, L. Liu, Z. Liu, F. Li, Q. Xie, K. Chen, C. Lv, Y. He, and F. Li, “A survey of ddos attack and defense technologies in multi-access edge computing,” *IEEE Internet of Things Journal*, 2024.

[116] J. M. DeAlmeida, C. F. Pontes, L. A. DaSilva, C. B. Both, J. J. Gondim, C. G. Ralha, and M. A. Marotta, “Abnormal behavior detection based on traffic pattern categorization in mobile networks,” *IEEE Transactions on Network and Service Management*, vol. 18, no. 4, pp. 4213–4224, 2021.

[117] X. Wu, R. Honnalli, and J. Farooq, “Poster: Triage Slicing: Online detection and containment of disruptive UEs in O-RAN slices,” in *Proceedings of the Twenty-sixth International Symposium on Theory, Algorithmic Foundations, and Protocol Design for Mobile Networks and Mobile Computing*, pp. 405–406, 2025.

[118] J. Moore, A. S. Abdalla, M. Zhang, and V. Marojevic, “SSxApp: Secure slicing for O-RAN deployments,” in *IEEE Military Communications Conference (MILCOM 2023)*, pp. 251–252, IEEE, 2023.

[119] F. Sharevski, “Towards 5G cellular network forensics,” *EURASIP Journal on Information Security*, vol. 2018, no. 1, p. 8, 2018.

[120] S. Brown, J. Gommers, and O. Serrano, “From cyber security information sharing to threat management,” in *Proceedings of the 2nd ACM workshop on information sharing and collaborative security*, pp. 43–49, 2015.

[121] J. Pan, I. S. Popa, K. Zeitouni, and C. Borcea, “Proactive vehicular traffic rerouting for lower travel time,” *IEEE Transactions on vehicular technology*, vol. 62, no. 8, pp. 3551–3568, 2013.

[122] T. Hauer, P. Hoffmann, J. Lunney, D. Ardelean, and A. Diwan, “Meaningful availability,” in *17th USENIX Symposium on Networked Systems Design and Implementation (NSDI 20)*, pp. 545–557, 2020.

[123] G. Deepak, A. Ladas, Y. A. Sambo, H. Pervaiz, C. Politis, and M. A. Imran, “An overview of post-disaster emergency communication systems in the future networks,” *IEEE Wireless Communications*, vol. 26, no. 6, pp. 132–139, 2019.

[124] S. A. A. Shah, E. Ahmed, M. Imran, and S. Zeadally, “5G for vehicular communications,” *IEEE Communications Magazine*, vol. 56, no. 1, pp. 111–117, 2018.

[125] K. Ito, J. Nakazato, R. Fontugne, M. Tsukada, and E. Hiroshi, “A multipath redundancy communication framework for enhancing 5G mobile communication quality,” *Computer Communications*, p. 108157, 2025.

[126] J. Zhong, H. Sanhedrai, F. Zhang, Y. Yang, S. Guo, S. Yang, and D. Li, “Network endurance against cascading overload failure,” *Reliability Engineering & System Safety*, vol. 201, p. 106916, 2020.

[127] S. Sevgican, M. Turan, K. Gökarşlan, H. B. Yilmaz, and T. Tugcu, “Intelligent network data analytics function in 5G cellular networks using machine learning,” *Journal of Communications and Networks*, vol. 22, no. 3, pp. 269–280, 2020.

[128] C. Benzaïd, N. Guerd, N. E. H. Rehouma, K. Zeraoulia, and T. Taleb, “A multi-layered zero trust microsegmentation solution for cloud-native 5g & beyond networks,” in *IEEE Wireless Communications and Networking Conference (WCNC 2025)*, pp. 1–7, IEEE, 2025.

[129] T. Tsourdinis, N. Makris, S. Fdida, and T. Korakis, “Drl-based service migration for MEC cloud-native 5G and beyond networks,” in *IEEE 9th International Conference on Network Softwarization (NetSoft 2023)*, pp. 62–70, IEEE, 2023.

[130] D. S. Fowler, Y. K. Mo, A. Evans, S. Dinh-Van, B. Ahmad, M. D. Higgins, and C. Maple, “A 5G automated-guided vehicle SME testbed for resilient future factories,” *IEEE Open Journal of the Industrial Electronics Society*, vol. 4, pp. 242–258, 2023.

[131] M. Mekki, S. Arora, and A. Ksentini, “A scalable monitoring framework for network slicing in 5G and beyond mobile networks,” *IEEE Transactions on Network and Service Management*, vol. 19, no. 1, pp. 413–423, 2021.

[132] D. Borsatti, C. Grasselli, C. Contoli, L. Micciullo, L. Spinacci, M. Settembre, W. Cerboni, and F. Callegati, “Mission critical communications support with 5G and network slicing,” *IEEE Transactions on Network and Service Management*, vol. 20, no. 1, pp. 595–607, 2022.

[133] J. Ortiz, R. Sanchez-Iborra, J. B. Bernabe, A. Skarmeta, C. Benzaid, T. Taleb, P. Alemany, R. Muñoz, R. Vilalta, C. Gaber, *et al.*, “INSPIRE-5Gplus: Intelligent security and pervasive trust for 5G and beyond networks,” in *Proceedings of the 15th International Conference on Availability, Reliability and Security*, pp. 1–10, 2020.

[134] E. N. Amachaghi, M. Shojafar, C. H. Foh, and K. Moessner, “A survey for intrusion detection systems in Open RAN,” *IEEE Access*, vol. 12, pp. 88146–88173, 2024.

[135] T. Han and N. Ansari, “Network utility aware traffic load balancing in backhaul-constrained cache-enabled small cell networks with hybrid power supplies,” *IEEE Transactions on Mobile Computing*, vol. 16, no. 10, pp. 2819–2832, 2017.

- [136] S. Cherrared, S. Imadali, E. Fabre, G. Gössler, and I. G. B. Yahia, “A survey of fault management in network virtualization environments: Challenges and solutions,” *IEEE Transactions on Network and Service Management*, vol. 16, no. 4, pp. 1537–1551, 2019.
- [137] J. Xing, J. Gong, X. Foukas, A. Kalia, D. Kim, and M. Kotaru, “Enabling resilience in virtualized rans with atlas,” in *Proceedings of the 29th Annual International Conference on Mobile Computing and Networking*, pp. 1–15, 2023.
- [138] L. Huang and Q. Zhu, “Duplicity games for deception design with an application to insider threat mitigation,” *IEEE Transactions on Information Forensics and Security*, vol. 16, pp. 4843–4856, 2021.
- [139] W. Casey, J. A. Morales, E. Wright, Q. Zhu, and B. Mishra, “Compliance signaling games: toward modeling the deterrence of insider threats,” *Computational and Mathematical Organization Theory*, vol. 22, pp. 318–349, 2016.
- [140] W. A. Casey, Q. Zhu, J. A. Morales, and B. Mishra, “Compliance control: Managed vulnerability surface in social-technological systems via signaling games,” in *Proceedings of the 7th ACM CCS international workshop on managing insider security threats*, pp. 53–62, 2015.
- [141] J. M. Vidal and M. A. S. Monge, “Framework for anticipatory self-protective 5G environments,” in *Proceedings of the 14th international conference on availability, reliability and security*, pp. 1–9, 2019.
- [142] M. M. Alnfiai, “AI-powered cyber resilience: a reinforcement learning approach for automated threat hunting in 5G networks,” *EURASIP Journal on Wireless Communications and Networking*, vol. 2025, no. 1, p. 68, 2025.
- [143] N. Fazrina, “Securing distributed sensor systems through adaptive encryption algorithms in 5G-based smart energy networks,” *Open Journal of Robotics, Autonomous Decision-Making, and Human-Machine Interaction*, vol. 9, no. 11, pp. 18–27, 2024.
- [144] G. H. Carvalho, I. Woungang, A. Anpalagan, and I. Traore, “When agile security meets 5G,” *IEEE Access*, vol. 8, pp. 166212–166225, 2020.
- [145] W. Fan, B. Shi, and C. Peng, “A novel 5G key reinstallation attack and defensive strategies,” in *2025 IEEE Wireless Communications and Networking Conference (WCNC)*, pp. 1–6, IEEE, 2025.

- [146] Z. Liu, Q. Wu, X. Shen, J. Tan, and X. Zhang, “Post-disaster robust restoration scheme for distribution network considering rerouting process of cyber system with 5G,” *IEEE transactions on smart grid*, vol. 15, no. 5, pp. 4478–4491, 2024.
- [147] Q. Zhu and T. Başar, “Disentangling resilience from robustness: contextual dualism, interactionism, and game-theoretic paradigms,” *IEEE Control Syst. Mag.*, vol. 44, no. 3, pp. 95–103, 2024.
- [148] Q. Zhu and Z. Xu, “Cross-layer design for secure and resilient cyber-physical systems,” *Cham, Switzerland: Springer*, 2020.
- [149] J. Chen and Q. Zhu, “Interdependent strategic security risk management with bounded rationality in the internet of things,” *IEEE Transactions on Information Forensics and Security*, vol. 14, no. 11, pp. 2958–2971, 2019.
- [150] Q. Zhu and T. Basar, “Game-theoretic methods for robustness, security, and resilience of cyberphysical control systems: games-in-games principle for optimal cross-layer resilient control systems,” *IEEE Control Syst. Mag.*, vol. 35, no. 1, pp. 46–65, 2015.
- [151] L. Bell, M. Brunton-Spall, R. Smith, and J. Bird, *Agile application security: enabling security in a continuous delivery pipeline.* ” O'Reilly Media, Inc.”, 2017.
- [152] O. Javed and S. Toor, “An evaluation of container security vulnerability detection tools,” in *Proceedings of the 2021 5th International Conference on Cloud and Big Data Computing*, pp. 95–101, 2021.
- [153] S. Pan, L. Bao, J. Zhou, X. Hu, X. Xia, and S. Li, “Towards more practical automation of vulnerability assessment,” in *Proceedings of the IEEE/ACM 46th International Conference on Software Engineering*, pp. 1–13, 2024.
- [154] S. Soltani, A. Amanloo, M. Shojafar, and R. Tafazolli, “Intelligent control in 6G Open RAN: security risk or opportunity?,” *IEEE Open Journal of the Communications Society*, 2025.
- [155] Y. He, D. Huang, L. Chen, Y. Ni, and X. Ma, “A survey on zero trust architecture: Challenges and future trends,” *Wireless Communications and Mobile Computing*, vol. 2022, no. 1, p. 6476274, 2022.
- [156] Y. Ge and Q. Zhu, “Mufaza: Multi-source fast and autonomous zero-trust authentication for 5g networks,” in *MILCOM 2022-2022 IEEE Military Commun. Conference (MILCOM)*, pp. 571–576, 2022.

- [157] A. Niakanlahiji, J. Wei, M. R. Alam, Q. Wang, and B.-T. Chu, “{ShadowMove}: A stealthy lateral movement strategy,” in *29th USENIX Security Symposium (USENIX Security 20)*, pp. 559–576, 2020.
- [158] D. Xu, L. Thomas, M. Kent, T. Mouelhi, and Y. Le Traon, “A model-based approach to automated testing of access control policies,” in *Proceedings of the 17th ACM symposium on Access Control Models and Technologies*, pp. 209–218, 2012.
- [159] B. Tang, V. K. Shah, V. Marojevic, and J. H. Reed, “AI testing framework for next-G O-RAN networks: Requirements, design, and research opportunities,” *IEEE Wireless Communications*, vol. 30, no. 1, pp. 70–77, 2023.
- [160] A. Basta, N. Basta, W. Anwar, and M. I. Essar, *Open-source Security Operations Center (SOC): A Complete Guide to Establishing, Managing, and Maintaining a Modern SOC*. John Wiley & Sons, 2024.
- [161] H. Lian, P. Li, and G. Wang, “Dynamic resource orchestration for cloud applications through AI-driven workload prediction and analysis,” *Artificial Intelligence and Machine Learning Review*, vol. 4, no. 4, pp. 1–14, 2023.
- [162] X. Wu, J. Farooq, and J. Chen, “Multi-agent resource orchestration based on D3QN for network slicing in 5G edge-cloud networks,” *IEEE Transactions on Network and Service Management*, vol. 1, no. 1, pp. 1–14, 2026.
- [163] S. Fang and Q. Zhu, “Fundamental stealthiness–distortion trade-offs in cyber-physical systems,” in *Security and Resilience in Cyber-Physical Systems: Detection, Estimation and Control*, pp. 37–60, Springer, 2022.
- [164] E. C. Balta, M. Pease, J. Moyne, K. Barton, and D. M. Tilbury, “Digital twin-based cyber-attack detection framework for cyber-physical manufacturing systems,” *IEEE Transactions on Automation Science and Engineering*, vol. 21, no. 2, pp. 1695–1712, 2023.
- [165] C. Fung, Q. Zhu, R. Boutaba, and T. Başar, “Smurfen: A system framework for rule sharing collaborative intrusion detection,” in *2011 7th International Conference on Network and Service Management*, pp. 1–6, IEEE, 2011.
- [166] A. Zidan, M. Khairalla, A. M. Abdrabou, T. Khalifa, K. Shaban, A. Abd Rabou, R. El Shatshat, and A. M. Gaouda, “Fault detection, isolation, and service restoration in distribution systems: State-of-the-art and future trends,” *IEEE Transactions on Smart Grid*, vol. 8, no. 5, pp. 2170–2185, 2016.

- [167] Z. Zhang, Y. Liu, Q. Li, Z. Liu, C. Peng, and S. Lu, “Dependent misconfigurations in 5G/4.5 G radio resource control,” *Proceedings of the ACM on Networking*, vol. 1, no. CoNEXT1, pp. 1–20, 2023.
- [168] J. Prados-Garzon, T. Taleb, and M. Bagaa, “Optimization of flow allocation in asynchronous deterministic 5G transport networks by leveraging data analytics,” *IEEE Transactions on Mobile Computing*, vol. 22, no. 3, pp. 1672–1687, 2021.
- [169] Q. Zhu, “Foundations of cyber resilience: The confluence of game, control, and learning theories,” in *Cyber Resilience: Applied Perspectives*, pp. 27–58, Springer, 2025.
- [170] J. Muniz, G. McIntyre, and N. AlFardan, *Security operations center: Building, operating, and maintaining your SOC*. Cisco Press, 2015.
- [171] B. S. Awoyemi, A. S. Alfa, and B. T. Maharaj, “Network restoration for next-generation communication and computing networks,” *Journal of Computer Networks and Communications*, vol. 2018, no. 1, p. 4134878, 2018.
- [172] R. Zhang and Q. Zhu, “Optimal cyber-insurance contract design for dynamic risk management and mitigation,” *IEEE Transactions on Computational Social Systems*, vol. 9, no. 4, pp. 1087–1100, 2021.
- [173] S. Liu and Q. Zhu, “Cyber insurance for cyber resilience,” *arXiv preprint arXiv:2312.02921*, 2023.
- [174] S. Liu and Q. Zhu, “Mitigating moral hazard in cyber insurance using risk preference design,” *arXiv preprint arXiv:2203.12001*, 2022.
- [175] R. Zhang, Q. Zhu, and Y. Hayel, “A bi-level game approach to attack-aware cyber insurance of computer networks,” *IEEE Journal on Selected Areas in Communications*, vol. 35, no. 3, pp. 779–794, 2017.
- [176] R. Zhang and Q. Zhu, “FlipIn: A game-theoretic cyber insurance framework for incentive-compatible cyber risk management of internet of things,” *IEEE Transactions on Information Forensics and Security*, vol. 15, pp. 2026–2041, 2019.
- [177] A. Jin, A. Kott, and I. Linkov, “Fundamental concepts of cyber resilience: Introduction and overview,” in *Cyber Resilience: Applied Perspectives*, pp. 1–23, Springer, 2025.
- [178] T. Li, K. Hammar, R. Stadler, and Q. Zhu, “Conjectural online learning with first-order beliefs in asymmetric information stochastic games,” *arXiv preprint arXiv:2402.18781*, 2024.

[179] K. Hammar, T. Li, R. Stadler, and Q. Zhu, “Automated security response through online learning with adaptive conjectures,” *arXiv preprint arXiv:2402.12499*, 2024.

[180] L. Huang and Q. Zhu, “Adaptive honeypot engagement through reinforcement learning of semi-markov decision processes,” in *Decision and Game Theory for Security: 10th International Conference, GameSec 2019, Stockholm, Sweden, October 30–November 1, 2019, Proceedings 10*, pp. 196–216, Springer, 2019.

[181] C. A. Kamhoua, C. D. Kiekintveld, F. Fang, and Q. Zhu, *Game theory and machine learning for cyber security*. John Wiley & Sons, 2021.

[182] Z. Qian, J. Fu, and Q. Zhu, “A receding-horizon mdp approach for performance evaluation of moving target defense in networks,” in *2020 IEEE Conference on Control Technology and Applications (CCTA)*, pp. 1–7, IEEE, 2020.

[183] J. Jin, Z. Pang, J. Kua, Q. Zhu, K. H. Johansson, N. Marchenko, and D. Cavalcanti, “Cloud-fog automation: The new paradigm towards autonomous industrial cyber-physical systems,” *IEEE Journal on Selected Areas in Communications*, 2025.

[184] A. Kott and I. Linkov, “To improve cyber resilience, measure it,” *Computer*, vol. 54, no. 2, pp. 80–85, 2021.

[185] Q. Zhu and H. Ishii, “Introduction to the special section on learning and security for multi-agent systems,” *Annual Reviews in Control*, vol. 53, pp. 249–251, 2022.

[186] J. Chen and Q. Zhu, “Control of multilayer mobile autonomous systems in adversarial environments: A games-in-games approach,” *IEEE Transactions on Control of Network Systems*, vol. 7, no. 3, pp. 1056–1068, 2019.

[187] H. Ishii and Q. Zhu, *Security and resilience of control systems*. Springer, 2022.

[188] Z. Xu and Q. Zhu, “Cross-layer secure cyber-physical control system design for networked 3d printers,” in *Proc. Amer. Control Conf. (ACC)*, pp. 1191–1196, 2016.

[189] Q. Zhu and T. Başar, “Game-theoretic approach to feedback-driven multi-stage moving target defense,” in *Decision and Game Theory for Security – 4th International Conference, GameSec 2013, Proceedings*, Lecture Notes in Computer Science, pp. 246–263, Springer, 2013. 4th International Conference on Decision and Game Theory for Security (GameSec 2013), November 11–12, 2013.

[190] T. Li, J. Guevara, X. Xie, and Q. Zhu, “Self-Confirming Transformer for Locally Consistent Online Adaptation in Multi-Agent Reinforcement Learning,” *arXiv*, 2023.

- [191] Y. Zhao, C. Rieger, and Q. Zhu, “Multi-agent learning for resilient distributed control systems,” 2022. arXiv:2208.05060.
- [192] T. Li, H. Lei, and Q. Zhu, “Self-Adaptive Driving in Nonstationary Environments through Conjectural Online Lookahead Adaptation,” *2023 IEEE International Conference on Robotics and Automation (ICRA)*, vol. 00, pp. 7205–7211, 2023.
- [193] Y. Pan, T. Li, and Q. Zhu, “On the Resilience of Traffic Networks under Non-Equilibrium Learning,” *2023 American Control Conference (ACC)*, vol. 00, pp. 3484–3489, 2023.
- [194] L. Huang, J. Chen, and Q. Zhu, “Distributed and optimal resilient planning of large-scale interdependent critical infrastructures,” in *Proc. Winter Simul. Conf. (WSC)*, pp. 1096–1107, 2018.
- [195] J. Chen, C. Touati, and Q. Zhu, “Optimal secure two-layer iot network design,” *IEEE Trans. Control Netw. Syst.*, vol. 7, no. 1, pp. 398–409, 2019.
- [196] J. Chen, C. Touati, and Q. Zhu, “A dynamic game approach to designing secure interdependent IoT-enabled infrastructure network,” *IEEE Transactions on Network Science and Engineering*, vol. 8, no. 3, pp. 2601–2612, 2021.
- [197] Y. Nugraha, A. Cetinkaya, T. Hayakawa, H. Ishii, and Q. Zhu, “Dynamic resilient network games with applications to multiagent consensus,” *IEEE Trans. Cont. Netw. Syst.*, vol. 8, no. 1, pp. 246–259, 2020.
- [198] Y. Nugraha, T. Hayakawa, A. Cetinkaya, H. Ishii, and Q. Zhu, “Subgame perfect equilibrium analysis for jamming attacks on resilient graphs,” in *2019 American Control Conference (ACC)*, pp. 2060–2065, IEEE, 2019.
- [199] M. J. Weisman, A. Kott, J. E. Ellis, B. J. Murphy, T. W. Parker, S. Smith, and J. Vandekerckhove, “Experimental measurements of cyber resilience,” in *Cyber Resilience: Applied Perspectives*, pp. 181–196, Springer, 2025.
- [200] M. J. Weisman, A. Kott, J. E. Ellis, B. J. Murphy, T. W. Parker, S. Smith, and J. Vandekerckhove, “Quantitative measurement of cyber resilience: Modeling and experimentation,” *ACM Transactions on Cyber-Physical Systems*, vol. 9, no. 1, pp. 1–25, 2025.
- [201] P. Cholda, A. Mykkeltveit, B. E. Helvik, O. J. Wittner, and A. Jajszczyk, “A survey of resilience differentiation frameworks in communication networks,” *IEEE Communications Surveys & Tutorials*, vol. 9, no. 4, pp. 32–55, 2007.

- [202] Z. Xu and Q. Zhu, “Secure and resilient control design for cloud enabled networked control systems,” in *Proc. 1st ACM Workshop Cyber-Phys. Syst.-Secur. priv.*, pp. 31–42, 2015.
- [203] Z. Xu and Q. Zhu, “Cross-layer secure and resilient control of delay-sensitive networked robot operating systems,” in *Proc. IEEE Conf. Control Technol. Appl. (CCTA)*, pp. 1712–1717, 2018.
- [204] G. Xu, H. Li, H. Ren, J. Sun, S. Xu, J. Ning, H. Yang, K. Yang, and R. H. Deng, “Secure and verifiable inference in deep neural networks,” in *Annual Computer Security Applications Conference*, pp. 784–797, 2020.
- [205] F. Miao and Q. Zhu, “A moving-horizon hybrid stochastic game for secure control of cyber-physical systems,” in *53rd IEEE Conference on Decision and Control*, pp. 517–522, IEEE, 2014.
- [206] Q. Zhu and T. Başar, “Robust and resilient control design for cyber-physical systems with an application to power systems,” in *2011 50th IEEE conference on decision and control and European control conference*, pp. 4066–4071, IEEE, 2011.
- [207] Q. Zhu, L. Bushnell, and T. Başar, “Resilient distributed control of multi-agent cyber-physical systems,” in *Control of Cyber-Physical Systems: Workshop held at Johns Hopkins University, March 2013*, pp. 301–316, Springer, 2013.
- [208] Y. Huang, L. Huang, and Q. Zhu, “Reinforcement learning for feedback-enabled cyber resilience,” *Annual reviews in control*, vol. 53, pp. 273–295, 2022.
- [209] Z. Xu and Q. Zhu, “A cyber-physical game framework for secure and resilient multi-agent autonomous systems,” in *2015 54th IEEE Conference on Decision and Control (CDC)*, pp. 5156–5161, IEEE, 2015.
- [210] M. H. Manshaei, Q. Zhu, T. Alpcan, T. Bacşar, and J.-P. Hubaux, “Game theory meets network security and privacy,” *ACM Computing Surveys (CSUR)*, vol. 45, no. 3, pp. 1–39, 2013.
- [211] Q. Zhu and S. Rass, “Game theory meets network security: A tutorial,” in *Proceedings of the 2018 ACM SIGSAC conference on computer and communications security*, pp. 2163–2165, 2018.
- [212] Q. Zhu, A. Clark, R. Poovendran, and T. Başar, “Deceptive routing games,” in *2012 IEEE 51st IEEE Conference on Decision and Control (CDC)*, pp. 2704–2711, IEEE, 2012.

- [213] S. Jajodia, V. Subrahmanian, V. Swarup, and C. Wang, “Cyber deception,” *Cham, Switzerland: Springer*, 2016.
- [214] E. Al-Shaer, J. Wei, W. Kevin, and C. Wang, “Autonomous cyber deception,” *Springer*, 2019.
- [215] S. Zhang, “An overview of network slicing for 5G,” *IEEE Wireless Communications*, vol. 26, no. 3, pp. 111–117, 2019.
- [216] S. Vassilaras, L. Gkatzikis, N. Liakopoulos, I. N. Stiakogiannakis, M. Qi, L. Shi, L. Liu, M. Debbah, and G. S. Paschos, “The algorithmic aspects of network slicing,” *IEEE Communications Magazine*, vol. 55, no. 8, pp. 112–119, 2017.
- [217] X. Foukas, G. Patounas, A. Elmokashfi, and M. K. Marina, “Network slicing in 5G: Survey and challenges,” *IEEE Communications Magazine*, vol. 55, no. 5, pp. 94–100, 2017.
- [218] Q. Zhu and L. Bushnell, “Networked cyber-physical systems: Interdependence, resilience and information exchange,” in *Proc. 51st Annual Allerton Conf. Commun., Control, Comput. (Allerton)*, pp. 763–769, 2013.
- [219] J. Chen and Q. Zhu, *A game-and decision-theoretic approach to resilient interdependent network analysis and design*. Springer, 2019.
- [220] S. Yüksel and T. Başar, *Stochastic Networked Control Systems: Stabilization and Optimization under Information Constraints*. Systems & Control: Foundations & Applications, Birkhäuser, Cambridge, MA, USA, 2013.
- [221] X.-M. Zhang, Q.-L. Han, and X. Yu, “Survey on recent advances in networked control systems,” *IEEE Trans. Ind. Inform.*, vol. 12, no. 5, pp. 1740–1752, 2015.
- [222] M. Long, C.-H. Wu, and J. Y. Hung, “Denial of service attacks on network-based control systems: Impact and mitigation,” *IEEE Trans. Ind. Inform.*, vol. 1, no. 2, pp. 85–96, 2005.
- [223] V. S. Dolk, P. Tesi, C. De Persis, and W. Heemels, “Event-triggered control systems under denial-of-service attacks,” *IEEE Trans. Cont. Netw. Syst.*, vol. 4, no. 1, pp. 93–105, 2016.
- [224] M. Chahbar, G. Diaz, A. Dandoush, C. Céerin, and K. Ghoumid, “A comprehensive survey on the e2e 5g network slicing model,” *IEEE Trans. Netw. Service Manage.*, vol. 18, no. 1, pp. 49–62, 2020.

[225] Y. Nugraha, A. Cetinkaya, T. Hayakawa, H. Ishii, and Q. Zhu, “Rolling horizon games of resilient networks with non-uniform horizons,” *Eur. J. Control*, vol. 68, p. 100693, 2022.

[226] M. J. Farooq and Q. Zhu, “On the secure and reconfigurable multi-layer network design for critical information dissemination in the internet of battlefield things (iobt),” *IEEE Trans. Wireless Commun.*, vol. 17, no. 4, pp. 2618–2632, 2018.

[227] A. Clark, Q. Zhu, R. Poovendran, and T. Başar, “An impact-aware defense against stuxnet,” in *Proc. Amer. Control Conf. (ACC)*, pp. 4140–4147, 2013.

[228] E. A. Hansen, D. S. Bernstein, and S. Zilberstein, “Dynamic programming for partially observable stochastic games,” in *AAAI*, vol. 4, pp. 709–715, 2004.

[229] K. Horák, Q. Zhu, and B. Bošanský, “Manipulating adversary’s belief: A dynamic game approach to deception by design for proactive network security,” in *Decision and Game Theory for Security: 8th International Conference, GameSec 2017, Vienna, Austria, October 23-25, 2017, Proceedings*, pp. 273–294, Springer, 2017.

[230] Y.-T. Yang, T. Li, and Q. Zhu, “Transparent tagging for strategic social nudges on user-generated misinformation,” *IEEE Transactions on Network Science and Engineering*, no. 99, pp. 1–14, 2025.

[231] Y.-T. Yang and Q. Zhu, “When to deceive: A cross-layer stackelberg game framework for strategic timing of cyber deception,” *arXiv preprint arXiv:2505.21244*, 2025.

[232] C. A. Holt and A. E. Roth, “The Nash equilibrium: A perspective,” *Proceedings of the National Academy of Sciences*, vol. 101, no. 12, pp. 3999–4002, 2004.

[233] E. Maskin and J. Tirole, “Markov perfect equilibrium: I. observable actions,” *Journal of Economic Theory*, vol. 100, no. 2, pp. 191–219, 2001.

[234] D. Fudenberg and J. Tirole, “Perfect Bayesian equilibrium and sequential equilibrium,” *Journal of Economic Theory*, vol. 53, no. 2, pp. 236–260, 1991.

[235] E. Winter, “The Shapley value,” *Handbook of game theory with economic applications*, vol. 3, pp. 2025–2054, 2002.

[236] J. Filar and K. Vrieze, *Competitive Markov decision processes*. Springer Science & Business Media, 2012.

[237] L. S. Shapley, “Stochastic games,” *Proceedings of the national academy of sciences*, vol. 39, no. 10, pp. 1095–1100, 1953.

[238] J. C. Harsanyi, “Games with incomplete information played by ?bayesian? players, i–iii part i. the basic model,” *Management science*, vol. 14, no. 3, pp. 159–182, 1967.

[239] R. Aumann and A. Brandenburger, “Epistemic conditions for nash equilibrium,” *Econometrica: Journal of the Econometric Society*, pp. 1161–1180, 1995.

[240] Q. Zhu, H. Tembine, and T. Başar, “Hybrid learning in stochastic games and its application in network security,” *Reinforcement Learning and Approximate Dynamic Programming for Feedback Control*, pp. 303–329, 2012.

[241] T. Li, G. Peng, Q. Zhu, and T. Başar, “The confluence of networks, games, and learning a game-theoretic framework for multiagent decision making over networks,” *IEEE Control Systems Magazine*, vol. 42, no. 4, pp. 35–67, 2022.

[242] Y. Pan, T. Li, and Q. Zhu, “Model-agnostic meta-policy optimization via zeroth-order estimation: A linear quadratic regulator perspective,” *arXiv preprint arXiv:2503.00385*, 2025.

[243] Y. Pan and Q. Zhu, “Model-agnostic zeroth-order policy optimization for meta-learning of ergodic linear quadratic regulators,” *arXiv preprint arXiv:2405.17370*, 2024.

[244] Y. Pan, T. Li, H. Li, T. Xu, Z. Zheng, and Q. Zhu, “A first order meta stackelberg method for robust federated learning,” *arXiv preprint arXiv:2306.13800*, 2023.

[245] A.-L. Barabási, “Network science,” *Philosophical Transactions of the Royal Society A: Mathematical, Physical and Engineering Sciences*, vol. 371, no. 1987, p. 20120375, 2013.

[246] P. Erdős, A. Rényi, *et al.*, “On the evolution of random graphs,” *Publications of the*, 1960.

[247] A.-L. Barabási and E. Bonabeau, “Scale-free networks,” *Scientific american*, vol. 288, no. 5, pp. 60–69, 2003.

[248] R. W. Heath, M. Kountouris, and T. Bai, “Modeling heterogeneous network interference using poisson point processes,” *IEEE Transactions on signal processing*, vol. 61, no. 16, pp. 4114–4126, 2013.

[249] J. Dall and M. Christensen, “Random geometric graphs,” *Physical review E*, vol. 66, no. 1, p. 016121, 2002.

[250] P. Balister, A. Sarkar, and B. Bollobás, “Percolation, connectivity, coverage and colouring of random geometric graphs,” *Handbook of large-scale random networks*, pp. 117–142, 2008.

[251] X. Fu, M. Small, and G. Chen, *Propagation dynamics on complex networks: models, methods and stability analysis*. John Wiley & Sons, 2013.

[252] R. Parshani, S. Carmi, and S. Havlin, “Epidemic threshold for the susceptible-infectious-susceptible model on random networks,” *Physical review letters*, vol. 104, no. 25, p. 258701, 2010.

[253] M. J. Farooq and Q. Zhu, “Modeling, analysis, and mitigation of dynamic botnet formation in wireless IoT networks,” *IEEE Transactions on Information Forensics and Security*, vol. 14, no. 9, pp. 2412–2426, 2019.

[254] C. Smidts, I. Ray, Q. Zhu, P. K. Vaddi, Y. Zhao, L. Huang, X. Diao, R. Talukdar, and M. C. Pietrykowski, *Cyber-security threats and response models in nuclear power plants*. Springer, 2022.

[255] Y. Zhao, L. Huang, C. Smidts, and Q. Zhu, “Finite-horizon semi-markov game for time-sensitive attack response and probabilistic risk assessment in nuclear power plants,” *Reliability Engineering & System Safety*, vol. 201, p. 106878, 2020.

[256] S. Uryasev and R. T. Rockafellar, “Conditional value-at-risk: optimization approach,” in *Stochastic optimization: algorithms and applications*, pp. 411–435, Springer, 2001.

[257] J. Pawlick, S. Farhang, and Q. Zhu, “Flip the cloud: Cyber-physical signaling games in the presence of advanced persistent threats,” in *Proc. Decis. Game Theory Secur.*, pp. 289–308, 2015.

[258] J. Pawlick and Q. Zhu, “Strategic trust in cloud-enabled cyber-physical systems with an application to glucose control,” *IEEE Trans. Information Forensics and Security*, vol. 12, no. 12, pp. 2906–2919, 2017.

[259] M. Rausand and A. Høyland, *System reliability theory: models, statistical methods, and applications*, vol. 396. John Wiley & Sons, 2003.

[260] A. Rauzy, “Toward an efficient implementation of the MOCUS algorithm,” *IEEE Transactions on Reliability*, vol. 52, no. 2, pp. 175–180, 2003.

- [261] I. L. Johansen and M. Rausand, “Foundations and choice of risk metrics,” *Safety science*, vol. 62, pp. 386–399, 2014.
- [262] P. Miziūla and J. Navarro, “Birnbaum importance measure for reliability systems with dependent components,” *IEEE transactions on reliability*, vol. 68, no. 2, pp. 439–450, 2019.
- [263] T. Kieras, M. J. Farooq, and Q. Zhu, “RIO TS: Risk analysis of iot supply chain threats,” in *IEEE 6th World Forum on Internet of Things (WF-IoT 2020)*, pp. 1–6, IEEE, 2020.
- [264] T. Kieras, M. J. Farooq, and Q. Zhu, “Modeling and assessment of IoT supply chain security risks: The role of structural and parametric uncertainties,” in *IEEE Security and Privacy Workshops (SPW 2020)*, pp. 163–170, IEEE, 2020.
- [265] T. Li, Y.-T. Yang, Y. Pan, and Q. Zhu, “From texts to shields: Convergence of large language models and cybersecurity,” *arXiv preprint arXiv:2505.00841*, 2025.
- [266] C. Peng and Q. Zhu, “Trust-aware resource management for secure and optimal network slicing in 5g mobile edge networks,” in *IEEE Conference on Computer Communications Workshops (INFOCOM WKSHPS 2023)*, IEEE, 2023.
- [267] S. Massari, N. Mirizzi, G. Piro, and G. Boggia, “An open-source tool modeling the ETSI-MEC architecture in the Industry 4.0 context,” in *29th Mediterranean Conference on Control and Automation (MED 2021)*, pp. 226–231, IEEE, 2021.
- [268] X. Wu, J. Farooq, and J. Chen, “Adaptive risk-aware resource orchestration for 5G microservices over multi-tier edge-cloud systems,” in *2024 IEEE International Conference on Communications Workshops (ICC Workshops)*, pp. 359–364, IEEE, 2024.
- [269] X. Wu, J. Farooq, and J. Chen, “Joint admission control and resource provisioning for URLLC traffic in O-RAN: A constrained multi-agent reinforcement learning approach,” in *IEEE International Conference on Communications (ICC 2025), Montreal, Canada*, pp. 1426–1431, 2025.